Princeton Plasma Physics Laboratory

PPPL-5444

Overview of Plasma Mass Filters for Nuclear Waste Remediation

S.J. Zweben, N.J. Fisch, R. Gueroult, I. Ochs, C.A. Gentile, A. Khodak, F.M. Levinton*

May 2018

Prepared for the U.S. Department of Energy under Contract DE-AC02-09CH11466.

Princeton Plasma Physics Laboratory
Report Disclaimers

Full Legal Disclaimer

Trademark Disclaimer

PPPL Report Availability

Princeton Plasma Physics Laboratory:

http://www.pppl.gov/techreports.cfm

Office of Scientific and Technical Information (OSTI):

http://www.osti.gov/scitech/

Related Links:

U.S. Department of Energy

U.S. Department of Energy Office of Science

U.S. Department of Energy Office of Fusion Energy Sciences

Overview of Plasma Mass Filters for Nuclear Waste Remediation

S.J. Zweben, N.J. Fisch, R. Gueroult, I. Ochs, C.A. Gentile, A. Khodak, F.M. Levinton*

Princeton Plasma Physics Laboratory, Princeton, NJ 08540

* Nova Photonics Inc., 200 Forrestal Rd, Princeton NJ 08540

Abstract

This PPPL Report presents an overview of plasma mass filters for nuclear waste remediation, based on studies at PPPL done during the period 2012-2017. The Introduction describes the motivations and goals, the experimental background, and options for nuclear waste separation. Section 2 describes various possible plasma physics mechanisms for ion mass filtering, such as ion gyro-orbit separation, drift-orbit separation, the vacuum arc centrifuge, steady-state rotating plasmas in various geometry, and several others. Section 3 describes some generic physics issues concerning these processes, such as the ion charge state, neutrals and molecules, collisions, radiation loss, and electric fields and fluctuations. Section 4 describes some generic technology issues such as the plasma source, plasma heating, and material handling. The last section outlines a possible R&D plan, including staged goals and specific research needs for theory and diagnostics. The last sub-section summarizes the findings of this report.

Outline

1. Introduction

This report summarizes an internal LDRD study of "Plasma Mass Filters for Nuclear Waste Remediation" done at PPPL during the period 2012-2017, including some new results and perspectives. Related work has already been published [1-8], and a more simplified tutorial on the more general topic of "Plasma Mass Separation" is being submitted [9]. The present Report is intended to archive many details of and references used for the work done for this study at PPPL, and will remain unpublished.

1.1 Motivations and goals

The main motivation for this work is to develop methods for using magnetized plasmas to separate atoms of widely differing mass ranges for various practical applications. The focus here is *not* on separating isotopes of a single atomic species, but rather on a coarser separation of high mass from low mass atoms at a much higher throughput than conventional isotope separation methods. This emerging topic of *differential confinement* in plasmas is also of considerable interest as basic plasma physics, and also relevant for some frontiers of magnetic fusion research, such as active control of the ion distribution functions in tokamaks.

Three potential applications of this technology have been described in a recent paper [7]: separation of nuclear waste into high-activity (high mass) and low-activity (low mass) components, separation of lighter lanthanides from chemically-similar but heavier (radioactive) actinides, and separation of high-mass (high value) rare earths in recycling processes. This report will focus on the first of these, namely, the separation of radioactive from non-radioactive components of nuclear waste, such a presently being stored at Hanford.

The goal of a plasma-based mass filter for nuclear waste remediation process is to reduce the volume of high-level radioactive waste (HLW) by increasing the concentration of radioactive materials in that waste stream [4]. This should reduce the high cost of conventional the vitrification of HLW for permanent storage in glass containers. A similar program of HLW concentration is also part of the conventional chemical processing of nuclear waste at Hanford, but plasma separation may have the advantage in that it does not produce additional liquid waste that would require additional treatment. The potential cost savings of plasma filtering techniques were discussed in [4], and metrics for comparing various mass plasma mass filters were discussed in [8].

A near-term goal of this research is to develop an experimental facility for plasma mass separation *via* differential ion confinement physics. Initially a small-scale experiment would explore and compare various physical mechanisms for ion separation, which are discussed in Sec. 2. After evaluation of the various physics issues involved in this process, as discussed in Sec. 3, this could evolve into an intermediate-scale facility to demonstrate high-throughput mass separation, initially using nonradioactive nuclear waste surrogates. Further engineering and testing would then be needed to develop the relevant technology, as discussed in Sec. 4. If this development is successful, a prototype plasma mass filter could then be tested with actual nuclear waste at a site such as Hanford , as outlined in the R&D plan in Sec. 5.

1. R. Gueroult and N.J. Fisch, Phys. Plasmas 19, 122503 (2012)
2. R. Gueroult, J.-M. Rax and N.J. Fisch, Phys. Plasmas 21, 020701 (2014)
3. R. Gueroult and N.J. Fisch, Plasma Sources Sci. Tech 23, 035002 (2014)
4. R. Gueroult, D.T. Hobbs and N.J. Fisch, J. Hazardous Mat. 297, 153 (2015)
5. R. Gueroult, E.S. Evans, S.J. Zweben, N.J. Fisch, and F. Levinton, PSST 25, 035024 (2016)

6. I.E. Ochs, R. Gueroult, N.J. Fisch, and S.J. Zweben, Phys. Plasmas 24, 043503 (2017)
7. R. Gueroult, J.-M. Rax, S.J. Zweben, and N.J. Fisch, Plasma Physics Control. Fusion 60, 104018 (2018)
8. A.J. Fetterman and N.J. Fisch, Phys. Plasmas 18, 103503 (2011)
9. S.J. Zweben, R. Gueroult, N. Fisch, submitted to Physics of Plasmas (2018)

1.2 Experimental Background

The mass spectrum of atoms and molecules is routinely determined for small samples using various types of mass spectrometers developed over many years [1,2]. These analytical devices can ionize and analyze a wide range of masses with an accuracy of ~1 amu, even including large biological molecules, using techniques such as quadrupole mass analysis, plasma or laser desorption mass spectroscopy, inductively coupled plasma mass spectroscopy, glow discharge mass spectroscopy, or Fourier transform ion cyclotron resonance mass spectroscopy, as described in standard textbooks [3,4]. Mass spectrometers measure charge/mass ratio of ions, but do not operate with higher density quasi-neutral plasmas. Thus their throughput is very small, i.e. ≤ 1 μgr/sec, and so they have no direct application to large-scale nuclear waste remediation.

Most previous work on plasma mass filtration has been done for isotope separation, but at relatively modest throughput, e.g. ~10^3 kg/year for the Manhattan project [5]. However, this is far too low to be useful for nuclear waste remediation of a site like Hanford (see Sec. 1.3), where the total waste volume is ~$2x10^5$ m^3 and the total waste mass is ~ $4x10^8$ kg. Plasma processing of 10^8 kg would require an average processing throughput of ~$3x10^6$ kg/year or ~100 gr/sec, assuming 30 year remediation period with 24/7 operation. Since the plasma densities of interest are ~10^8 times lower than solid or liquid densities, plasma mass filtration tends to have a lower throughput than conventional chemical separation methods.

The rest of this section contains a brief history of plasma mass separation experiments, including isotope separation, as summarized in Table 1. Note that the information about these experiments is often limited due to classification or proprietary interests, and not all plasma separation work is covered. Some parameters of these devices are shown in Table 1.2, and parameters of similar basic plasma physics experiments are shown in Table 1.3. Further discussion of the theoretical mechanisms for plasma mass separation is given in Sec. 2.

The first large effort on plasma-based separation of uranium isotopes was made using calutrons from 1941-45 for the Manhattan project [5-8]. Natural uranium was turned into gas molecules (apparently UCl_6), which were then singly ionized by an electron beam and electrostatically accelerated to form multiple ~35 keV ion beams within a magnetic field of B~5 kG. The U^{235} and U^{238} ions were then separated using their 0.6% different ion gyroradii (typically ~100 cm), and ~10% of the ionized atoms were recovered using mechanical slits and deposition on graphite receivers. The total uranium throughput was apparently ~10^{-3} gr/sec per calutron, and there were ~1000 calutrons at ORNL by 1945. Since that time a few of these calutrons have been used for producing ~10-100's of grams/year of stable isotopes of many different elements for medical and industrial purposes [8].

The next experiments on plasma mass separation shown in Table 1.1 was done during 1966-71 using a rotating plasma in a toroidal magnetic chamber with B~6000 Gauss [9]. This was motivated in part by the theory of gas centrifuges, in which radial mass separation was expected at high rotation speeds. The gases used were H, D, Ne and Ar, and gaseous samples were extracted from inside the plasma with a collector probe at various locations, and analyzed with a mass spectrometer well after the ~10 msec plasma

discharges. The relative concentration ratio of Ar/H_2 was observed to increase with the radius of the sampling probe, at least qualitatively in agreement with the expected centrifugal separation process.

Table 1.1 – Experiments on plasma mass separation

Device (country)	species	year(s)	Ref's
calutron (Berkley, ORNL)	U isotopes	1941-present	5-8
FI torus (Sweden)	H/Ar	1966-71	9
ICR (US, USSR, France)	many isotopes/elements	1976-present	10-13
plasma centrifuge (Yale)	metal isotopes and elements	1980-87	14-16
vacuum arc centrifuge (Australia)	Cu/Zn and their isotopes	1989-99	17-19
PCEN vacuum arc centrifuge (Brazil)	C, Al, Mg, Zn, Cd, Pb etc.	1987-98	20-23
Archimedes filter (San Diego)	Xe/Ar and Cu/Ag/Au ?	1998-05	24-31
linear device with electrodes (Kyushu)	Ar, Xe	2007	32
POMS-E-3 (Irkutsk)	N, Ar, Kr	2010-15	33,34
vacuum arc separator (Irkutsk)	Ni, Cr, Fe, W	2011-15	35,36
PMFX (PPPL)	Ar/Kr	2013-14	37,38
SNF separator (JIHT Moscow)	U, Gd, He	2013-16	39-44

Table 1.2 Parameters for some previous plasma separation devices

Device	Length /Diam.	B field (Gauss)	Density (cm-3)	Temp. (eV)	Power source	Gas Type	Outflow g/sec
Q-machine (TRW)	100 cm X 6 cm	4000	.01-0.1x 10^12	e: 0.2 eV i: 0.2 eV	ICRH	K	n/a
Vac Arc Ct (Yale)	160 cm x 15cm	5000 G	10-100x 10^12	e: 1-2 eV i: 1-2 eV	metal arc	Cu, Ni, C, Ti, Al etc	~3 mg/ sec ?
PCEN (Brazil)	105 cm x22 cm	500-3000 G	7-33x 10^12	e: 2-6 eV i: 3 eV	metal arc	C, Mg, Al, Ni, Cu, etc	~60 mg/ sec ?
ERIC (Saclay)	200 cm X12 cm	30,000 G	0.6x 10^12	e: 1.4 eV i: ~200 eV	oven + sputter	Li, Ca, Zn, Yb	10^-4 g/ sec est.
SIRENA (Kurchatov)	80 cm X 6 cm	250	n/a	e: 1.4 eV i: ~200 eV	Li arc	Li	n/a
Archim. DEMO	390 cm 70 cm	1600 G	3-20 x 10^12	e: 3 eV i: 7 eV	Helicon 4-6 MHz	Na, Ar	~1 g/sec
Kyushu JJAP '07	170 cm 45 cm	<700 G	0.2-2 x 10^10	e: 3-6 eV i: 1 eV	Helicon 7 MHz	Ar, Xe	~10^-2 g/sec ?

Table 1.3 Various basic plasma physics devices

Device	Length/ Diam.	B field (Gauss)	Density (cm-3)	Temp. (eV)	Power source	Gas Type
LAPD (UCLA)	2100 cm x 60 cm	1000 G	2x10^12	e: 5 eV	Biased cathode	He
CSDX (UCSD)	280 cm x 20 cm	1000 G	5-30x 10^12	e: 1-3 eV i: ≤ 1 eV	Helicon 13.5 MHz	Ar
VINETA (Greifswald)	450 cm x 40 cm	1000 G	20 x10^12	e: ≤ 3 eV i: ~0.2 eV	Helicon/ ICP	Ar
LHPD (Kyushu)	480 cm x 74 cm	140 G	10^8 – 10^12	e: 3-5 eV	Helicon 7 MHz	Ar
HelCat (UNM)	400 cm x 40 cm	≤ 2200 G	0.5-50 x10^12	e: 3-12 eV i: ≤ 1 eV	Helicon + cathode	He, Ar
Helix (WVU)	150 cm x 10 cm	<1400 G	10 x 10^12	e: 4 eV i: 0.2 eV	Helicon 6-18 MHz	He, Ar
Wombat (ANU)	200 cm x 90 cm	200 G	15x10^12	e: 1.5 eV i: 0.1 eV	Helicon 7 MHz	Ar

The next entry in Table 1.1 are ion cyclotron resonance (ICR) experiments for isotope separation, originally proposed by Dawson et al in 1976 [10]. The first results showed selective ICR acceleration of ions in a linear Q-machine at a magnetic field of B~2.5 kG, densities of $\leq 10^{11}$ cm^{-3}, and temperature of T_e ~0.2 eV, along with a significant variation in the measured ≤50 eV ion populations of K^{39} vs. K^{41} as the magnetic field was varied slightly [10]. Many further ICR separation experiments have been done in the US, France, and the USSR to resonantly increase the gyroradius of various elements and isotopes in a linear magnetic field configuration, and to collect the separated ions using carefully designed baffles at the far end. Extensive reviews of such experiments are in Refs. 11-13, including results for large devices with superconducting magnets and plans for separation of spent nuclear fuel [13]. These devices have successfully separated many ion species and isotopes, and seem to be considerably more efficient than calutrons in terms of cost per gram [12]. The measured isotope production rates have been $\leq 10^{-3}$ gr/sec of the Ni^{62} isotope at TRW and $\leq 10^{-5}$ gr/sec of Li^6 at Kurchatov [12], and an estimated (potential) production rate for Ca^{48} was 5 kg/year [12]. It is not clear whether this technique could be adapted to have a high enough throughput for the remediation of nuclear waste.

The next entry in Table 1.1 is the plasma centrifuge as developed by Krishnan et al during 1980-87 [14-16]. This device has a metal cathode electrode as the source of the material to be separated, located at one end of a ~1-2 m long chamber with a magnetic field of B~7 kG. A metal vapor plasma is created by applying a ~4 kV voltage to the cathode with respect to the chamber wall, which forms a ~5 kA arc for ~1 msec. An azimuthal plasma rotation was created by the self-consistent electric fields with speeds of up to $V_\theta \sim 5x10^6$ cm/sec. The metallic cathode elements were deposited at the far end of the device and their mass spectrum was measured with SIMS and x-ray photoelectron spectroscopy [15,16]. Radial separation of

Al/Ti, Cu/Ni mixtures with a separation ratio of ~2, and enrichment of heavy isotopes of Mg, Ca, Tl by a factor of ~2 were observed, roughly consistent with a fluid model for the vacuum-arc centrifuge. The energy cost for separation in this device was estimated to be $7x10^4$ eV/atom [16], or 100 MJ/gr at A=70, which translates into ~ $5/gr, or $500B for a $\sim 10^8$ kG inventory, which would be prohibitively high.

The next entry in Table 1.1 is on vacuum arc centrifuge work done in Australia using a similar device, but with significant hardware and diagnostic improvements. The experimental results on elemental and isotope separation were qualitatively similar to Krishnan et al, for example, in the mass separation of Zn and Cu isotopes with increasing radius [17]. However, they also point out some caveats; for example, due to the differing melting/boiling point of Zn/Cu in the electrodes, and systematic errors in the x-ray spectroscopy analysis technique. This group also has done theoretical analysis of non-uniform axial magnetic fields [18] and an improved theoretical analysis of the Yale experiments [19].

Similar vacuum arc centrifuge experiments were also done in Brazil using a wide variety of metal cathodes, but with a strong axial gradient in the magnetic field [20-22]. Isotope separation of carbon was observed using a quadrupole mass spectrometer [23]. The azimuthal velocity for Mn, Zn, Cd, and Pb cathodes decreased with atomic mass and was just below the Alfven critical velocity [21]. Detailed measurements of plasma electron parameters, axial velocities, erosion and deposition were measured for 8 different metal cathodes [22]. Large coherent fluctuations were apparently observed in all vacuum arc centrifuges, and a theoretical analysis of plasma instability in a vacuum arc centrifuge was done jointly by the Australian and Brazilian groups [23].

Perhaps the largest experimental effort on plasma mass separation since WWII was made at the privately-funded Archimedes Technology Group in San Diego ca. 2002-2005, based on a theory of single-particle ion orbit confinement by Ohkawa [25]. There is some information on the plans for this project [26-27], but no experimental results on mass separation were ever published. Their DEMO device design aimed to process surrogate Hanford nuclear waste with a throughput ~0.7 MT (metric tons)/day with energy cost per ion of ~0.5 keV/ion, which is ~100 times lower the estimated energy cost for the plasma centrifuge. A linear helicon plasma device was built with a length of 3.9 m, a diameter of 0.4 m, and a magnetic field of $B \leq 1.6$ kG, which was heated with ~3 MW of 6 MHz RF power, and which created a rotating plasma with end electrodes biased at ≤700 Volts [26-29]. Data on plasma density profiles without biasing was published [28], but no data is available on the claimed separation of Xe/Ar and Cu/Ag/Au in an argon based plasma [29]. The latest description of the project plans were in [30], and some additional information is available from the many patents filed by this company [31].

An initial experiment to test the mass separation effect of radial electric fields in a linear magnetized plasma device was done by Shinohara et al [32]. A saturation in the azimuthal flow speed was observed in Xe plasmas but not in Ar plasmas, apparently consistent with the mass-dependent orbit loss model of Okhawa. This experiment was done at very low density $n \sim 10^{10}$ cm^{-3}, which is appropriate for studying collisionless orbit effects, but leads to very low throughput for a given machine size.

A significant experimental effort on plasma mass separation has been ongoing at Irkursk (Russia) since ~2010, apparently by two independent groups. The Paperny group uses a pulsed vacuum arc in a ~200 G curved magnetic field, where the ion gyroradius is comparable to the chamber size. They reported spatial separation of Fe and W ions based on x-ray fluorescence measurement of metallic films deposited on targets [33], and energy spectra of various ion charge states [34]. The Bardakov group focuses on the POMS concept ("plasma optical mass separation"), involving a region of strong magnetic field B~0.5 T along with

various biased electrodes [35,36]. An attempt to separate N, Ar, and Kr in ions was not successful, apparently due to the ion energy spread or possible collective effects.

The next entry in Table 1.1 is the Plasma Mass Filter Experiment (PMFX), operated at the Princeton Plasma Physics Laboratory during 2013-14 [37]. This experiment was based on an existing steady-state linear helicon device with RF heating of ~1 kW at 13.6 MHz and an axial magnetic field of B ≤1 kG. Three coaxial end electrodes were biased to test the effect of applied electric fields on plasma rotation and noble gas ion separation. Slight differences were measured in the radial profiles of singly ionized Ar vs. Kr lines as a function of biasing, which suggested (but did not prove) differential ion confinement. Subsequent theoretical analysis showed that significant device modifications would be needed to produce ion separation due to the high collisionality in this experiment [38].

The final entry in Table 1.1 represents the work on Spent Nuclear Fuel (SNF) processing at the Joint Institute for High Temperatures in Moscow [39-44]. This comprises theoretical work [39,40], design and construction of a separation device with a diameter of 0.9 m, length of 2.0 m, and a field of B=2.1 kG [41]. Preliminary measurements were made of the electrostatic potential profile in discharges biased with a cathode potential of 1190 Volts [42], and a diffuse vacuum arc plasma source was developed which produced ~3 mg/sec of metal ions with an average charge of about +1 [43,44]. This seems to be the most active plasma separation program, although no results on actual separation have been published yet.

An thorough and critical review of proposals and experiments for nuclear waste and spent nuclear fuel separation has recently been published [45], which is especially helpful in referencing the extensive Russian literature. An alternative optically pumped magnetic separation device was also recently developed for isotope separation [46] .

[1] A.J. Dempster, Phys. Rev. 11, 316 (1918)
[2] http://www.thermofisher.com/us/en/home/industrial/mass-spectrometry
[3] J.H. Gross, Mass Spectroscopy, A Textbook, Springer 2011
[4] E. de Hoffmann and V. Stroobant, Mass Spectroscopy, Principles and Applications, Third Edition, Wiley 2007
[5] A.L. Yergey and A.K. Yergey, J. Am. Soc. Mass. Spectrom. 8, 943 (1997)
[6] L.P. Smith et al, Physical Review 72, 989 (1947)
[7] W.E. Parkins, Physics Today 58, 45 (2005)
[8] P. Maier-Komor, Nucl. Inst. and Methods in Physics Res. A613, 465 (2010);
J.G. Tracy and W.S. Aaron, Nucl. Inst. Methods in Physics Research A, 334, 45 (1993);
B.J. Egle, K.J. Hart, W.S. Aaron, J. Radioanal. Nucl. Chem. 299, 995 (2014);
https://www.ornl.gov/research-area/isotope-development-and-production
[9] B. Bonnevier, Plasma Physics 13, 763 (1971)
[10] J.M. Dawson et al, Phys. Rev. Lett. 37, 1547 (1976)
[11] A. Compant La Fontaine, V.G. Pashkovsky, Phys. Plasmas 2, 4641 (1995)
[12] D.A. Dolgolenko and Yu. A. Muromkin, Physics-Uspekhi 52, 345 (2009)
[13] A.V. Timofeev, Physics-Uspekhi 57 990 (2014)
[14] M. Krishnan et al, Phys. Rev. Lett. 46, 36 (1981)
[15] M. Geva et al, J. App. Phys. 56, 1398 (1984)
[16] R.R. Prasad and M. Krishnan, Nucl. Inst. and Meth. in Phys. Research B26, 65 (1987)
[17] P.J. Evans et al, J. Appl. Phys. 66, 116 (1989)
[18] M.J. Hole and S.W. Simpson, Phys. Plasmas 4, 3493 (1997)

[19] M.J. Hole and S.W. Simpson, IEEE Trans. Plasma Sci. 27, 620 (1999)
[20] E. del Bosco et al, App. Phys. Lett. 50, 1716 (1987)
[21] E. del Bosco et al, J. Phys. D: App. Phys. 24, 2008 (1991)
[22] R. S. Dallaqua et al, IEEE Trans. Plasma Science 26, 1044 (1998)
[23] M.J. Hole et al, Phys. Rev. E 65, 046409 (2002)
[24] T. Okhawa and R.L. Miller, Phys. Plasmas 9, 5116 (2002)
[25] J. Gilleland et al, WM'02 Conference paper, Tuscon AZ (2002), http://netserver.aip.org/epaps/phys_plasmas/E-PHPAEN-10-007301/WM2002Paper.pdf ;
[26] Freeman *et al.*, AIP Conf. Proc., AIP, 2003, 694, 403-410 http://aip.scitation.org/doi/abs/10.1063/1.1638067
[27] A. Litvak et al, 30th EPS Conference on Contr. Fusion and Plasma Phys., St. Petersburg, 7-11 July 2003 ECA Vol. 27A, O-1.6A
[28] B.P. Cluggish et al, Phys. Plasmas 12, 057101 (2005)
[29] J. Gilleland et al, WM'05 Conference paper, Tuscon AZ (2005), http://www.wmsym.org/archives/pdfs/5370.pdf
[30] C.E. Ahlfeld et al, 21st IEEE/NPSS Symposium on Fusion Engineering, SOFE 05, 81 (2006)
[31] Archimedes patent list: http://patents.justia.com/assignee/archimedes-technology-group-inc
[32] S. Shinohara and S. Horii, Japanese J. Appl. Phys. 46,4276 (2007)
[33] V.L. Paperny et al, Plasma Sources Sci. Tech. 24, 015009 (2015)
[34] V.L. Paperny et al, Contrib. Plasma Phys. 54, 635 (2014)
[35] V.M. Bardakov et al, Phys. Plasmas 21, 033505 (2014)
[36] V.M. Bardakov et al, Plasma Science and Technology 17, 862 (2015)
[37] R. Gueroult et al, Plasma Sources Sci. Tech. 25, 035024 (2016)
[38] I. Ochs et al, Phys. Plasmas 24, 043503 (2017)
[39] V.P. Smirnov et al, Plasma Physics Reports, 39, 456 (2013)
[40] A.A. Samokhin et al, Technical Physics, 61, 283 (2016)
[41] N.A. Vorona et al, Physics of Atomic Nuclei, 78, 1624 (2015).
[42] A.V. Gavrikov et al, Journal of Physics: Conference Series 774 (2016) 012197
[43] R. Kh. Amirov et al, Plasma Physics Reports 41, 808 (2015)
[44] R. Kh. Amirov et al, Physics of Atomic Nuclei 78, 1631 (2015)
[45] D.A. Dolgoenko and Yu. A. Muromkin, Physics-Uspekhti 60, 994 (2017)
[46] T.R. Mazur, B. Klappauf, and M.G. Raizen, Nature Physics 10, 601 (2014)

1.3 Nuclear waste characterization

The nuclear waste at Hanford came from the production of plutonium for nuclear weapons, starting in 1943 and continuing until 1987. The plutonium was created by bombarding ^{238}U with neutrons from early high-powered nuclear fission reactors designed in part by Fermi, Wigner, and Wheeler. The reactors were cited near the Columbia river to use its water for cooling. The plutonium was extracted from the fuel rods in large plants nearby using various chemical processes, which produced most of the present waste material. Hanford produced a total of about 57 metric tons of ^{239}Pu used for most of the US nuclear weapons.

The nuclear waste repository at Hanford has already been characterized in great detail, for example, in a recent report from Pacific Northwest National Laboratory [1]. This report characterizes the waste as follows (Sec. 3.7):

"The 177 large underground waste storage tanks are distributed into 149 single-shell tanks and 28 double shell tanks and the wastes are grouped into three chemical-physical types: low-solubility sludge, generated from polyvalent metal ions such as Fe(III), Cr(III), Ca(II), and La(III) that have precipitated from the original acidic process solutions by being made alkaline for discharge to the mild-steel-lined waste tanks; aqueous supernatant solutions; and saltcakes generated by crystallization of water-soluble salts from concentrated supernatant solutions. The solutions generally exist above the settled sludge and saltcake layers but are also contained interstitially within sludge and saltcake beds. Of the total 56.2 million gallon (213,000 m3) tank waste volume, supernatant solutions constitute about 37 volume%, solution-bearing saltcake about 42 volume%, and the solution-bearing sludge about 21 volume% (Rodgers 2010). The tank capacity available for additional waste storage is constrained by the obligation to eliminate solutions in the single-shell tanks, many of which have leaked, thus compelling solution transfer to the double-shell tanks. Aside from constructing more double-shell tanks or easing requirements for flammable gas control such as density limits or headspace requirements, the only way to increase capacity is through Waste Concentration operations."

The chemical component inventory of the Handford waste is specified in Fig. 3.1 of that report, reproduced below as Fig. 1.1 (note the log scale). The dominant waste elements are aluminum and sodium, and the dominant waste compounds are water, NO_3 (nitrate) and OH (hydroxide) ions. There are a large number of relatively minor chemical components, including of course many radioactive elements. The total inventory in Hanford high level waste is ~$1.5x10^8$ kg, of which 99% is non-radioactive elements with A<65, e.g. aluminum and nickel.

The main (but not only) environmental concern in the Hanford waste tanks is the radioactive elements. The main source of radioactivity are the relatively short-lived isotopes of Cs^{137} (~75%) and Sr^{90} (~24%), with the remaining ~1% of the radiation due to other elements such as C^{14}, Tc^{99}, I^{129}, and various isotopes of U and Pu. Note that almost all of these radioactive elements have a atomic mass A≥90, which is the basis for plasma mass separation in the waste remediation process. Additional environmental concerns are highly corrosive and toxic chemicals, and flammable gases (e.g. hydrogen) present in all tank wastes.

Estimates of the waste inventories of key radionuclides at various Hanford tanks sites are shown in Table 1.5, taken from [2]. Each radioactive element emits a characteristic form of radiation, mainly alpha, beta, and gamma rays, and each has a characteristic lifetime. These waste inventories are huge by any standard; for example, typical commercial laboratory source of Cs^{137} is 1-10 μCi, and there are about $5x10^7$ Ci of Cs^{137} in the Hanford tanks (which contain ~2/3 of the high level radioactive waste in the US). The inventory of ~$2x10^6$ kG of uranium is equivalent a volume of ~100 m^3, or about 1% of the tank waste mass. The total inventory of plutonium is much smaller, less than 1000 kg. A complete inventory of the nuclear waste at Hanford has been published [3]. A recent general assessment of the basic research needs for remediating these wastes was done by DOE in 2016 [4].

A large fraction (≥ 99%) of the radioactive inventory of ~$2x10^8$ Ci at Hanford is due to elements with an atomic weight above A~90 [5]. The fractional mass of all elements with A≤90 (radioactive and non-radioactive) in the Hanford solid waste (sludge) is ~62-97%, depending on the waste tank [6]. The fractional mass of radioactive fission products with A=80-160 is~0.7%, and the fractional mass of radioactive actinides with A=225-250 is ~0.4.

Two photographs of the Hanford waste tanks are shown in Fig. 1.2. At the left is one of the tanks under construction. At the right is an image of the surface of waste found inside double-shell tank 101-SY at the Hanford Site, April 1989 [7].

Since the nuclear waste inventory at Hanford is very heterogeneous, it is an open question as to what type of and how much of this waste could or should be separated using plasma processing. Solid waste is the fraction for which efficient remediation techniques have yet to be found (as opposed to liquid waste for which flowcharts are in place). Solid waste at Hanford accounts for just under 10^8 kg, which is about 25% of the total waste mass, but by water-washing this waste it goes down to about $0.2x10^8$ kg. We will use for

this report a target goal of 10^8 kg, but the ultimate need for plasma processing will depend on its effectiveness and cost with respect to other processing options, which can not yet be determined since these processes are not finalized.

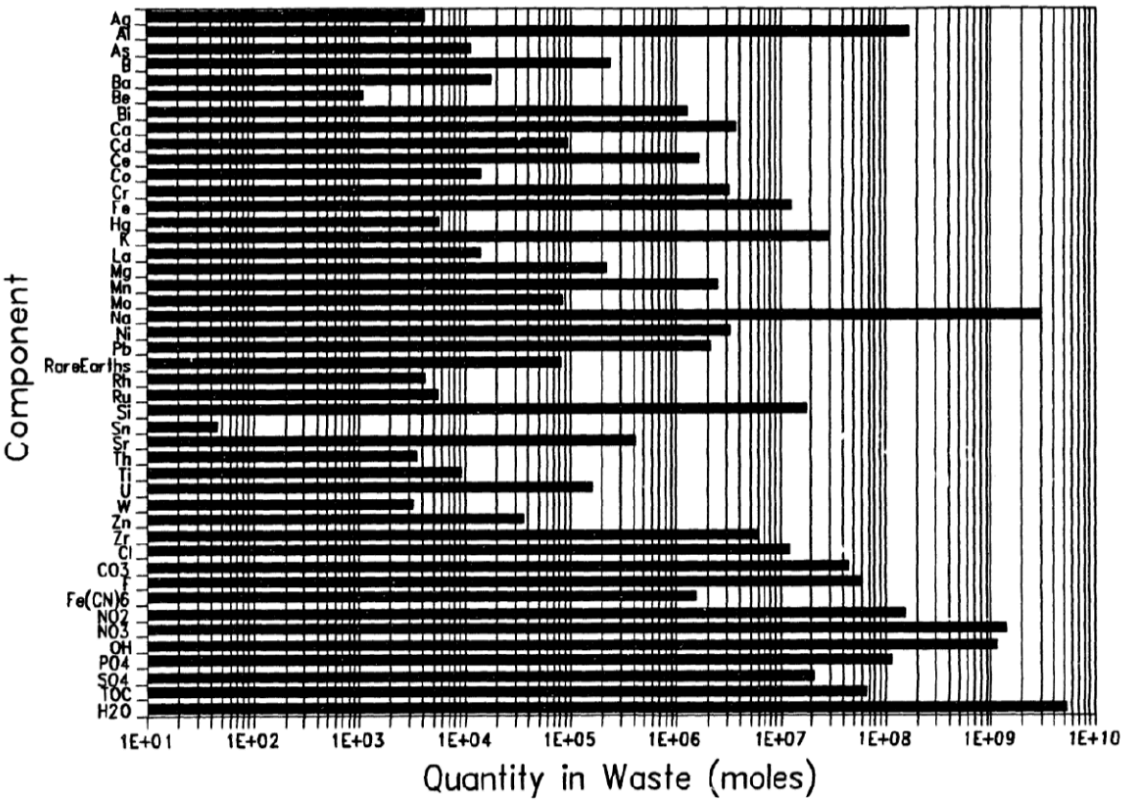

Figure 3-1. Hanford Site Tank Waste Chemical Component Inventory (Delegard et al. 1994, based on Boomer et al. 1993)

Fig. 1.1 Hanford site tank waste chemical component inventory

Table 1-3. Total Hanford defined waste inventories of key radionuclides in Hanford tanks, listed by quadrant (taken from Cragnolino et al., 1997). Values are in curies, with the exceptions of U and Pu (kg). Although Pu-239 and Pu-241 are the only fissile Pu isotopes, they comprise more than 95 percent of waste Pu by mass. Therefore, total Pu is reasonably representative of the relative fissile Pu content.

Quadrant	C-14	Sr-90	Tc-99	I-129	Cs-137	U (kg)	Pu (kg)
NE	8.4×10^2	2.3×10^7	5.3×10^3	1.0×10^1	6.7×10^6	1.1×10^6	2.7×10^2
SW	1.5×10^3	1.9×10^7	1.1×10^4	2.0×10^1	1.3×10^7	6.2×10^5	1.4×10^2
NW	4.1×10^2	1.9×10^6	2.9×10^3	5.6×10^0	4.5×10^6	4.9×10^5	1.2×10^2
SE	2.1×10^3	1.8×10^7	1.4×10^4	2.7×10^1	2.3×10^7	1.9×10^5	2.5×10^2

Table 1.4 Total Hanford defined waste inventories of key radionuclides in Hanford tanks

Fig. 1.2 Hanford waste tank construction (left) and present interior surface of a waste tank (1989)

[1] C.H. Delegard and S.A. Jones, PNNL-23466 Rev. 1 "Chemical Disposition of Plutonium in Hanford Waste Tanks", 2015

[2] R.T. Pabalan et al, CNWRA 97-008 Rev. 1, "Hanford Tank Waste Remediation System High-Level Waste Chemistry Manual", Center for Nuclear Waste Regulatory Analysis, San Antonio Texas, 1998

[3] C.T. Kincaid et al, "Inventory Data Package for Hanford Assessments", PNNL-15829 (2006)

[4] DOE Report (2016) "Basic research needs for environmental management" (http:// science.energy.gov/~/media/bes/pdf/reports/files/ BRNEM_rpt.pdf)

[5] A. Fetterman and N.J. Fisch, Phys. Plasmas 18, 103503 (2011)

[6] R. Gueroult et al, Journal of Hazardous Materials 297, 153 (2015)

[7] from "Hanford Site" in Wikipedia https://en.wikipedia.org/wiki/Hanford_Site; https://en.wikipedia.org/wiki/Hanford_Site#/media/File:Hanford_waste_tank.jpg https://commons.wikimedia.org/wiki/File:Hanford_site_tank_interior.jpg

1.4 Conventional chemical separation

The conventional strategy for nuclear waste remediation is to concentrate the highly radioactive components of the waste to reduce its volume, then dissolve this highly radioactive component into impermeable glass (vitrify), and then put the glass into steel containers which would be buried deep underground. The much larger volume of less radioactive waste can then be mixed with grout or concrete to limit its mobility, then buried nearer the surface. This process should result in the removal of most or all of the nuclear waste from the temporary storage tanks at Hanford to safer and more permanent storage. An illustration of the scale of the present Hanford waste treatment plant is shown in Fig. 1.3.

Chemical processing of the nuclear waste is the conventional approach to this remediation goal. There has been a huge amount of work in this area, as summarized for example in [1,2]. Despite success with vitrification at the Savannah River Site (SRS), there are still many difficulties and unresolved issues for the Hanford site, for example as outlined in [3-7]. There is of course a very large body of academic and industrial work on chemical separation of non-radioactive mixtures, which comprise closed and open systems, bulk flows both parallel and perpendicular to the various separation forces, acting on multiple phases of solids, liquids and gases [8]. A review of chemical nuclear waste pretreatments for Hanford and SRS had the following conclusion [2]:

"Radiochemical and physical separation technologies, applicable to the pretreatment of radioactive wastes to prepare them for immobilization, have developed and evolved for over 60 years. Crossflow filtration and rotary microfiltration represent the state-of-the-art for removing solids from liquid waste streams. Ion exchange (e.g., with SRF resin) and solvent extraction (i.e., with calix-crown compounds) are the currently preferred methods for removing 137Cs from alkaline waste solutions. Inorganic sorbents (e.g., MST) can be used to separate TRU and 90Sr from alkaline tank wastes that do not contain significant amounts of complexants, but treatment with permanganate and isotopic dilution with nonradioactive Sr is required to remove these radionuclides from complexed waste. Leaching with caustic and permanganate have been demonstrated to be effective at removing Al and Cr, respectively, from radioactive tank-waste sludges."

Fig. 1.3 - the Hanford waste treatment plant in January 2017 [6]

[1] R. Gueroult, D.T. Hobbs, and N.J. Fisch, Journal of Hazardous Materials 297, 153 (2015)
[2] W.R. Wilmarth et al, Solvent Extraction and Ion Exchange 29, 1 (2011)
[3] "Advice on the Department of Energy's Cleanup Technology Roadmap: Gaps and Bridges", National Academies Press (2009) https://www.nap.edu/catalog/12603/advice-on-the-department-of-energys-cleanup-technology-roadmap-gaps
[4] "Research Needs for High-Level Waste Stored in Tanks and Bins at U.S. Department of Energy Sites:

Environmental Management Science Program, The National Academies Press, 2001
http://www.nap.edu/catalog.php?record id=10191
[5] R. Carreon et al, "Selection of Pretreatment Processes for removal of radionuclides from Hanford tank waste", Waste Management '02 Conference,
https://digital.library.unt.edu/ark:/67531/metadc783130/
[6] D. Kramer, "Cleanup of Cold War nuclear waste drags on", Physics Today 70, 28 (2017)
[7] T.C. Perry and C.B. Abraham, "Money for Nothing", IEEE Spectrum July 2002
[8] K.K. Sirkar, "Separation of Molecules, Macromolecules, and Particles", Cambridge Univ. Press, 2014

1.5 Physical waste separation (without plasma)

Physical separation of nuclear waste would involve the separation of the radioactive elements from the non-radioactive elements through physical rather than chemical means. Many of these physical methods are summarized in a textbook [1], and employ the forces generated by centrifuges, gravitation, convection, electrostatic and magnetic fields, acoustic pressure, capillary action, surface tension, aerodynamic or hydrodynamic drag, thermal gradients, radiation pressure, and many types of physical membranes. Some physical separation methods which could be particularly useful for radioactive nuclear waste are listed in Table 1.5, all of which have already been implemented using conventional technology.

separation mechanism	**Measurement/sorting technique**	**present applications**
radiation	α, β, γ, neutron detectors	nuclear physics, radio-medicine
mass density	sedimentation, centrifuge	recycling, purification, sorting cells
atomic mass	x-ray transmission	medical imaging, airport scanners
particle charge	electric fields	electrostatic precipitator
temperature	infrared imaging	human body imaging

Table 1.5 Physical separation mechanisms for radioactive species (without plasma)

The efficacy of these physical separation methods for nuclear waste depends to a large extent on the size-scale over which the radioactive and non-radioactive components are mixed within the tanks. For example, it would be easy to separate cm-scale pellets of uranium from the bulk waste using x-ray transmission measurements, e.g. with an automated conveyer belt with robotic sorting. On the other hand, it would be nearly impossible to physically separate uranium uniformly mixed into the waste on an atomic or molecular scale by any of the physical separation methods of Table 1.5.

The general presumption seems to be that tank waste is mixed on near-molecular level, based on the origin of the waste and history of the tanks, and on limited sampling measurements done over time *in situ*. If so, then physical separation would not be possible and chemical or plasma separation would be necessary. However, it is also known that the large-scale structure of the tank waste is quite inhomogeneous, e.g. with liquid, sludge and solid components at various levels, and with large variations in composition from tank-to-tank and even within a single tank over time. Thus a strategy for physical processing of nuclear waste would be to first determine the degree of mixing of sample waste on various size scales, and then to design a

system to transform the waste into particles of a size-scale in which there is a significant particle-to-particle variation in radioactivity. These particles could then be sorted robotically using the physical mechanisms of Table 1.5.

For example, the simplest method to separate radioactive waste from non-radioactive waste is to measure the radioactive decay itself. This method would work best for Cs^{137} and Sr^{90}, which constitute 99% of the tank radioactively, and which emit beta particles with a range of a few millimeters (see Table 1.6). A related method would be to sort small waste particles electrostatically using the charge created by the radioactivity; for example, electrical levitation of dust from the PPPL fusion device TFTR was observed due to charging from beta decays of tritium [2]. It might also be possible to separate the radioactive waste components by sorting with temperature measurements using IR camera technology, since bulk heating due to radiation in the tanks can be significant.

species	half-life (year)	decay products	range in water	charging rate (elect/μgr)
U-235	$7x10^8$	α (4.6 MeV)	0.05 mm	~ 1 (positive)
P-239	$2.4x10^4$	α (5.2 MeV)	0.05 mm	~ 10^4 (positive)
Sr-90	30	β (0.5 MeV)	0.2 cm	~ 10^7 (negative)
Cs-137	30	β (1.2 MeV) γ (662 keV)	0.5 cm 10 cm	~ 10^7 (negative)

Table 1.6 – major radioactive species in nuclear waste

There are also several simple and conventional methods to separate the high density (radioactive) components of the waste from low density components, such as centrifuges for liquid waste, differential evaporation or sedimentation, or the differential particle motion in air for powdered waste. If the desired separation goals can be achieved using conventional physical separation methods, then plasma (or chemical) separation techniques are not necessary, since they will probably be more complicated and expensive.

[1] K.K. Sirkar, "Separation of Molecules, Macromolecules, and Particles", Cambridge Univ. Press, 2014
[2] C.H. Skinner et al, Fusion Science and Technology 45, 11-14 (2004)

1.6 Generic plasma separation device configuration

A generic configuration for a plasma separation device is illustrated in Fig. 1.4. The central section is a vacuum chamber containing the main plasma confined by a magnetic field of typically ~10^3-10^4 Gauss (0.1-1 Tesla). There will also be neutral gas in this chamber at a pressure of ~1-10 mTorr (10^{-6} to 10^{-5} bar). At the left is a plasma source, into which is fed the nuclear waste or waste surrogate, and at the right is the plasma exhaust or waste extraction section. Note that the source and exhaust sections could be in different places for different types of experiments. Some alternative end sections are shown at the bottom of Fig. 1.3.

Table 1.7 shows a set of generic machine and plasma parameters for a device like that in Figure 1.4. The ion charge will normally be +1 at an electron temperature of T_e ~ 1-10 eV. The plasma density would

normally be in the range n_e~10^{13} -10^{14} cm^{-3}, and the neutral (unionized) atom density n_o would be in the same range. The maximum possible ion throughput will depend on the ion speed v_i, which depends on the ion temperature T_i. Making optimistic assumptions of an assumed T_i=10 eV, an average ion mass A=40 and Z=1, and an ion density of n_i~10^{14} cm^{-3}, the the maximum axial ion flux is roughly $\Gamma \sim \frac{1}{2} n_i v_i \sim 2.5 \times 10^{19}$ ions/(cm^2 sec). Assuming an exhaust area of ~10^4 cm^2, this is equivalent to a mass throughput of ~10-20 gr/sec, which is not too far from the desired throughput of ~100 gr/sec for remediation of ~10^8 kg of the Hanford nuclear waste within 30 years (see Sec. 1.2). Perhaps the required throughput could be obtained with ~20 plasma devices each with a throughput of ~5 gr/sec.

There are clearly many difficulties in achieving a successful plasma technology of this type. First, the basic physical mechanism has to be demonstrated which can efficiently separate ions of different mass, as discussed in Sec. 2. Next, various other plasma physics process which constrain this separation mechanism must be evaluated, as discussed in Sec. 3. Third, an efficient source of ionized nuclear waste must be developed, and practical means of extracting the separated waste from the plasma vacuum chamber must be designed, all consistent with the serious ES&H issues, as discussed in Sec. 4. A possible R&D route to this development is outlined in Sec. 5.

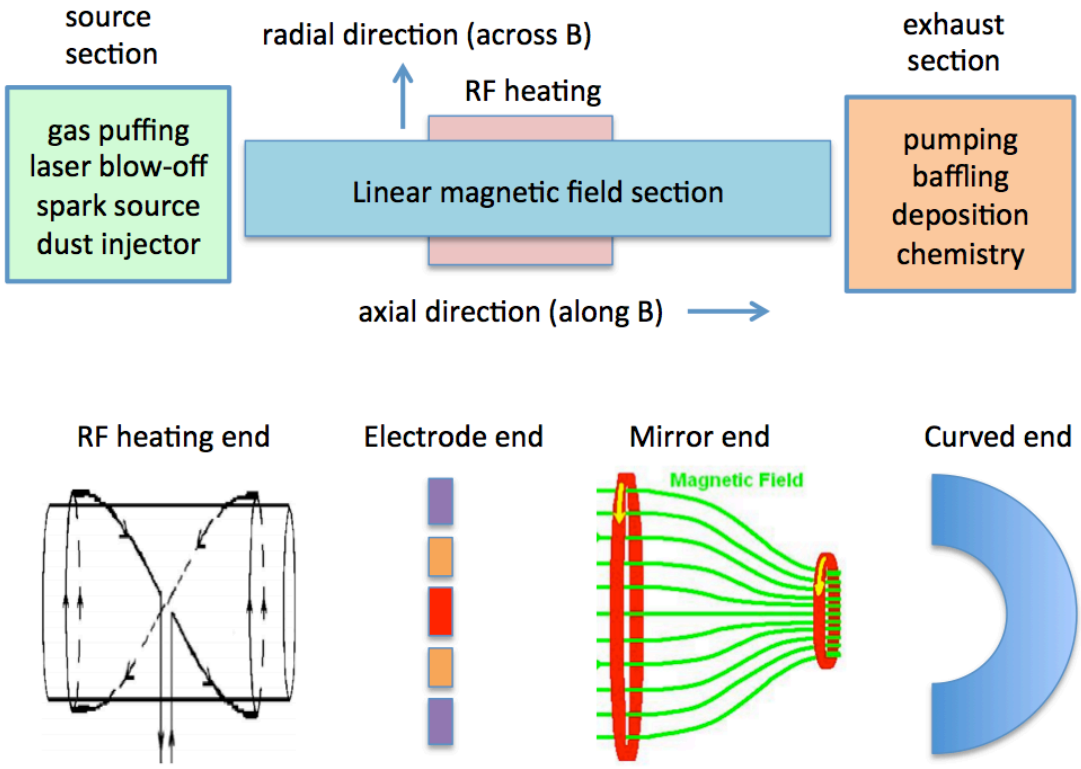

Fig. 1.4 - Generic configuration for plasma separation experimental device

Table 1.7 Generic plasma separation device parameters

Parameter	nominal	approx. range
L (axial length)	2 m	2-4 m
a (radial width)	0.2	0.1-0.3 m
B_z (magnetic field)	0.1 T	≤1 T (pulsed)
P_{rf} (RF power)	5 kW	≤100 kW (pulsed)
M_i (ion mass)	40 (Ar)	4-130
n_e (electron density)	10^{13} cm^{-3}	10^{11}-10^{14} cm^{-3}
n_o (neutral density)	10^{14} cm^{-3}	10^{11} -10^{14} cm^{-3}
T_e (electron temperature)	3 eV	1-10 eV
T_i (ion temperature)	1 eV	0.1-10 eV
Ω_{ci} (ion cyclotron freq.)	40 kHz	0.01-1 MHz
ρ_i (ion gyroradius)	0.6 cm	0.1-5 cm

2. Mechanisms for plasma separation

There are many different plasma mechanisms which could be used to separate ions of different mass for nuclear waste remediation. Some have been tested in previous small-scale experiments (see Sec. 1.2), but none has yet been done with a high enough throughput for nuclear waste remediation. Further experiments with nuclear waste surrogates are needed to optimize the process, and the best process will depend to some extent on the composition of the waste and the separation targets.

Plasmas in this section are assumed to be quasi-neutral with $n_e=n_i$ and (unless otherwise noted) all ions are assumed to have a charge of +1, which is typical of low temperature plasmas. We do not assume that the plasmas are fully ionized, since typically the neutral density is $n_o \sim n_e$. Although neutrals can be useful for ion separation, they will themselves not be separated in any of these process.

The following sub-sections each describe one of the basic plasma mechanisms in Table 2.1. These brief descriptions are highly idealized and simplified, and do not treat the generic physics issues discussed further in Sec. 3, or the engineering issues involving the waste source and extraction discussed in Sec. 4.

2.1 Finite ion gyroradius separation

Perhaps the simplest method for separating ions of different mass in a magnetized plasma would be to exploit the differences in ion gyroradius with M_i, as used in WWII calutrons. Assuming an ion charge of Z=+1, the ion gyroradius is:

$$\rho_i = v_i/\omega_{ci} \sim 100\ [M_i\,(\text{amu})\ T_i\,(\text{eV})]^{1/2} / B\,(\text{Gauss}) \qquad \text{Eq. 2.1.1}$$

where $v_i = (kT_i/M_i)^{1/2}$ is a typical ion velocity at an ion temperature of T_i, B is the magnitude of the magnetic field, and ω_{ci} is the ion cyclotron frequency (radians/sec). For example, the average ion gyroradii for typical noble gas experiments at T_i= 10 eV and B = 1 kG would be $\rho_i \sim 1.4$ cm for neon (M_i=20) and $\rho_i \sim$

3.6 cm for xenon (M_i=130). Note that there will be an order-of-unity variation in the range of gyroradius for each ion species, depending on the angle of the ion with respect to the magnetic field and on the ion velocity within the thermal ion distribution function. Thus this separation mechanism is not very sharp, at least for thermal ions, and obviously requires ions to complete at least one gyro-orbit without pitch-angle scattering due to collisions (see Sec. 3.3 for definition of collisionality).

A schematic illustration of a plasma mass filter based on this mechanism is shown in Fig. 2.1. The ions created in the source at the left could be heated in the main plasma chamber by an RF system like ICRH (ion cyclotron resonance heating) in order to increase the gyroradius of selected ions, such as those with the largest mass and hence the lowest gyrofrequency [1]. The heated ions ρ_i larger than the chamber radius could be collected radially by cylindrical "heavy ion loss collectors" inside the vessel, while lower energy ions which exit at the right could be further separated by gyroradius using carefully designed slits and baffles, as discussed in a review of such schemes [1].

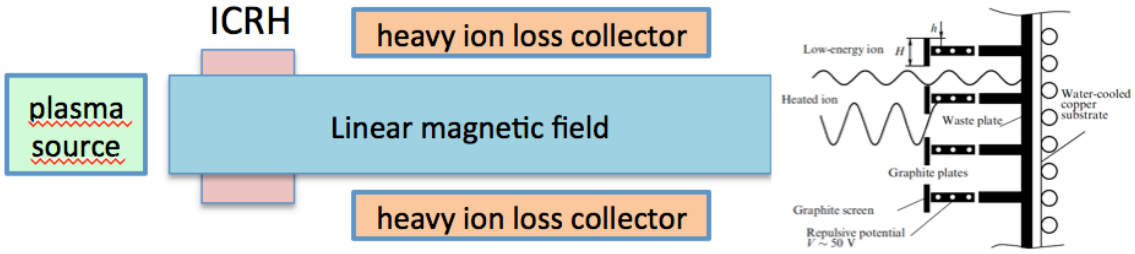

Fig. 2.1 - ion gyroradius separation (section at right from [1]).

The main advantage of this system is its simplicity, for example compared with the methods below which large plasma potentials and/or rotation. The main disadvantages are the difficulty of the ICRH coupling and heating physics, especially at high plasma density and high throughput [1], and the difficulty of waste extraction from the large-area radial heavy ion collectors. For application to nuclear waste processing, the energy cost of ICRH will also limit the maximum ion energy (and corresponding gyroradius) to $T_i < 1$ keV.

This scheme with end collector plates as shown at the right has already been used for use with isotope separation in Russia [1] and in the ERIC device at Saclay [2]. The scheme with radial heavy ion collectors is also similar (but not identical) to the Archimedes proposal [3], since their theoretical "band gap" cutoff condition $M_i/Z > eB^2a^2/8V_{dc}$ is equivalent to $\rho_i > a/8$, assuming the ion velocity is the ExB rotation speed with $E_{rad} = V_{dc}/a$ (although the electric field depends linearly on the radial position in the Archimedes scheme).

[1] D.A. Dolgolenko and Yu. A. Muromkin, Physics-Uspekhi 52, 345 (2009); D.A. Dolgoenko and Yu. A. Muromkin, Physics-Uspekhti 60, 994 (2017)
[2] A. Compant La Fontaine, V.G. Pashkovsky, Phys. Plasmas 2, 4641 (1995)
[3] T. Okhawa and R.L. Miller, Phys. Plasmas 9, 5116 (2002)

2.2 Ion drifts in a curved magnetic field

Another simple mass filter mechanism would use the well-known ion grad-B and curvature drifts of collisionless particles in a curved magnetic field. As shown in standard textbooks [1], ions with a gyroradius ρ_i in a magnetic field with radius of curvature R (with $\rho_i < R$) will drift perpendicular to B and grad-B at a velocity:

$$v_\perp = (\rho_i/R)\, v_i \qquad \text{Eq. 2.1.1}$$

where v_i is the ion velocity and $\rho_i = v_i/\omega_{ci}$ is the ion gyroradius, which depends on the ion temperature and mass through Eq. 2.1.1. Thus the vertical deflection $\delta_\perp$ of an ion with a parallel speed of $\sim v_i$ in a half-torus would be about π times the ion gyroradius, and increases with ion mass M_i and ion temperature T_i (assuming an ion charge Z=+1) as:

$$\delta_\perp \sim (2v_\perp/v_i)\pi R \sim \pi\rho_i \sim\ 320\ [M_i\,(\text{amu})\ T_i\,(\text{eV})]^{1/2} / B\,(\text{Gauss}) \qquad \text{Eq. 2.1.2}$$

A schematic illustration of a plasma mass filter based on this mechanism is shown in Fig. 2.1. The ions created in the source at the left would be heated in the linear magnetic field section to increase their temperature, and some of them would drift along the axial magnetic field into the curved magnetic field section, in which they would be separated vertically (into the page), according to Eq. 2.1.2.

To illustrate this separation effect for an experiment with noble gas ions, we can assume T_i=10 eV and B=1 kG in the curved section; then the vertical drifts through a half-torus would be $\delta_\perp \sim 4.5$ cm for neon (M_i=20) and $\delta_\perp \sim 11.5$ cm for xenon (M_i=130). The electrons will drift in the opposite vertical direction, leading to a charge separation and a vertical electric field which can also affect the ion drift motion. This electric field would cause the same outward drift for all species, depending on the magnitude of the electric field inside the plasma (which can not be simply evaluated).

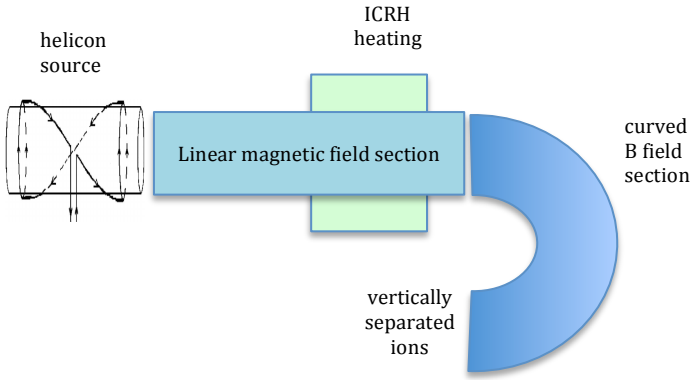

Fig. 2.2 – ion drift in curved magnetic field

Early experiments on plasma transmission through 90º magnetic field bends were done at PPPL [2] and in Russia [3] using pulsed plasma sources, which showed a reduction in heavy ion impurities after the bend as seen by ion energy analyzers. Further experiments on the ion drift motion were done at Columbia

[4] and in Japan [5] using a steady-state Q-machines, which showed a short-circuiting of the expected ExB drift due to nearby conductors and electron drift along the magnetic field. The use of a curved magnetic field for separation of ions has been reviewed in the context of plasma processing of spent nuclear fuel [6], and a related concept of ion separation in a bent magnetic mirror was proposed [7]. It might be possible to use permanent magnets to create a curved field, which would reduce the complexity and cost of a plasma mass separation device.

The main advantage of this mechanism is that the ion separation occurs passively without an externally applied electric field. A second advantage is the possibility of increased separation by increasing the T_i of the heavy species, e.g. using ion cyclotron heating. The separation might increase with ion collision frequency (at least up to the cyclotron frequency) due to increased residence time in the curved section, since the vertical drift direction is independent of the parallel ion direction, at least in the range where ions have near-collisionless gyro-orbits. A significant difficulty is the self-generated electrical field created by the separation of ions and electrons, causing outward ExB drifts of all species together, thus removing the separation effect. Another difficulty is that the source profile would have to be shaped into horizontal "slits" for the vertical curvature-induced separation to result in spatial separation at the far end. This separation mechanism is reduced at higher magnetic fields where the plasma density and throughput would be increased. Note that this separation is independent of the radius of field curvature, but does require $R>\rho_i$. The separation distance increases with the toroidal angle of the field bend, and could potentially be increased using multi-turn orbits inside a vertically elongated torus like a Helimak [8].

[1] F.F. Chen, Introduction to Plasma Physics and Controlled Fusion, 2nd Edition (1984)
[2] H.P. Eubank and T.D. Wilkerson, Phys. Fluids 6, 914 (1963)
[3] V.S. Voitsenya et al, Sov. Phys.-Tech. Phys. 9, 221 (1964)
[4] S. Ejima, T.C. Marshall and S.P. Schlessinger, Phys. Fluids 17, 163 (1974)
[5] A. Komori et al, Plasma Physics 19, 283 (1977)
[6] A.V. Timofeev, Physics-Uspekhi 57 990 (2014)
[7] R. Gueroult and N.J. Fisch, Phys. Plasmas 19, 112105 (2012)
[8] K.W. Gentle, Plasma Sci. Technol. 10, 284 (2008)

2.3. Plasma centrifuge (vacuum arc centrifuge)

The separation mechanism of a plasma centrifuge (a.k.a. vacuum arc centrifuge) is similar to a liquid or gaseous centrifuge, in that more massive particles are forced radially outward by rapid azimuthal rotation. The density profiles of two ion species of different masses was calculated using radial force balance in a two-fluid model for masses M_i with charges Z_i in a plasma rotating with azimuthal ExB velocity V_θ [1-4]:

$$n_1(r)/n_2(r) = [n_1(0)/n_2(0)] \exp [(Z_1M_2 - Z_2M_1)(V_\theta^2/2kT)] \qquad \text{Eq. 2.3.1}$$

The radial separation should be significant if the ions are rotating near $V_\theta \sim V_i \sim c_s$ (i.e. when $T_i \sim T_e$), where heavy Z=1 ions should equilibrate at significantly larger radii. A similar radial mass separation mechanism for high (M,Z) ions has been seen in rotating tokamak plasmas [5,6].

An illustration of the original experimental device of this type is shown in Fig. 2.3, taken from [1]. In this configuration the source is the solid metal target, to which is applied a pulsed electrical voltage to

create a metal vapor arc. As discussed in Sec. 1.2, isotope and elemental separation has previously been measured with such devices, although at low throughput and a relatively high energy cost per ion. It might be possible to rapidly repeat pulses in this system for higher throughput, although this has not yet been done. Thus it is not clear that this arc mechanism is suitable for high-throughput applications.

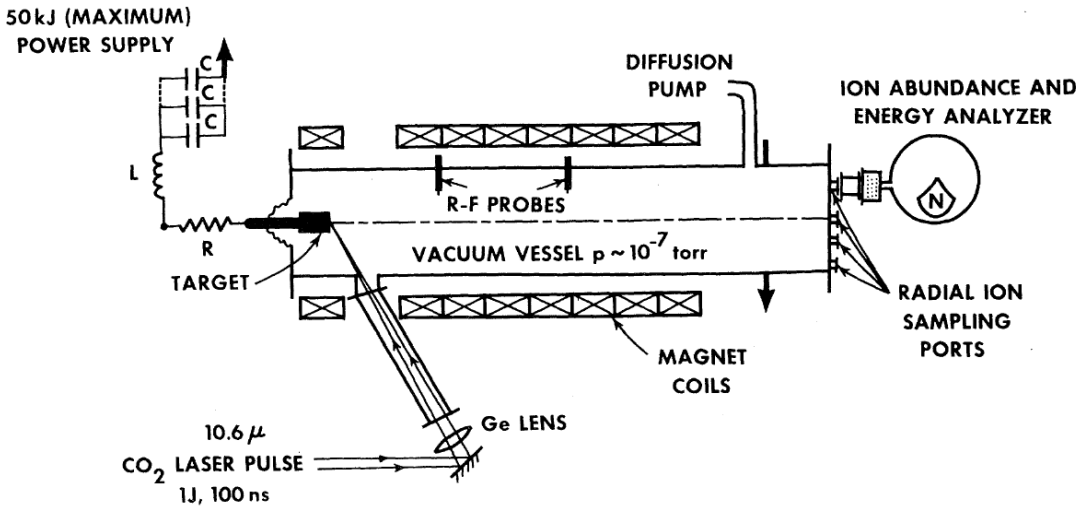

Fig. 2.3 plasma centrifuge (from [1])

The advantages of this separation mechanism are its simplicity and its operation in a fluid regime, in which the separation should be relatively insensitive to the species mix and collisionality. Two strong disadvantages of this system are the likely presence of plasma instabilities [2,4], which can cause mixing, and its requirement for a conducting solid target, which may not be the case for solid nuclear waste. If the energy cost of this method is 70 keV/atom, as estimated in [7], then the cost would also be too high to process the large volume of nuclear waste, as mentioned already in Sec. 1.2. A recent review of plasma centrifuge literature can be found in [8].

[1] M. Krishnan et al, Phys. Rev. Lett. 46, 36 (1981)
[2] R.R. Prasad and M. Krishnan, J. Appl. Phys. 61, 113 (1987)
[3] M.J. Hole and S.W. Simpson, IEEE Trans. Plasma Sci. 27, 620 (1999)
[4] T. Ikehata et al, Nucl. Instr. and Methods in Phy. Research B70, 26 (1992)
[5] R. Dux et al, Nucl. Fusion 39, 1509 (1999);
[6] H. Chen et al, Phys. Plasmas 7, 4567 (2000)
[7] R.R. Prasad and M. Krishnan, Nucl. Inst. and Meth. in Phys. Research B26, 65 (1987)
[8] D.A. Dolgolenko and Yu. A. Murimkin, Physics-Uspekhi 60, 994 (2017)

2.4 Rotating plasmas (uniform magnetic field)

The centrifugal forces due to rotation can also cause mass separation in steady-state uniformly magnetized plasmas when the rotation is created by radial electric fields imposed by annular electrodes, as illustrated schematically in Fig. 2.4. As reviewed in Ref. [1], the guiding center orbits of ions in low collisionality plasmas can produce a radial separation of mass species similar to that a plasma centrifuge, for either radial vs. axial mass separation similar to the Archimedes filter, or radial mass separation in a

"double-well" mass filter [2], depending on the shape and magnitude of the imposed radial potential. The ExB rotation velocities needed for significant separation in this regime are fairly high, i.e. $\omega_{ExB}/\omega_{ci} \geq 0.1$, where $\omega_{ExB} = V_{ExB}/a$, where a is the plasma minor radius and:

$$V_{ExB} = 10^8 \, E(V/cm)/B(Gauss) \qquad \text{Eq. 2.4.1}$$

The potential advantages of this method are its capability for allowing external control through biased electrodes, and its geometric simplicity. However, the requirement for near-collisionless plasmas will limit the plasma density and throughput, depending on the temperature (see Sec. 3.3). The fluid rotation speed in partially ionized plasma may also be limited by the "critical ionization velocity" $V_{CIV} \sim (2eI_i/M_i)$, where I_i is the ionization energy of the neutrals [3]. Other potential disadvantages are the difficulty of controlling the radial electric field with end electrodes (see Sec. 3.4), and the presence of various plasma instabilities which can cause mixing (see Sec. 3.5)

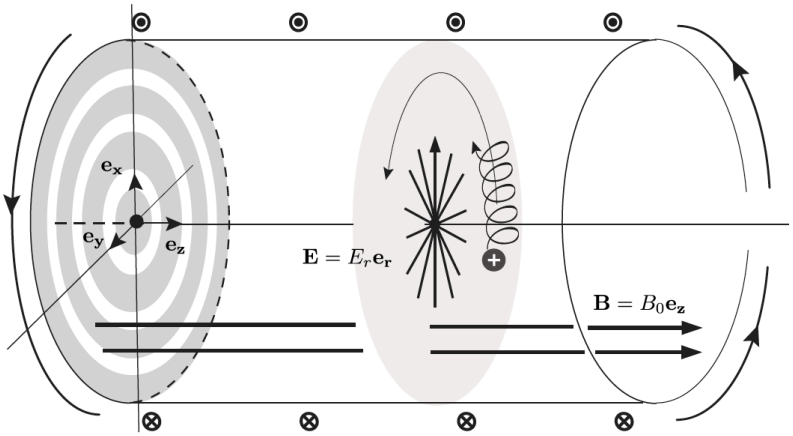

Fig. 2.4 - configuration for rotating plasma separation [1]

The Archimedes plasma operated in a regime similar to Fig. 2.4 with electrodes at both ends of a 3.9 m vessel with helicon wave heating at B = 1.6 kG [4]. The PPPL plasma mass filter experiment also operated in a similar configuration, with three electrodes at one end which were biasable up to ±100 Volts in a linear helicon-driven plasma with B ~ 1 kG [5]. Azimuthal rotation speeds were controllable to a limited extent by biasing in both devices, and some preliminary indications of radial ion mass separation were observed spectroscopically. However, further analysis of the PMFX conditions showed that the plasmas were too collisional to produce separation by a gyro-orbit mechanism, since the ion-ion collision frequency was much larger than the ion gyrofrequency [6]. Possible solutions to improve the prospects for ion mass separation were to increase the magnetic field or decrease the plasma density.

[1] R. Gueroult et al, Plasma Phys. Control. Fusion 60, 014018 (2018)
[2] J.-M. Rax and R. Gueroult, J. Plasma Phys. 82, 595820504 (2016)
[3] C. Theodorescu et al, Phys. Plasma 17, 052503 (2010)
[4] B.P. Cluggish et al, Phys. Plasmas 12, 057101 (2005)
[5] R. Gueroult et al, Plasma Sources Sci. Tech. 35, 035024 (2016)
[6] I.E. Ochs, R. Gueroult, N.J. Fisch and S.J. Zweben, Phys. Plasmas 24, 043503 (2017)

2.5 Rotating plasmas (variable magnetic fields)

Addition of a spatially varying magnetic field to the geometry of Fig. 2.4 can in principal improve the mass separation capability of near-collisionless plasmas, as illustrated in Fig. 2.5 taken from Ref. [1]. For example, a particle at radius r with negative v_{II} in part (a) of Fig. 2.5 sees a centrifugal potential barrier:

$$d\phi = m\omega^2(r^2-r_m^2)/2 \qquad \text{Eq. 2.5.1}$$

Interestingly, this potential barrier is proportional to the particle mass, so for a given parallel energy there exists a rotation velocity ω for which the light particle can reach r_m while the heavy particle can not. Assuming a two-ion species plasma in thermal equilibrium, this result can in principle be used to preferentially collect light ions on the left side, as illustrated part (b) in Fig. 2.5.

Another possible configuration adds a magnetic mirror field to the geometry, as shown in part (c) in Fig. 2.5, taken again from Ref. [1]. In configuration $r_m/r > 1$, so that a particle with zero parallel velocity is only confined if:

$$v_\perp^2 > [(r_m/r)^2 - 1]\,(B_m/B - 1)^{-1}\, r^2\omega^2 \qquad \text{Eq. 2.5.2}$$

which creates a loss cone modified by rotation in which the heavy ions are preferentially lost, as shown in part (d) of Fig. 2.5.

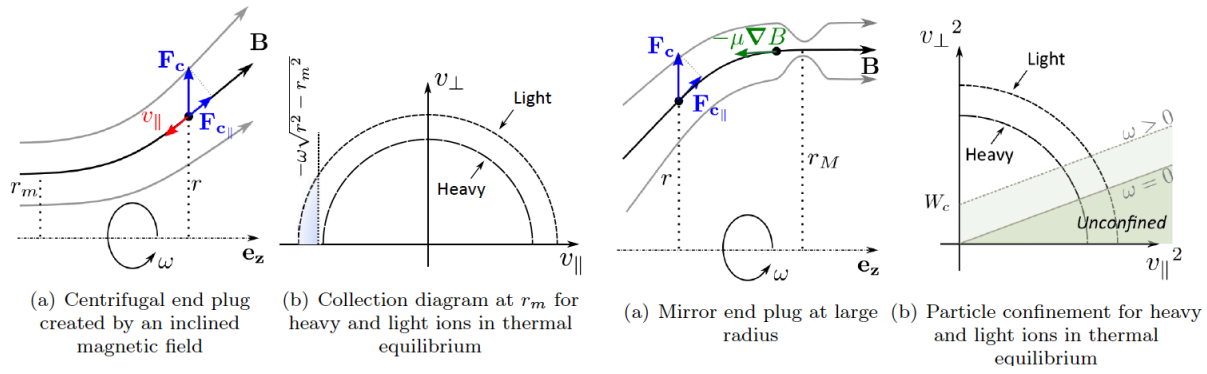

(a) Centrifugal end plug created by an inclined magnetic field

(b) Collection diagram at r_m for heavy and light ions in thermal equilibrium

(a) Mirror end plug at large radius

(b) Particle confinement for heavy and light ions in thermal equilibrium

Fig. 2.5 rotating plasmas with variable magnetic field (from [1])

These two effects, namely preferential loss of light ions at smaller radius in Fig. 2.5(a) and preferential loss of heavy ions through a magnetic mirror at large radius in Fig. 2.5(c), are the basis of the Magnetic Centrifugal Mass Filter (MCMF) [2]. In this device, collisionality has to be large enough for ion-ion pitch angle scattering to scatter ions into the small radius side loss cone, but low enough to limit perpendicular transport. The mass separation capabilities were confirmed through preliminary numerical simulations [3], and additional constraints imposed by collisionality were recently clarified [4]. However, no experimental results have yet been obtained on any of these variable magnetic field configurations.

An entirely different mechanism for mass separation was envisions using rotating magnetic fields [1,5]. Preliminary estimates suggest that rotating plasma separators might satisfy the throughput requirement

and be energetically attractive for spent fuel reprocessing applications. This novel approach could be valuable for advanced closed nuclear fuel cycles [5]. However, several challenges such as optimization, screening and extraction remain to be addressed in order to design an industrial isotope and mass separator.

[1] R. Gueroult et al, Plasma Phys. Control. Fusion (2017)
[2] A.J. Fetterman and N.J. Fisch, Phys. Plasmas 18, 094503 (2011)
[3] R. Gueroult and N.J. Fisch, Phys. Plasmas 19, 122503 (2012)
[4] I.E. Ochs, R. Gueroult, N.J. Fisch and S.J. Zweben, Phys. Plasmas 24, 043503 (2017)
[5] J.-M. Rax and R. Guerolt, J. Plasma Phys. 82, 595820504 (2016)

2.6 Azimuthal magnetic field

An alternative magnetic geometry for ion separation employs a azimuthal magnetic field and a radial electric field, as illustrated in Fig. 2.6 [1,2]. In this concept, a large steady current ~100 kA is driven in a central conductor which creates the azimuthal magnetic field, which decreases as 1/r from the central conductor. Additional electric fields are formed using ~1 kV electrodes immersed in the plasma (dotted lines in left figure), on which the magnetic field lines terminate. The electric potential is assumed have the radial dependence (ln r) and to be independent of the axial direction z. Ions are injected either radially or along the z-axis through an annular radial slit. The motion of heavy (A=238) and light (A=152) ions are calculated in this geometry, and it is claimed that that separation of spent nuclear fuel with high efficiency can be obtained without deposition of ions on the electrodes. No experimental results on this mechanism have been obtained so far. Further information can be found in a recent review [3].

[1] V.P. Smirnov et al, Plasma Physics Reports, 39, 456 (2013)
[2] A.A. Samokhin et al, Technical Physics, 2016, Vol. 61, No. 2, pp. 283–289
[3] D.A. Dolgoenko and Yu. A. Muromkin, Physics-Uspekhti 60, 994 (2017)

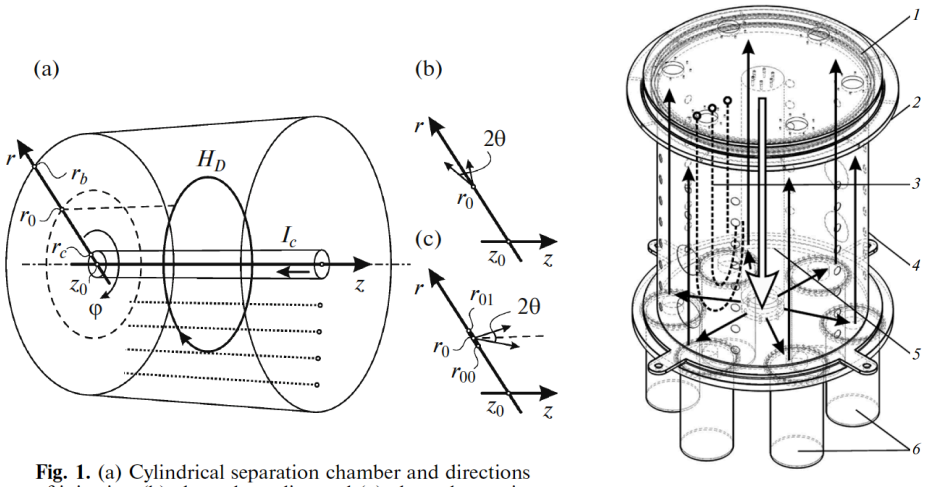

Fig. 1. (a) Cylindrical separation chamber and directions of injection (b) along the radius and (c) along the *z* axis. Dotted lines in (a) conditionally show the electrodes producing the potential in the chamber.

Fig. 13. Sketch of a coaxial system for plasma SNF separation: (*1*) insulator, (*2*) side current conductor, (*3*) electrodes, (*4*) shell, (*5*) central current conductor, and (*6*) plasma source.

Fig. 2.6 azimuthal magnetic field separation

2.7 Ion mobility in an electric field

Highly collisional plasmas are interesting for mass separation purposes since they occur at relatively high density, which could produce high throughput, and at relatively low temperature, which reduces the need for auxiliary plasma heating. At low enough electron temperature the plasma will contain molecular ions (with either a positive or negative charge), which could potentially assist in nuclear waste separation, since the heavy atom species with A≥90 will most likely dominate the total molecular mass. The radioactive charging effects of nuclear waste molecules will be negligible, since the half-life of these atoms is much longer than their residence time in the separation device.

The response of collisional ions to a DC electric field E in a plasma is defined by the mobility μ, where the ion drift speed is $v_d = \mu E$ and [1]:

$$\mu = q/(M_i \nu_i) \qquad \text{Eq. 2.7.1}$$

where q is the charge on the ion of mass M_i, and ν_i is the total ion collision frequency with all species. The corresponding flux of this ion species with a density n_i in the direction of the electric field E is:

$$\Gamma = n_i v_d = \mu\, n_i\, E = q\, n_i\, E\, /\, (M_i \nu_i) \qquad \text{Eq. 2.7.2}$$

The main difficulty in evaluating Eq. 2.7.2 is the ion collision frequency, which has a different form for ion collisions with other ions, neutrals, and electrons. For ions colliding with neutrals, the ion-neutral collision frequency is approximately independent of ion velocity in the low-temperature limit ($T_i < 3$ eV), with $\nu_{io} = K\, n_o$, where K depends on the neutral species and ion mass [1,2]. In this case, the flux of ions along the direction of the electric field will depend inversely on the ion mass, which is a fairly strong separation mechanism. For heavy ions colliding with light ions, the collision frequency also depends inversely on the heavy ion mass M_i, but also on the light ion mass $M_j^{1/2}$ [2]. In general, the mobility of heavy ions tends to be lower than light ions due to their lower thermal speed.

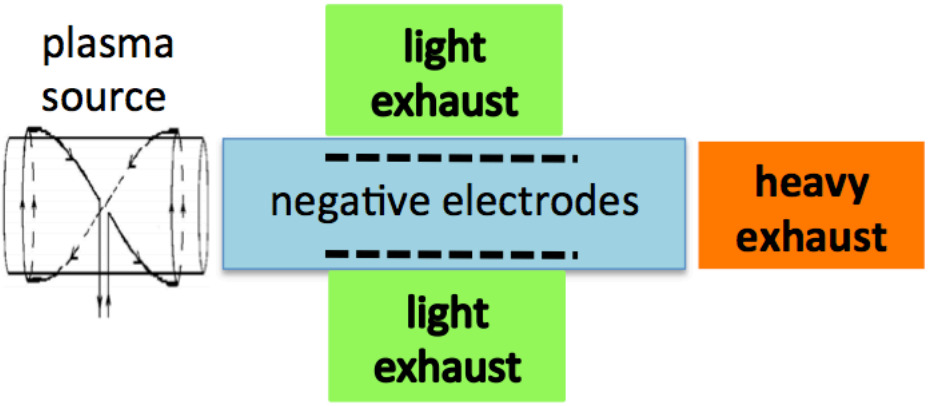

Fig. 2.7 – mass separation using ion mobility

A conceptual design for high-throughput plasma mass separation based on ion mobility is shown in Fig. 2.7. The plasma could be created by a separate source or by RF within the main (blue) chamber itself. A mesh electrode could be located just in front of the light exhaust sections (green), where presumably the lighter ions would be preferentially attracted if the electrode potential was negative. The heavier less mobile ions would be exhausted in the orange chamber at the right. Obviously there are a wide variety of electrode and exhaust geometries which could be based on this concept. Note that there is no need for a magnetic field in this device, except perhaps to guide the plasma from the source to the main chamber or from the main chamber to the exhaust chamber.

The throughput of such a device will depend (among other things) on the average ion drift speed, which depends on the ion energy gain in the electric field over a collision mean free path L_{coll}, or roughly:

$$v_d/v_i \sim (E\, L_{coll}/T_i)^{1/2} \qquad \text{Eq. 2.7.3}$$

For a helicon plasma like that in PMFX [2] with $n_i \sim 10^{13}$ cm^{-3} and $T_i \sim 1$ eV, the ion-ion collision length for a heavy ion with M_i=80 (krypton) on a background of light ions with M_j=40 (argon) is roughly $L_{coll} \sim 0.1$ cm, so an electric field of E=1 V/cm will produce a drift speed of roughly $v_d \sim 0.3 v_i$, which seems consistent with a reasonably high throughput.

Despite its conceptual simplicity, there are many potential difficulties in implementing such an electrostatic mass separation scheme, and there are apparently no such devices yet for high-throughput ion mass separation. First, the directed ion flux due to the mobility will have to compete with the random motion due to thermal ion collisional diffusion, which will set a minimum level of the electric field required for separation. Second, most of the electric field will be shielded from the plasma by a Debye sheath of $\lambda_d << 1$ mm, although the electric field of the larger pre-sheath region has been seen to cause mobility-limited ion flow [3]. Third, any electrode inside a plasma with nuclear waste could become coated with various insulating films, which would have to be removed *in situ* (e.g. by heating). Fourth, the ion lifetimes may be limited by charge exchange reactions, the cross-sections for which are largely unknown for the complex molecules in nuclear waste. Finally, the extraction efficiency in a geometry like Fig. 2.7 may be very low, thus increasing the energy cost of mass separation.

On the other hand, there already exist several sophisticated ion mobility mass spectrometry techniques (IMMS) to analyze the mass spectrum of organic compounds, based on (un-neutralized) ion drift motion in a buffer gas in static or time-dependent electric fields, as described in reviews such as [4,5]. For example, there are 50,000 handheld analytical mass spectrometers of this type being used for chemical weapons and explosives monitoring. However, these devices are designed to work with microscopic samples, and are not useful for high-throughput applications such as nuclear waste separation.

[1] M.A. Lieberman and A.J. Lichtenberg, Principles of Plasma Discharge for Materials Processing (John Wiley & Sons, 1994)
[2] I.E. Ochs, R. Gueroult, N.J. Fisch and S.J. Zweben, Phys. Plasmas 24, 043503 (2017)
[3] X. Wang and N. Hershkowitz, Phys. Plasmas 13, 053503 (2006)
[4] A.B. Kanu et al, Journal of Mass Spectroscopy 43, 1 (2008)
[5] H. Borsdorf et al, Applied Spectroscopy Reviews 46, 472 (2011)

2.8 Radial advection in rotating plasmas

Low temperature plasmas in linear magnetic field devices tend to spontaneously rotate in the azimuthal direction, even without externally applied electric fields [1-3]. This rotation is due in part to due a radial electric field $E_{rad} \sim 3T_e/a$ caused by the Debye sheath at the axial end, typically resulting a velocity $V_\theta = E_{rad}xB \leq 1$ km/sec. If there is a frictional force F_θ on this azimuthal ion rotation which depends on the ion mass, this will cause a radial drift $v_{rad} = F_\theta xB$ which might be useful for ion mass separation. For example, collisional ion simulations of one case for the PMFX device showed that the radial drift due to ion-neutral advection was much larger than the radial diffusion due to ion-neutral collisions [4]. Since this ion separation mechanism could occur spontaneously in linear plasma devices, it is worth investigating in more detail, especially since it might compete with more active separation methods.

Very little is known experimentally about the radial advection of ions in linear plasma devices, but outward flow speeds of a surprisingly large ~500 m/sec were measured for ArII ions in a helicon device using LIF [2]. It is possible that radial ion mass separation could already be occurring in linear devices, but is masked by the recycling of the usual noble gas species from the walls. The physics of perpendicular ion currents due to inertial and viscosity in partially ionized plasmas were treated theoretically in [5], but not yet well measured or understood experimentally. Radially inward pinching of high M,Z impurities is also a well-known phenomenon in tokamak plasmas [5], due to either fluctuations or orbit effects. Particle drift and separation in collisionality gradient has recently been analyzed in Ref. 7.

[1] C. Holland et al, Phys. Rev. Lett 96, 195002 (2006)
[2] E. Scime et al, Phys. Plasmas 14, 043505 (2007)
[3] S. C. Thakur et al, Phys. Plasmas 23, 082112 (2016)
[4] I.E. Ochs, R. Gueroult, N.J. Fisch and S.J. Zweben, Phys. Plasmas 24, 043503 (2017)
[5] V. Rozhansky, Phys. Plasmas 20, 101614 (2013)
[6] C. Angioni and A.G. Peeters, Phys. Rev. Lett. 96, 095003 (2006)
[7] I.E. Ochs, J.M. Rax, R. Gueroult, and N.J. Fisch, Phys. Plasmas 24, 083503 (2017)

2.9 Ionization energy

A simple concept for ion mass separation would use electron temperature control within the plasma to differentially ionize atomic or molecular species. The electron temperature can in principle be controlled by localized heating, e.g. using electron beams or ECH resonance with a magnetic field, and an applied electric field can be used to collect the ions, as in Fig. 2.7. Such differential ionization processes could also be relevant in the boundary region between plasmas and neutral gas [1] or in chemical separation of astrophysical plasmas [2].

The ionization energy of cesium is the 2nd lowest of all elements (3.9 eV) [3], and so its ionization threshold might be useful to separate the radioactive isotope Cs^{137} from other species, assuming the Cs was in atomic form. The ionization energy of most molecules are in the range of ~7-15 eV [4-6], generally somewhat higher than the ionization energy of their elements. However, since the cross-sections for ionization of atoms and molecules are slowly varying functions of electron energy, and even more slowly varying functions of the electron temperature of a plasma, it is unlikely that a sharp separation threshold for ionization can be obtained for any component in a complicated nuclear waste environment. Also, molecular ions can charge exchange and/or react quickly in plasmas to form other compounds, so control of the plasma

chemistry of the nuclear waste would be needed to some extent, and could be quite difficult.

[1] B. Bonnevier, Astrophysics and Space Science 40, 231 (1976)
[2] G.T. Marklund, Nature 277, 370 (1979)
[3] http://www.lenntech.com/periodic-chart-elements/ionization-energy.htm
[4] http://webbook.nist.gov/chemistry/ie-ser/
[5] J.H. Gross, Mass Spectroscopy, A Textbook, Springer 2011, Chapter 2
[6] A. Fridman, Plasma Chemistry, Cambridge University Press (2008)

2.10 Dusty plasma separation

Dusty plasmas are suspensions of micron-sized charged particles in a plasma environment, in which dust particles can stay levitated indefinitely since the electrical forces are larger than the gravitational forces. If there was a significant variation in the radioactive heavy atom composition of nuclear waste on the dust size scale, then plasma separation of charged dust might be very effective, since the effective density and throughput could be higher than that for atomic or molecular plasmas. Note that dusty plasma separation would be different from the usual electrostatic precipitation of dust since dusty plasma are electrostatically neutralized by electrons. While separation of dust in plasmas with respect to particle size has been shown [1–3], there is little or no research on separation of dust (or aerosols) in plasmas with respect to density or atomic number. Radioactive dusty plasmas have been discussed mainly in magnetic fusion research, since radioactive dust from the walls could be a significant safety hazard in future devices such as ITER [4,5]. However, the radioactive charging of dust will always be negligible with respect to the charging by plasma electrons or ions, even at the lowest possible plasma density.

Many aspects of the physics of dusty plasmas under tightly-controlled laboratory conditions are well understood [6], and there are several interesting technological applications [7]. However, dusty plasmas regimes of most interest for nuclear waste separation have not been studied in laboratory settings, namely: regimes of high dust velocity and mass throughput, regimes of intense plasma heating together with evaporating dust, and regimes of dust with mixed densities, sizes, shapes, electrical conductivities and chemical compositions. These regimes are more closely related to natural dusty plasmas found in astrophysical dust clouds [8], planetary or comet dust [9], or dust levitated on the surface of the Moon [10]. In general, there are many types of forces on charged dust particles in plasmas [6], each of which might be used for nuclear waste separation: the electric fields (including the electrode sheath), gravity, ion drag, thermophoresis (due to temperature gradients), neutral drag, radiation pressure, and various particle-particle interactions.

A schematic illustration of a dusty plasma mass separator is shown in Fig. 2.8. Dust could be separated based on net charge using auxiliary electrodes (blue), using either DC or AC electric fields. Another possible separation mechanism is driven by buffer gas flow (e.g. argon), which could spin the dust through collisional coupling. The centrifugal force on the rotating dust might be used to separate the dust according to density, as in a gas centrifuge. The plasma or dust particles might also be heated to provide additional non-equilibrium drive to the system, e.g. by an electron beam or lasers. No applied magnetic field is needed for these mechanisms, although magnetized dusty plasmas are an area of current research [12]. There are also many unsolved aspects of the relationship between flows and electric fields in dusty plasmas [13]. Of course, the fundamental issue in applying these mechanisms to separate nuclear waste is the unknown relationship between the dust size and/or charge to the relative concentration of radioactive materials in the dust. This would need to be understood before proceeding in this direction.

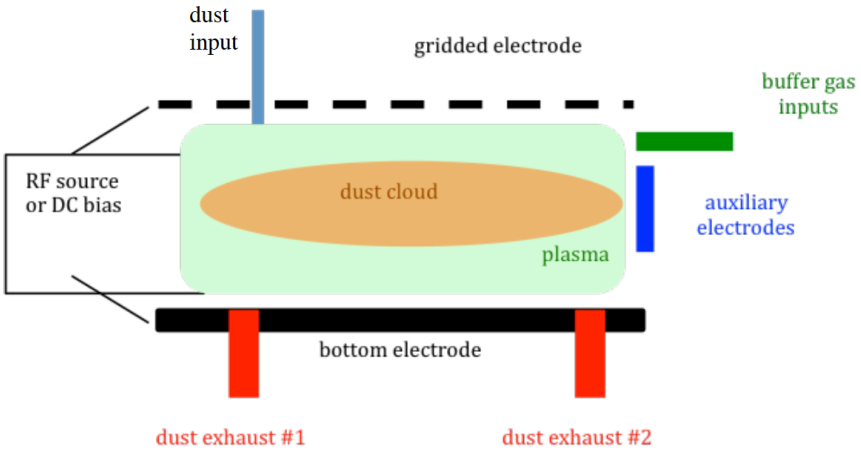

Fig. 2.8 - dusty plasma separation device

[1] C. Killer et al, Phys. Rev. Lett. 116, 115002 (2016)
[2] A. V. Zobnin et al, AIP Conference Proceedings 649, 293 (2002)
[3] E. S. Dzlieva et al, Technical Physics 57, 945 (2012)
[4] J. Winter et al, Journal of Nuclear Materials 290-293, 509 (2001).
[5] F. Le Guern et al, Fusion Engineering and Design 86, 2753 (2011).
[6] A. Melzer and J. Goree, Fundamentals of Dusty Plasmas, in Low Temperature Plasmas: Fundamentals, Technologies and Techniques (Wiley, 2007),
[7] K. R. Sutterlin et al, Phys. Rev. Lett. 102, 085003 (2009).
[8] G. E. Ciolek et al, Astrophysical Journal, Part 1 425, 142-160 (1994).
[9] P. K. Shukla and A. A. Mamun, Introduction to Dusty Plasma Physics (Taylor and Francis, 2001).
[10] J. Wang et al, IEEE Transactions on Plasma Science 36, 2459-2466 (2008).
[11] S. Jaiswal et al, Review of Scientific Instruments 86, 113503 (2015).
[12] E. Thomas et al , Physics of Plasmas 22, 113708 (2015).
[13] V. N. Tsytovich, Physics-Uspekhi 50, 409 (2007).

2.11 Radial diffusion in linear magnetic field

A conceptually simple mechanism for plasma mass separation would be a differential radial transport in a linear magnetic field geometry, as illustrated in Fig. 2.9. For example, if the collisional radial transport of ions across a magnetic field depended on the ion mass, then a mixture of ions introduced near the axis (at the left) could be separated by mass using a set of nested annular exhaust collectors (at the right). A basic limitation of this mechanism is that the source diameter needs to be much smaller than the radial range of diffusion, which may limit the throughput. A basic advantage of this scheme is that it requires no applied electric fields, and in principle operates only on collisional diffusion.

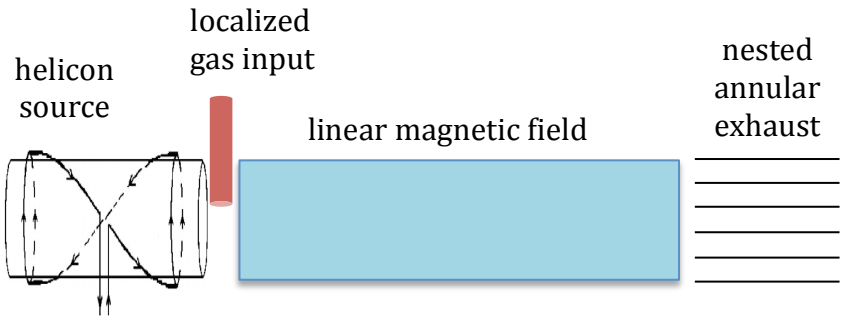

Fig. 2.9 radial ion diffusion in a linear magnetic field

From the theory in Ref. [1], in the limit where ions are magnetized $\tau_M = 1.5\ \Omega_{ci}/\nu_{ii} > 1$, where Ω_{ci} is the ion gyrofrequency and $\nu_{ii} = 2.3\text{x}10^{-7}\ n_j\ \lambda\ M_j^{1/2}\ M_i^{-1}\ T_i^{-3/2}$ is the ion-ion collision frequency, the classical collisional diffusion rate of heavy ions of M_i across the magnetic field in a (much more dense) background of lighter background ions of M_j is [1]:

$$D_{ii} \sim \tfrac{1}{2}\ \rho_i^2 \nu_{ii} \sim 1.2\text{x}10^{-3}\ n_j(\text{cm}^{-3})\ \lambda\ M_j^{1/2}\ T_i^{-1/2}\ (\text{eV})/B(\text{G})^2\ \ \text{cm}^2/\text{sec} \qquad \text{Eq. 2.11.1}$$

where n_i is the heavy ion density and λ is the Coulomb logarithm. For M_j=40, Ti=10 eV, λ=5, and B=10^3 kG, the resulting diffusion coefficient is $D_{ii} \sim 10^5$ cm^2/sec. In this case the heavy ion diffusion coefficient is independent of the heavy ion mass M_i, since its larger gyroradius is offset by its smaller ion collision frequency. However, in general the heavy ion diffusion coefficient may be different from the light ion diffusion coefficient, e.g. if the dominant collisions were with the background neutral gas. Diffusive separation in a collisional plasma is discussed in more detail in [2].

There have been some experimental measurements of "classical" collisional ion diffusion in quiescent linear plasma devices [3-6], but only in regimes where electrostatic fluctuations are small. If a simple diffusive mechanism was dominant in a geometry like Fig. 2.9, it might be possible to feed the annular exhausts into subsequent stages for extra separation. However, no clear ion separation has been obtained using this simple diffusion mechanism, as far as we know.

References:

[1] I.E. Ochs, R. Gueroult, N.J. Fisch and S.J. Zweben, Phys. Plasmas 24, 043503 (2017)
[2] I.E. Ochs, J.M. Rax, R. Gueroult, and N.J. Fisch, Phys. Plasmas 24, 083503 (2017)
[2] M. Siddiqui et al, Phys. Plasmas 22, 122103 (2015)
[3] J.P. Boeuf et al, Phys. Plasmas 19, 113509 (2012)
[4] A. Perry et al, Phys. Plasmas 9, 3171 (2002)
[5] A. Fasoli et al, Phys. Rev. Lett. 68, 2925 (1992)

2.12 Transit time separation

Atoms are routinely analyzed and separated by mass using high resolution TOFMS (time-of-flight-mass spectroscopy), where ions are created with pulsed source and detected with microchannel plates [1,2].

Spatial separation has been also obtained in distance-of-flight spectroscopy with a modified instrument and phosphor plate detection [3]. However, these devices have only a microscopic throughput due to space charge limits.

It might be possible to extend this simple principle to high throughput mass separation using a pulsed plasma source and a rotating collector plate synched with the source. For this purpose the ions should have a well defined energy, perhaps obtained using a pulsed sputtering target with ion energy control grids. If the ion energy was 10 eV, the difference in transit time for ions of A=40 and A=250 over a drift length of 10 meters would be ~3 msec, which would produce a spatial separation of ~3 cm on a collection plate moving at ~10 m/sec. This is a small spatial separation, but not much different than that used in the original calutron devices (Sec. 2.1).

A schematic illustration of this scheme is shown in Fig. 2.10. In a device of this type, the ions could be guided along the drift tube by an axial magnetic field, but the collisionality must be low enough to avoid significant scattering. The ions need to be accelerated to a near-constant energy, with electrostatic grids at either or both ends. Fixed radial slits at the far end would allow spatial dispersion on the rotating collector plate. An advantage of this geometry is that a rotating collector plate could be mechanically segmented and the collected material could be readily segregated when the plate is removed. Difficulties include the need for a near-monoenergetic low energy ion beam, the inefficiency due to the slit transmission and pulsed duty cycle, and the mechanics of rapid rotary motion in a vacuum system.

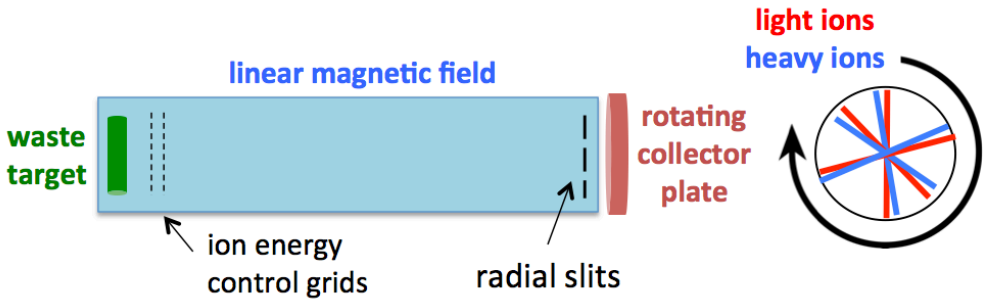

Fig. 2.10 - transit time plasma mass separation

[1] R.E. Steiner et al, J. Anal. At. Spectrom. 14, 1537 (1999)
[2] E. de Hoffmann and V. Stroobant, Mass Spectrometry, Principles and Applications (Wiley, 2012)
[3] A. Gundlach-Graham et al, J. Anal. At. Spectrom. 28, 1385 (2013)

2.13 Collisionality gradient

In the presence of a collision gradient perpendicular to a magnetic field, gyrating ions drift to regions of higher collisionality [1]. Consider, for example, regimes for super-thermal ions such that the dominant collisional term is a drag term resulting from slowing down on lighter buffer ions. In the presence of a collisionality gradient, this drag force will be greater on the more collisional part of the orbit, as illustrated in Fig. 2.10, which shows collisionality increasing in the y direction. Now because ions tend to

lose energy on the high collision side of their orbit, then there will be a net force in the x direction. Thus, preliminary considerations give a drift in the y direction,

$$\mathbf{v}_D = \frac{1}{2}\frac{v_\perp^2}{\Omega^2 + \nu_s^2}\nabla\nu \approx \frac{1}{2}\rho^2\nabla\nu, \qquad \text{Eq. 2.13.1}$$

Since ions that are not magnetized will not drift, they will be separated. Importantly, the drift is independent of the atomic mass, since $\nu \sim m^{-1}$. In order to maintain the drift, the ions can be heated by waves. The heating, though unbiased with respect to drift, can be resonant, and therefore sensitive to mass, thereby sustaining the drift only in the resonant ions. Thus, separation occurs because either only the magnetized or heated ions acquire the drift. For reasonable numbers, the effect can be large. Consider heavy (200 amu) ions in a typical laboratory plasma, with a density of 10^{12} cm^{-3}, a temperature on the order of 1 eV, and in a 10^3 Gauss magnetic field. Then we will have $\rho \sim 5$ cm and $\nu \sim 10^2$ Hz. Assuming the gradient in the collisionality occurs on a scale length of ~10 cm, we then have $v_d \sim 1$ m/s, which is more than ample for fast separation.

[1] I.E. Ochs, J.M. Rax, R. Gueroult, and N.J. Fisch, Phys. Plasmas 24, 083503 (2017)

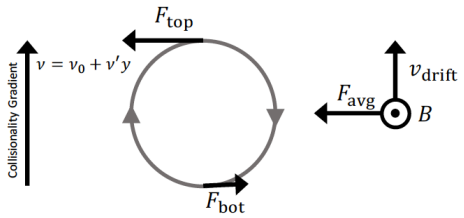

Figure 2.11 Drift in collisionality gradient

3. Generic physics issues

This section describes some generic physics issues which need to be considered in designing a plasma-based nuclear waste separation device. Some generic technology issues are discussed in Sec. 4.

3.1 Charge state and radiated power

In order to efficiently separate ions using the mechanisms of Sec. 2, it is highly desirable to maintain a single ion charge state of $<Z>=1$, since the separation usually operates on the charge/mass ratio. It is also desirable to limit the power radiated from the plasma, since this energy loss must be balanced by plasma heating. The average ion charge and radiated power per atom generally increase with the atomic number, electron temperature and electron density. However, these dependences vary significantly with each atom, so detailed calculations are needed for each species.

For example, the calculated average ion charge state and radiated power for sodium (Z=11) and gold (Z=79) vs. electron temperature is shown in Fig. 3.1 for three assumed electron densities, based on an IAEA atomic physics database [1]. Sodium is the most common metallic element in the Hanford nuclear waste (see Sec. 1.3), and gold is the highest Z in this database. Similar databases can be found elsewhere [2,3], but all are based on simplified atomic physics models (e.g. assuming equilibrium), and not on direct experimental measurements.

Based on Fig. 3.1, the desirable average charge state of Z=1 for sodium and gold occurs at $T_e \sim$ 1-2 eV, independent of electron density in the range $n_e = 10^{12}$-10^{14} cm^{-3}. Above this temperature the average charge state increases to Z=2 at $T_e \sim 5$ eV, at which point most ion separation mechanisms will be compromised due to the change in the charge/mass ratio. Thus the requirement of Z=1 most likely constrains the device operation to $T_e \sim$ 1-2 eV, even without considering the radiated power. Note that since there are many species and (most likely) a spatially varying electron temperature within the device, there will be a spread in the ionization state distribution in every operating condition (see Sec. 3.1.2).

The calculated radiated power for a 100% sodium plasma at $n_e = 10^{13}$ cm^{-3} reaches a minimum of $P_{rad} \sim 10^{-10}$ erg/atom-sec at T_e=2 eV [1]. This corresponds to a relatively small $P_{rad} \sim 100$ Watts/m^3, i.e. less than the RF heating power in typical helicon experiments. The calculated radiated power at this density increases to $P_{rad} \sim 10$ kW/m^3 at T_e=5 eV, which should still be acceptable. However, the calculated radiation power for gold at $n_e = 10^{13}$ cm^{-3} peaks at $P_{rad} \sim 5 \times 10^{-4}$ erg/atom-sec at T_e=2 eV, which is $\sim 5 \times 10^6$ times higher than for sodium at this temperature. Thus the calculated radiated power for a plasma with only 1% gold at $n_e = 10^{13}$ cm^{-3} and T_e=2 eV is about $P_{rad} \sim 5$ MW/m^3, which is very high in terms of plasma heating and wall cooling technology. Qualitatively similar constraints on tungsten exist for a tokamak fusion reactor.

Obviously the charge state distribution and radiated power should be calculated specifically for each plasma mass filter device, depending on the species mix and plasma density and temperature profiles. For example, at T_e=2 eV and $n_e = 10^{13}$ cm^{-3} the average charge of aluminum (another common metal in the Hanford waste) is near Z=2 instead of Z=1, and the radiated power is ~100x larger than for sodium, i.e. $P_{rad} \sim 10^{-8}$ erg/atom-sec [1]. The atomic physics calculations become much more complicated for high atomic mass atoms; for example, for tungsten (Z=74) in ITER tokamak edge plasmas [5]. There the average charge state at $n_e = 10^{14}$ cm^{-3} was found to be $<Z> \sim 1$ at T_e = 1 eV and $<Z> \sim 2$ at T_e = 2 eV, and the radiated power was ~ 1-2×10^{26} W cm^3, or ~1-2 MW/m^3 for a tungsten density of 10^{-2} n_e.

It would be useful to know the total energy radiated per ion in order to estimate the energy costs for plasma mass separation. A lower limit to this cost is the atomic ionization energy, which comes from the energy in the electron distribution function. This varies from ~4 eV for cesium to ~14 eV for nitrogen and oxygen [4], or roughly ~3-25 MJ/kg assuming M_i=100 [6]. However, the total radiated power depends on both the radiation rate and the confinement time of the ion in the system. For example, if an aluminum ion radiated at $P_{rad} \sim 10^{-8}$ erg/atom-sec at T_e=2 eV and $n_e = 10^{13}$ cm^{-3} and was confined for 1 msec, the total radiated power would be ~6 eV/ion, which is about the same as its ionization energy. Since the ion confinement time is highly variable depending on the specific separation mechanism, the radiation energy cost can not be calculated per atom without further information about history of the atoms in the system.

For more realistic modeling of the radiation energy loss, the assumptions of a thermal electron distribution function and an equilibrium ion charge state need to be re-evaluated, especially for an RF heated linear device with a small ion confinement time. There are many possible charge exchange processes which also need to be included in the ion modeling, the cross-sections for which generally not well known (see Sec. 3.3). Thus a quantitative model for the atomic physics and radiation in a plasma separation device will be extremely complicated and is not likely to provide predictive capabilities, especially since the nuclear waste composition will is variable and not well characterized.

[1] IAEA Atomic Molecular Data https://www-amdis.iaea.org/FLYCHK/
[2] D.E. Post and R.V. Jensen, ATOMIC DATA AND NUCLEAR DATA TABLES 20, 397-439 (1977)
[3] Atomic Data and Analysis Structure (ADAS) http://open.adas.ac.uk/
[4] http://www.lenntech.com/periodic-chart-elements/ionization-energy.htm
[5] J. Abdallah Jr et al, J. Phys. B: At. Mol. Opt. Phys. 44, 075701 (2011)
[6] R. Gueroult, J.-M. Rax, S.J. Zweben, and N.J. Fisch, accepted by PPCF (2017)

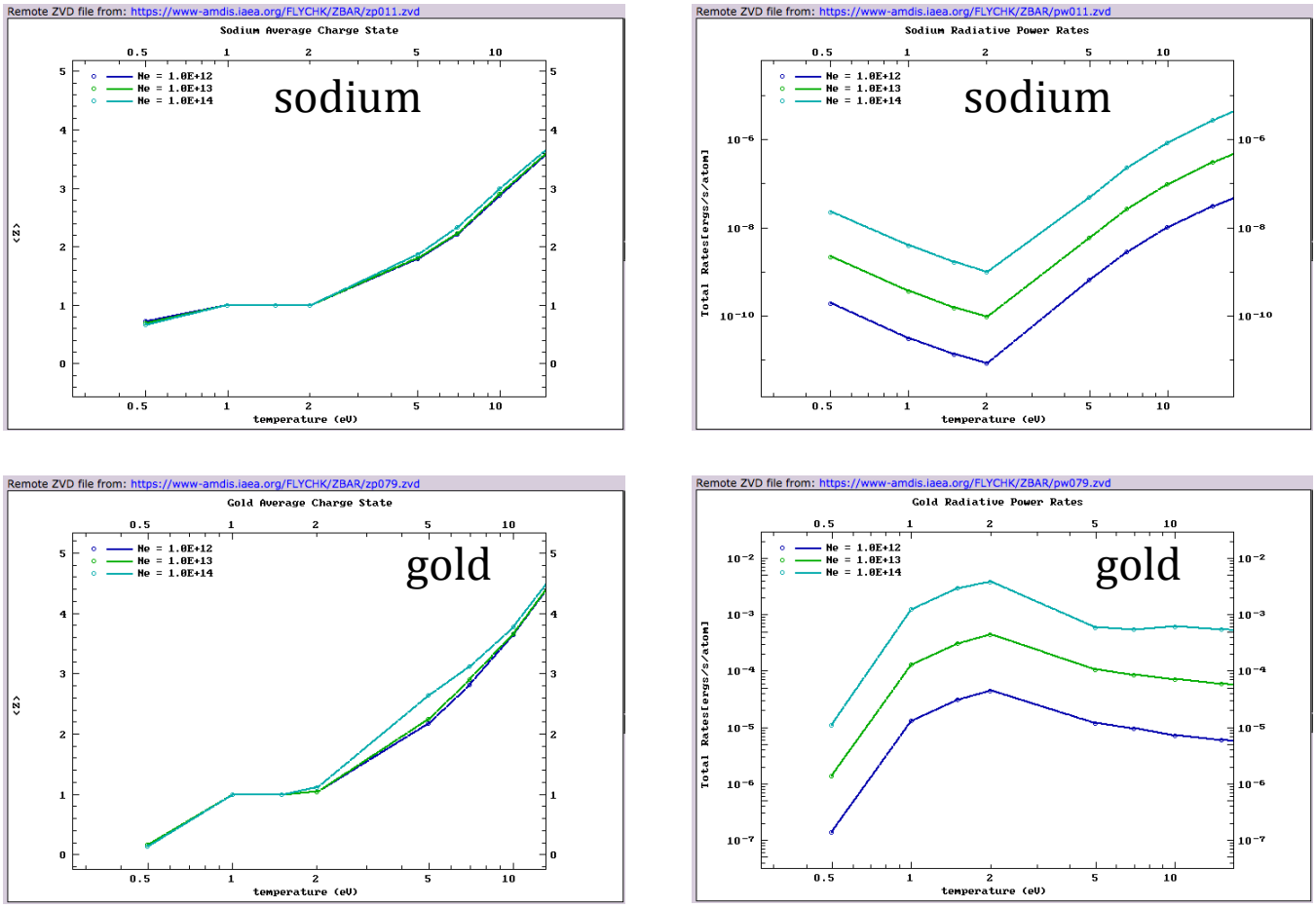

Fig. 3.1 - charge state (left) and radiated power (right) in erg/atom-sec for sodium (top) and gold (bottom) vs. electron temperature for three electron densities Ne (cm^{-3})

3.2 Molecular ions and plasma chemistry

The previous section assumed that all species were in atomic form. However, much of the nuclear waste consists of metallic oxides, nitrides, water, and many other molecular compounds (see Sec. 1.3). Thus at low electron temperatures there will probably be significant molecular ion components in nuclear waste plasmas in addition to simple atomic ion species. The subject of molecular ionization and dissociation is treated extensively in the literature of mass spectroscopy [1,2], where it is desirable to ionize molecules without breaking them apart, and in plasma chemistry and plasma processing, where molecular reactions and plasma-surface interactions are dominant [3,4].

The main molecular ion issues in plasma mass separation of nuclear waste are to determine the expected charge, effective mass, and concentration of molecules at the electron temperatures of interest. Although most of the mechanisms of Sec. 2 will work for molecular ions as well at atomic ions, the presence of molecules with a variable charge/mass ratio for each heavy species will make it more difficult to separate low mass atoms from high mass atoms in a plasma. In general, the behavior of even simple molecules in plasmas is extremely complicated, involving many distinct processes such as electron impact ionization and dissociation, recombination, electron attachment and detachment for negative ions,

metastable states, charge exchange reactions, and vibrational and rotational excitations. For example, in [4] there is a table of 33 selected second order reaction rate constants for oxygen discharges, including O, O_2, O_3, O^+,O^-, O_2^+, O_2^- and O_3 components and their metastable states, with cross-sections which vary greatly with electron energy over the range ~0.1-10 eV.

The ionization energy of many molecules is tabulated in the NIST Chemistry WebBook [5]. Essentially no molecules have an ionization energy below that of a cesium atom (3.9 eV) or above that of a helium atom (24.6 eV), and so the range of molecular ionization energy largely overlaps that of single atom species. For example, the ionization energy of an Na atom is 5.1 eV and an NaCl molecule is 8.9 eV, and a U atom is 6.2 eV and a UCl_4 molecule is 9.2 eV. Thus the average ionization state of the molecules in a plasma device should be roughly similar to that of the constituent atoms, so if the plasma is optimized to have $<Z>=1$ for atoms at T_e=1-2 eV, the ionization state of the molecules in this plasma should be similar. An exception to this is negative ion states, which will behave completely differently than singly-charged positive ion atoms or molecules in a plasma separation device.

Obviously the molecular mass can be significantly larger than the mass of its heaviest atom, e.g. NO_3 (mass 62) is a common molecules in the Hanford tank waste [6]. However, a coarse plasma mass filtration process with a cutoff at ~90 amu at Z=1 should still be able to separate the heavy radioactive metals such as Sr^{90}, Cs^{137}, U^{235} and Pu^{239} (or their oxides) from almost all non-radioactive molecules, with a few exceptions, e.g. Na_2CO_3 (mass 106).

The concentration of molecular ions in a nuclear waste plasma is difficult to estimate from first principles, but will depends on the ionization source technique (see Sec. 4.1) and the rate of molecular dissociation, given the plasma electron temperature and density within the separation volume. The energy required for breaking molecular bonds is typically in the range ~1-10 eV, e.g. 1.5 eV for an O-O bond and 8 eV for NaCl [7]. Thus it is likely that many of the molecules created in an ion source will remain in their original molecular state inside the plasma separation device, as in analytical mass spectrometers [1,2]. There has been some mass spectroscopy of nuclear waste [8-10], but not enough to guide estimates of the molecular concentration in a plasma mass separation device.

In general, molecular dissociation is a complex process which depends on the excitation states of the bound electrons and the electron energy distribution [12]. Most likely this issue will need to be studied with a dedicated plasma chemistry model and simulation code such as used for plasma processing [11] and/or plasma chemistry [3]. If there are molecules in a nuclear waste plasma, there could also be chemical reactions as well. The plasma chemistry of nuclear waste seems to be an unexplored field.

[1] J.H. Gross, Mass Spectroscopy, A Textbook, Springer 2011
[2] E. de Hoffmann and V. Stroobant, Mass Spectrometry, Principles and Applications (Wiley, 2012)
[3] A. Fridman, Plasma Chemistry, Cambridge University Press (2008)
[4] M.A. Lieberman and A.J. Lichtenberg, Principles of Plasma Discharge for Materials Processing (John Wiley & Sons, 1994)
[5] http://webbook.nist.gov/chemistry/ie-ser/
[6] https://energy.gov/sites/prod/files/EIS-0391-FEIS-Volume2_AppD-G-2012.pdf
[7] http://lamp.tu-graz.ac.at/~hadley/ss1/crystalbinding/bonds/bonds.php
[8] M.L. Alexander et al, Applied Surface Science 127-129, 255 (1991)
[9] J.A. Campbell et al, J. Radioanalytical Nuclear Chemistry 250, 247 (2001)
[10] I.W. Croudace et al, J. Anal. At. Spectrom. 32, 494 (2017)
[11] M.J. Kushner, J. Appl. Phys. 63, 2532 (1988)

3.3 Charge exchange and recombination

The ion separation mechanisms discussed in Sec. 2 will be compromised if the ions inside the plasma turn into neutrals before they can be separated. When an ion exchanges an electron with a neutral atom or molecule, the process is known as charge exchange (or a charge transfer reaction). When an ion and an electron combine to form a neutral atom or molecule, it is known as recombination.

The distance an ion will travel before a charge exchange reaction will be:

$$L_{cx} = 1/(n_o \sigma_{cx}) \qquad \text{Eq. 3.3.1}$$

where n_o is the neutral atom density for any species of interest and σ_{cx} is the charge exchange cross-section for that specific ion-neutral pair, which depends on their relative velocity and electronic states. In general, there can be both resonant charge exchange reactions between atoms and ions of the same species, and non-resonant charges exchange reactions between ions and atoms of different species.

In the context of plasma mass separation, the charge exchange processes of interest are mainly those between heavy ions and light neutral atoms (or molecules), and *vice versa.* For example, if a heavy ion is being separated axially using an electric field (Sec. 2.7), its transport and extraction will be inhibited when L_{cx} is less than the system size. Charge exchange between a heavy ion and a heavy neutral atom will also be important if the separation mechanism depends on the ion energy, which can be changed by this reaction.

The cross-sections for resonant charge exchange of noble gas ions were measured to increase monotonically with decreasing energy up to $\sigma_{cx} \sim 3\text{x}10^{-15}$ cm^{-3} at T_i=4 eV for He, Ne, and Ar [1]. Several measurements and modeling of argon resonant charge-transfer cross-sections also showed $\sigma_{cx} \sim 3\text{-}4\text{x}10^{-15}$ cm^{-3} over the range T_i=1-10 eV [2], as illustrated in Fig. 3.2. For a cross-section of $\sigma_{cx} \sim 3\text{x}10^{-15}$ cm^{-3} and neutral density of 10^{14} cm^{-3} (see Sec. 3.5), the resulting charge exchange distance is roughly $L_{cx} \sim 3$ cm, which is smaller than a typical plasma size, and so charge exchange is important in the discharge modeling.

The resonant charge exchange cross-sections for other monatomic gases in the range $v_i \sim 10^5\text{-}10^7$ cm/sec are have been approximated analytically, as illustrated in Fig. 3.2 [3]. These cross-sections generally increase with decreasing ionization potential and decreasing particle velocity; for example, the calculated cesium resonant cross-section at T_i=4 eV is a large $\sim 3\text{x}10^{-14}$ cm^2, and the measured value is apparently even higher [3]. This implies a very small charge exchange distance of $L_{cx} \sim 0.3$ cm at a neutral cesium density of 10^{14} cm^{-3}, which could make this a dominant process in the motion of cesium ions in a cesium plasma. Many other charge transfer cross-sections can be found in the IAEA Aladdin database [4], and some in the Atomic Data and Nuclear Data Tables (ADNDT) [5], and the Plasma Data Exchange Project (PDEP) [6]. For example, the charge transfer cross-section between Na^+ and O^- ions is $\sigma_{cx} \sim 30\text{x}10^{-15}$ cm^2 at a relative velocity of $4\text{x}10^5$ cm/sec [7], which would again be a dominant process.

Recombination is a three-body process in which an ion transforms into a neutral in the presence of an electron and a third particle. For example, the electron-ion recombination rate coefficient for $e + N_2^+ = N + N$ for room temperature ions with T_e = 1 eV is $k=3\text{x}10^{-8}$ cm^3/sec [8]; thus N_2^+ has a lifetime of only ~3 μsec at $n_e=10^{13}$ cm^{-3}, so this could be an important process in a nuclear waste plasma. Obviously, the detailed analysis of charge exchange and recombination in a nuclear waste plasma would require an extensive data mining for cross-sections and detailed computational simulation. Even so, since many cross-sections are apparently unavailable, the resulting code would very likely have limited predictive value.

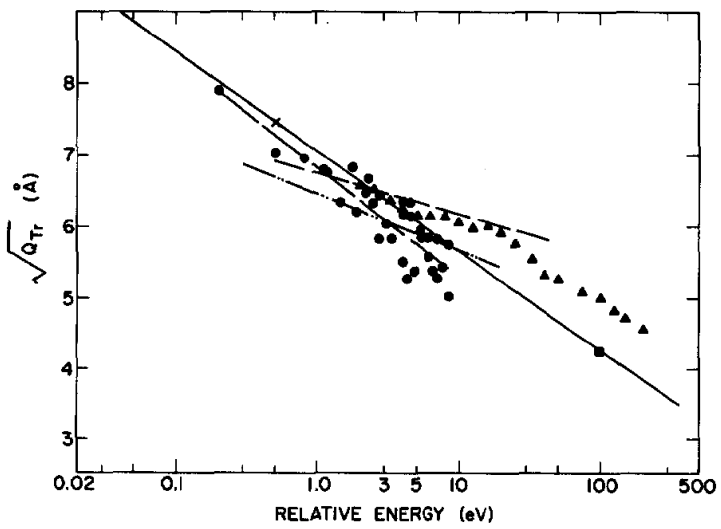

FIG. 1. Charge-transfer cross sections Ar^+–Ar vs relative energy. ×, Ref. 13; ▲, Ref. 14; ●, – –, Ref. 15; –•••–, ■, Ref. 16; - - -, Ref. 17; —, semiempirical, this work.

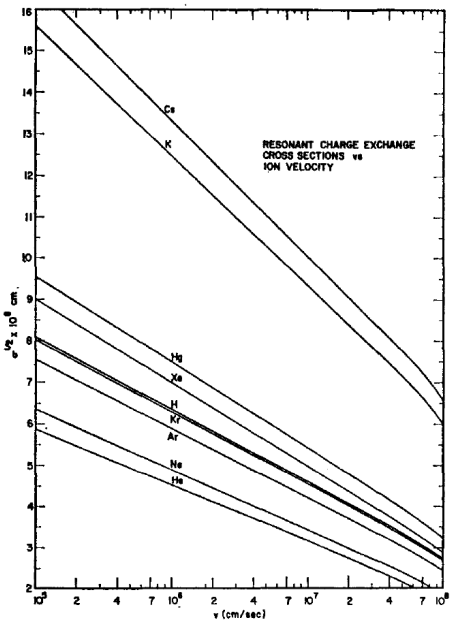

FIG. 2. Calculated cross sections for resonant charge exchange between monatomic ions and their parent gases. Interpolation can be made for other gases in terms of their ionization potential (listed in Table I).

Fig. 3.2 charge exchange cross-sections from [2] (left) and [3] (right)

[1] M.A. Lieberman and A.J. Lichtenberg, Principles of Plasma Discharge for Materials Processing (John Wiley & Sons, 1994)
[2] R.S. Devoto, Phys. Fluids 16, 616 (1973)
[3] D. Rapp and W.E. Francis, J. Chem. Phys. 37, 2631 (1962)
[4] https://www-amdis.iaea.org/ALADDIN/collision.html
[5] http://www.sciencedirect.com/science/journal/0092640X?sdc=1
[6] https://fr.lxcat.net/data/set_type.ph
[7] D.A. Hayton and B. Peart, J. Phys. B: At. Mol. Opt. Phys. 28 L279 (1995)
[8] A. Fridman, Plasma Chemistry, Cambridge Univ. Press 2008

3.4 Neutral gas transport

A major issue in plasma-based ion mass separation is the presence of neutral atoms, which will be not be separated by the mechanisms of Sec. 2, and which will tend to spatially mix the neutral species in the plasma. In fact, the neutral density was often larger than the plasma density in the plasma separation experiments of Table 1.2, and in the similar noble gas experiments in Table 1.3. Thus the separation efficiency of a plasma mass filter may be significantly reduced by the presence of neutrals, compared with idealized calculations assuming a fully ionized plasma.

A significant constraint in plasma separation is the need to avoid doubly ionized species, since the charge/mass ratio normally determines the separation mechanism. This limits the electron temperature to T_e ~1-2 eV for most atoms (see Sec. 3.1), so the neutral fraction at a given temperature will tend to be higher for species with a larger ionization potential, and higher for regions of the plasma below the peak electron temperature. Thus the charge state distribution will need to be carefully evaluated for specific plasmas to

minimize the neutral density, e.g. using an equilibrium distribution like the Saha equation, or more realistic non-equilibrium models.

For example, the calculated equilibrium charge state distributions for a low ionization potential cesium @ 3.9 eV and a high ionization potential argon @ 15.8 eV are shown in Fig. 3.3 at various electron temperature, taken from the same IAEA database as for Fig. 3.1 [1]. At T_e = 1 eV the dominant charge state for argon is "0" (i.e. neutral) while for cesium it is "1", while at T_e = 2 eV the dominant charge state for argon is "1" (i.e. neutral) while for cesium it is "2". Thus it is difficult to maintain a charge of +1 for both species at the same electron temperature, and even more difficult given the spatial variations of temperature and density within the plasma.

The transport rate of neutrals through a plasma mass separation device will depend on the neutral speed, the neutral collisionality, and the neutral pumping process. If the neutrals were at room temperature their transport through the system would be relatively slow compared with the ions, and their mixing effect may be relatively small. However, it is likely that ion-neutral collisions and charge exchange will heat the neutrals to near the ion temperature, in which case the local flux of neutral atoms would be larger than the ion flux. The quantitative effect on separation will then depend on the collection or exhaust mechanism for ions vs. neutrals. If the ions were collected in a way that excluded neutrals, e.g. using ion deposition onto a charged plate, then the neutrals might be recycled back into the main separation chamber without diluting the separation. However, if the ions were first neutralized and then exhausted, e.g. by a vacuum pump, then the background neutrals could seriously reduce the separation efficiency. The result will also depend on the mechanisms by which ions and neutrals interact with surfaces, which itself quite complicated.

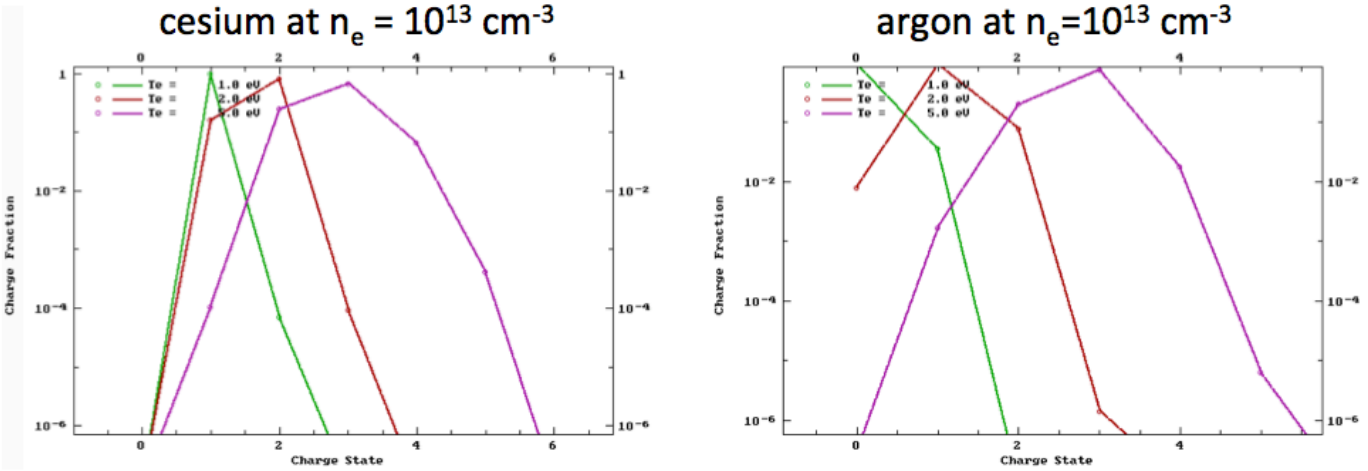

Fig. 3.3 calculated charge state distributions for Cs (left) and Ar (right) vs. T_e [1]

A simple model for neutral transport in a plasma mass filter loosely based on the PMFX experiment at PPPL is illustrated in Fig. 3.4. In this model a 50/50 mixture of argon and krypton is input into the left box, and the goal is to increase this ratio in the box at the right using a mass-dependent leak rate through the aperture between the boxes. The results are found to depend on the assumed ion/neutral fraction, neutral speed, the relative ion and neutral leak rates through the aperture, and the relative pumping speed for both species. It is hard to obtain good separation in this model when the ion/neutral ratio in the left box is ≤0.3 due to the streaming of neutral gas through the aperture.

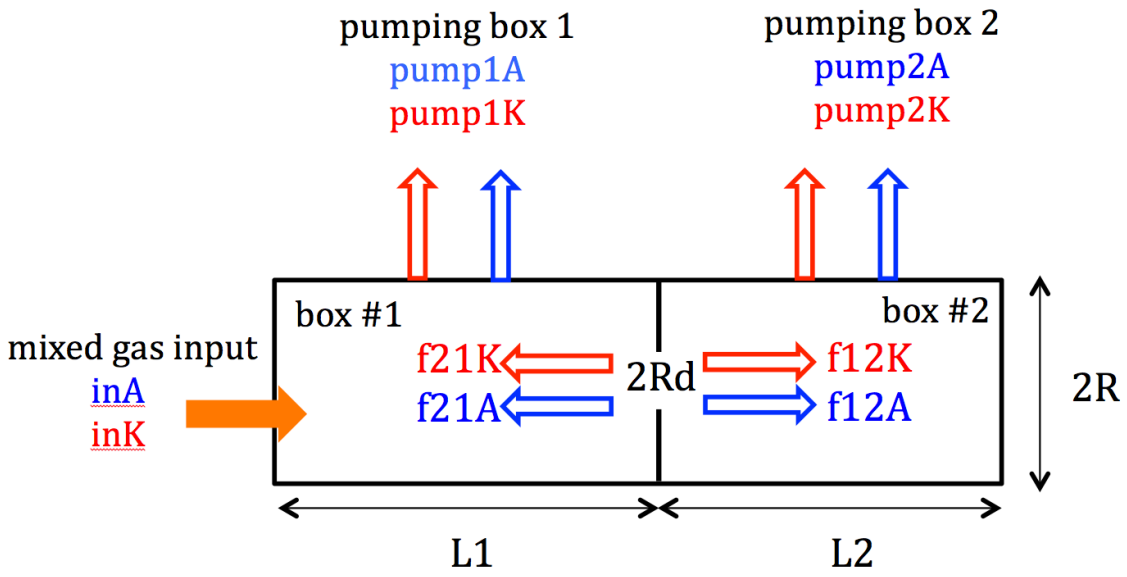

Fig. 3.4 simple model of neutral transport in a mass filter device (see Appendix I)

Another approach to modeling the neutral gas behavior in a plasma mass filter is to use a multi-fluid model in the computational fluid dynamics code CFX within the ANYSYS Workbench [2], as illustrated in Fig. 3.5. In this model an equal mix of argon and krypton enters the left box at the bottom, and no *ad hoc* mass-dependent leak rate between boxes or plasma effects are included. In most regions the mixture remains near 50/50 (green), but the results do indicate a weak separation effect with two neutral gases, with molar flow rate of krypton is 1.3% higher at Outlet 1 and 1.8% lower at Outlet 2. This may be explained by the fact that heavier krypton molecules tend to deviate less from a straight pass than lighter argon molecules, so krypton molecules dominate path to the Outlet 1, which is straighter than path to Outlet 2. The mixing rate is very low for such rarified gas, resulting in the areas where krypton is completely displaced by argon. When mixing rate is increased such areas disappear. Although this model is capable of including ions as a separate species, but is mainly useful to evaluate the potentially complex neutral flows in a realistic geometry.

Up to this point it was tacitly assumed that the majority of the plasma would be composed of the nuclear waste species. However, few if any real plasmas have been made with such a complicated and variable composition, and most experiments on processing plasmas are done in an inert gas background, e.g. using argon. Thus it is possible (or even likely) that in a practical device the dominant species being an inert "buffer gas" like argon, with a relatively small fraction of nuclear waste species. In this case the argon neutrals could be the dominant species in the system, but one which does not need to be separated. The argon will be chemically non-reactive, recycle from the chamber walls, and can be pumped out of the system and returned to the main chamber for steady-state plasma operation. The presence of a buffer gas will reduce the throughput of nuclear waste for a given set of plasma parameters, but should reduce the time-dependent plasma changes due to a highly variable waste composition.

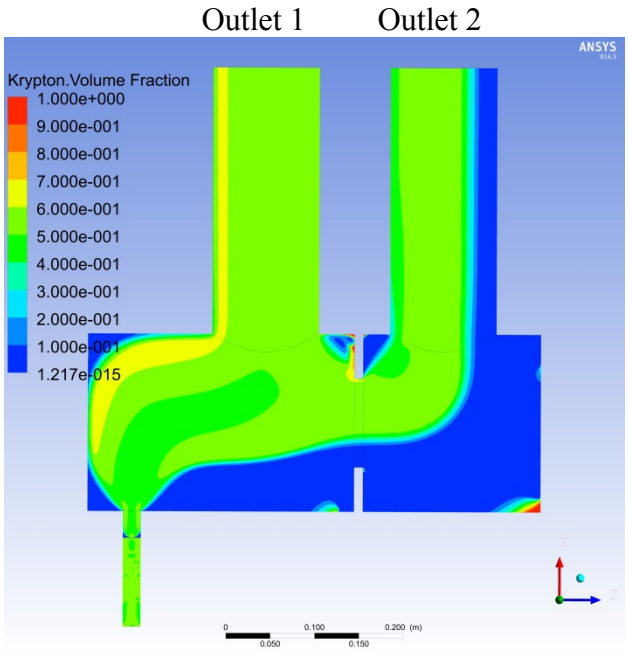

Fig. 3.5 krypton volume fractions in a CFX model of argon/krypton separation (see Appendix II)

[1] IAEA Atomic Molecular Data https://www-amdis.iaea.org/FLYCHK/
[2] ANSYS CFX http://www.ansys.com/products/fluids/ansys-cfx/ansys-cfx-features

3.5 Droplets, dust and nanoparticles

It is likely that most attempts to convert the solid/liquid forms of nuclear waste into an atomic or molecular plasma will be incomplete, resulting in macroscopic droplets (~100 μm), dust (~1 μm), and/or nanoparticles (~10 nm) in the plasma. For example, liquid droplets or macro-particles are normally evaporated from metallic cathodes in vacuum arc plasmas (see Sec. 4.1.6), and dust injection is one way to fuel the plasma with nuclear waste (see Sec. 4.1.8). The effects of these large particles on a separation device will depend on their species composition, charge/mass ratio, number density within the plasma, and their flow speed.

Typical surface charges on a large droplet ≥10 μm will be negligible with respect to their mass, with charge/atom ratios of roughly $<10^{-8}$, as shown in Table 3.2. These droplets will act essentially as neutral particles and will not be separated in a plasma mass separation device, as notesd in vacuum arc devices [1]. Smaller macro-particles of ≤10 μm in pulsed vacuum arcs can be deflected by electric and magnetic fields [2], but are not helpful for nuclear waste separation unless they already have mass-separated composition.

size of particle	average charge/atom
droplet (≥ 10 μm)	$< 10^{-8}$
dust (~1 μm)	$< 10^{-6}$
nanoparticle (~10 nm)	$\sim 10^{-3}$ (?)
molecular (~0.1-1 nm)	≤ 0.5
atomic (≤ 0.1 nm)	~ 1-2

Table 3.2 estimated charge/atom ratio for possible components of a nuclear waste plasma

Typical charges on micron-sized dust in steady-state low temperature laboratory "dusty plasmas" are $\sim 10^3$-10^4 electrons, with typical dust particle densities $\sim 10^4$ cm^{-3} and dust flow velocities ≤ 10 cm/sec [3-5]. Thus the average charge per atom is $< 10^4$ e^- / $6x10^{10}$ atoms/particle (e.g. for 1 μm aluminum dust), i.e. $< 10^{-6}$ e^-/atom, as shown in see Table 3.2. Thus even though charged dust in plasmas does respond to electric and magnetic fields, the mechanisms of Sec. 2 which are designed to separate singly charged atoms will not work for such dust particles. For dust particles to have a negligible mass density compared with the plasma, their number density needs to be $<10^2$ cm^{-3}, which is considerably lower than the dust density in a typical dusty plasma experiment. The expected dust evaporation rate needed to fuel a nuclear waste plasma is discussed in Sec. 4.1.6.

Smaller nanoparticles or "clusters" of ~1-10 nm in size with $\sim 10^5$-10^8 atoms are sometimes formed in low temperature processing plasmas [6], and have also been studied in the context of femtosecond laser-plasma interactions [7,8]. It is not clear whether or how such clusters would be formed in a complicated nuclear waste plasma, or if so, whether their composition would segregate high mass from low mass atoms. However, since their charge/atom ratio would still be much less than for singly-charged atoms or molecules, they would not be separated in the same way as the atoms or molecules.

The conclusion from this section is that the plasma source and plasma heating systems in a nuclear mass separation device need to be carefully designed to avoid particles larger than molecules, unless the separation mechanism specifically takes these larger particles into account (e.g. Sec. 2.10). This will probably require diagnostics of the particle size distribution in these plasmas, e.g. using lasers [9].

[1] V.L. Paperny et al, PSST 24, 105009 (2015)
[2] I.I. Beilis et al, J. Ap. Phys. 85, 1358 (1999)
[3] S. Jaiswal et al, Phys. Plasmas 86, 113503 (2015)
[4] E. Thomas et al, Phys. Plasmas 6, 4111 (1999)
[5] R.L. Merlino et al, Phys. Plasmas 5, 1607 (1998)
[6] A. Fridman, Plasma Chemistry, Cambridge Univ. Press (2008) Secs. 8.8-8.9 and references therein
[7] T. Ditmire et al, Phys. Rev. A 53, 3379 (1996)
[8] A.S. Boldarev et al, Laser and Particle Beams 35, 397 (2015)
[9] S. Yatom et al, Carbon 117, 154 (2017)

3.6 Collisional effects

The transport and separation of ions through a plasma mass filter system will be strongly modified by Coulomb collisions with other ions, electrons, and neutrals. These collisions will generally impede the flow of ions through the system, but the differences in collision rate between ions may also play a role in the separation process. For simplicity, in this section we consider collisional effects only for singly charged atoms, but similar collisional effects will occur for multiply charged atoms, molecules, and neutrals.

A detailed theoretical analysis of collisional effects in axial-collection plasma mass filters has been published recently [1], focusing mainly on cylindrical linear magnetic devices like the PMFX at PPPL [2]. This model includes ion-ion and ion-neutral collisions and ion gyroradius motion, and calculates radial and parallel transport timescales for low mass (M_j=40) vs. high mass (M_i=80) ions due to collisional diffusion and advection. The ion-ion collision frequency ν_{ii} for 90º scattering of minority ions M_i on majority ions M_j at a common ion temperature T_i is (see Sec. 2.11 for definitions):

$$\nu_{ii} = 2.3x10^{-7}\, n_j\, \lambda\, M_j^{1/2}\, M_i^{-1}\, T_i^{-3/2} \qquad \text{Eq. 3.6.1}$$

which can be used to determine the parallel ion diffusion rate $D_{||}$ for heavy ions:

$$D_{||} = (3/2)v_i^2/\nu_{ii} \qquad \text{Eq. 3.6.2}$$

and so the collisional confinement time of an ion parallel to (or without) a magnetic field is:

$$\tau_{||D} = (L_{||}/2)^2/D_{||} = L_{||}^2\, \nu_{ii}/6v_i = 4.0x10^{-20}\, n_j\, \lambda\, L_{||}^2\, M_i^{1/2}\, T_i^{-5/2} \qquad \text{Eq. 3.6.3}$$

For example, for the plasma parameters of PMFX* shown at the left of Table 3.3, the parallel heavy ion confinement time is $\tau_{||D}$ = 32 msec, while for PMFX-U at a 3x higher T_i it is $\tau_{||D}$ = 2 msec, and for the low density in PMFX-LD it goes down to $\tau_{||D}$ = 1 msec (as shown at the right in Table 3.3). Thus the heavy ions are highly collisional in all these cases, since the confinement time for a collisionless ion would be only $\tau_{||} \sim (L_{||}/2)/v_i \sim$ 0.1-0.2 msec.

These results were also summarized in the form of dimensionless parameters which need to be greater than 1 to insure that collisions do not destroy effective mass filtering, as shown at the bottom right of Table 3.3 for three different versions of a PMFX-like device. The $\tau_M = 1.5\Omega_i/\nu_{ii}$ parameter describes the average number of gyroradii completed before an ion-ion collision, which must be larger than 1 for normal gyro-orbit motion and drifts to occur, as needed for the mechanisms of Sec. 2.1, 2.2, 2.8 and several other mechanisms. The PMFX experiment in its slightly modified form PMFX* did not satisfy this criterion due to the relatively low ion temperature, which made the ion-ion collision rate large, and the low magnetic field which made the gyro-frequency relatively small. The proposed upgrade devices PMFX-U and PMFX-LD were designed to reduce the ion collisionality using a 15x higher magnetic field and 30x lower ion density, respectively.

	PMFX*	PMFX-U	PMFX-LD
n_j (cm^{-3})	10^{13}	10^{13}	3×10^{11}
n_n (cm^{-3})	10^{14}	10^{14}	10^{13}
B (G)	950	15 000	2500
E (V/cm)	2	5	5
μ_i (a.m.u.)	80	80	80
μ_j (a.m.u.)	40	40	40
T_i (eV)	1	3	1
T_e (eV)	5	5	5
$L_\parallel$ (cm)	40	40	40
$L_\perp$ (cm)	8	12	12

	PMFX*	PMFX-U	PMFX-LD
v_{thi} (cm/s)	1.1×10^5	1.9×10^5	1.1×10^5
t_{pD} (s)	3.2×10^{-2}	2.1×10^{-3}	9.7×10^{-4}
ρ_i (cm)	0.94	0.10	0.36
$v_{E\times B}$ (cm/s)	2.1×10^5	3.3×10^4	2.0×10^5
Ω_i (s^{-1})	1.1×10^5	1.8×10^6	3.0×10^5
ν_{ii} (s^{-1})	1.5×10^6	2.8×10^5	4.4×10^4
ν_{in} (s^{-1})	2.9×10^4	2.9×10^4	2.9×10^4
τ_M	0.12	9.6	10
τ_c	4.0×10^{-2}	12	13
τ_n	4.0×10^{-2}	8.1	4.8
τ_B	1.5×10^{-2}	8.3	3.0

Table 3.3 Assumed parameters (left) and collisional effects (right) for axial collection mass filters [1]

Continuing the discussion of Table 3.3, the dimensionless parameter τ_C is the ratio of the ion confinement time for ion-ion collisional diffusion across the magnetic field to the ion confinement time for parallel ion-ion diffusion along the magnetic field. For ions which satisfy $\tau_M > 1$, this ratio is $\tau_C = (L_\perp/L_{II})^2 \tau_M$, where $L_\perp$ is the length perpendicular to the magnetic field and L_{II} is the parallel length scale. This ratio was also less than 1 for PMFX*, indicating that ions would exit the system radially before being collected axially, which would prevent the desired axial ion separation. The upgrades PMFX-U and PMFX-LD increased this parameter by increasing τ_M, as described above.

The dimensionless parameter τ_N is the ratio of the ion confinement time for ion-neutral transport across the magnetic field to the parallel ion confinement time. Assuming a dominant advective radial transport due to ExB sheath-driven flows in a stationary neutral background (see Sec. 2.8), this parameter can be approximated as $\tau_N/\tau_C = (5.6/\alpha_R^{1/2})\ (\nu_{ii}/\nu_{in})\ (T_i/T_e)$, where α_R is the relative polarizability of the neutral atom. Thus even if the ion-neutral collision frequency was a factor of x5-10 lower than the ion-ion collision frequency, the relatively low (T_i/T_e) in PMFX* would have caused enough ion-neutral collisional loss to prevent the desired axial ion separation. The final dimensionless parameter τ_B in Table 3.3 refers to Bohm diffusion loss, and is discussed further in Sec. 3.8.

The conclusion from this section is that ion-ion and ion-neutral collisions are very important for nuclear waste separation in plasmas of this type. The basic cross-sections for most simple atomic collisions are available in textbooks [3,4] or databases [5]. Other collisional processes may also need to be considered, such as inelastic (energy absorbing) collisions of molecules, and particle-particle collisions for dust and clusters. It should also be noted that these plasmas may not have Maxwellian electron or ion distribution functions, especially in the presence of strong RF heating, and so collisional effects may need to be calculated using a kinetic model.

[1] I.E. Ochs et al, Phys. Plasmas 24, 043503 (2017)
[2] R. Gueroult et al, Plasma Sources Sci. Technol. 25, 035024 (2016)
[3] M.A. Lieberman and A.J. Lichtenberg, Principles of Plasma Discharge for Materials Processing (John Wiley & Sons, 1994)
[4] A. Fridman, Plasma Chemistry, Cambridge Univ. Press (2008)
[5] https://www-amdis.iaea.org/databases.php

3.7 Electric fields and rotation

Many of the ion mass separation mechanisms of Sec. 2 involve the imposition of DC electric fields to the plasma, either to differentially transport ions (Sec. 2.7, 2.9, 2.10), or to control plasma rotation through ExB drifts (Sec. 2.3-2.6 and 2.8). Surprisingly, the degree to which an electric field penetrates along or across a magnetic field is difficult to calculate theoretcially, and so understanding and controlling electric fields and rotation in these plasmas is a major issue in plasma mass separation. For example, the effects of electrodes on the radial potential profiles in linear RF devices such as PMFX [1], CSDX [2], and HelCat [3] was not well understood, although the plasma ExB rotation in these devices and in plasma centrifuges [4,5] is apparently consistent with the measured potential profiles.

The main reason for this difficulty is the complicated physics of cross-field electrical conductivity in magnetized plasmas, which depends on the ion-ion and ion-neutral friction (including charge exchange), which determines the perpendicular ion viscosity [6]. The difficulty is further increased by the complexities of sheath physics, even in an un-magnetized plasma [7,8], and by the cross-field conductivity and/or plasma flows which could be created by turbulence, as discussed in Sec. 3.8. Since the electrostatic potential distribution is determined by both the radial and parallel currents, the electric fields will depend on the full 3d geometry of the device, making experimental validation of theoretical models difficult [9]. Any small conducting path can "short out" the attempt to imposed a desired electric field.

Thus the self-consistent electric fields within a plasma mass separation device can not be calculated from first principles without knowing the plasma density and temperature profiles, the neutral density profile, and the plasma instabilities, thus coupling together many of the physics issues of this section. A similar complex situation exists in fusion plasmas, especially in the edge region where neutrals and radial electric fields can also be important [10]. Sophisticated computational codes such as BOUT++ [11] and XGC1 [12] are being developed to handle such problems.

[1] R. Gueroult et al, Plasma Sources Sci. Technol. 25, 035024 (2016)
[2] S.C. Thakur et al, Phys. Plasmas 20, 012304 (2013)
[3] M. Gilmore et al, J. Plasma Phys. (2015) 81, 345810104
[4] R.R. Prasad and M. Krishnan, J. Appl. Phys. 61, 113 (1987)
[5] M.J. Hole and S.W. Simpson, Phys. Plasmas 4, 3493 (1997)
[6] V. Rozhansky, Phys. Plasmas 20, 101614 (2013)
[7] N. Hershkowitz, Phys. Plasmas 12, 055502 (2005)
[8] X. Wang and N. Hershkowitz, Phys. Plasmas 13, 053503 (2006)
[9] M. U. Siddiqui et al, Phys. Plasmas 23, 057101 (2016)
[10] R.R. Weynants and G. Van Oost, Plasma phys. Control. Fusion 35, B177 (1993)
[11] P. Vaezi et al, Phys. Plasmas 24, 042306 (2017)
[12] R.M. Churchill et al, Plasma Phys. Control. Fusion 59, 105014 (2017)

3.8 Plasma fluctuations and mixing

The desired mass separation for most of the mechanisms of Sec. 2 can be compromised by spatial mixing associated with plasma fluctuations, which were not incorporated into any of those models. In general, the longer an ion is confined within the plasma volume, the more likely it will be that plasma

fluctuations will affect its spatial separation. The physics of plasma fluctuations is notoriously nonlinear and sensitive to the details of plasma parameters, plasma flows, electric fields, and boundary conditions.

Plasma fluctuations have been seen in many previous experiments on ion mass separation, including the arc plasmas used in uranium isotope separation, which motivated the Bohm diffusion coefficient [1]:

$$D_B \sim 6x10^6\ T_e\ (eV) / B\ (G)\ \ cm^2/sec \qquad \text{Eq. 3.8.1}$$

Even though there is no clear physical basis for this formula, it is still used as a benchmark to estimate turbulent transport in plasmas, e.g. in the dimensionless parameter τ_B in Table. 3.3 [2]. This ratio was estimated to be $\tau_B << 1$ in PMFX*, suggesting (but not demonstrating) that Bohm diffusion could dominate the ion transport in such a device, which would be bad for ion separation.

Although plasma fluctuations were observed in all plasma arc centrifuges [3,4] and in the PMFX experiment [5], there has not been a direct measurement of their effect on ion diffusion or spatial mixing in these separation experiments. However, it is clear that linear helicon devices like PMFX, CSDX, HelCat and HELIX can become very unstable and turbulent at $B \geq 1$ kG [5-8], as illustrated Fig. 3.6, with potential fluctuations of $e\phi/Te \geq 1$ [7] which can extend over much of the radial profile. If these fluctuations created an azimuthal electric field $E \sim e\phi/T_e \sim 5$ Volts over a radius of ~5 cm at B=1 kG, the resulting radial ExB drift is $V_r \sim 10^5$ cm/sec, which is comparable to the heavy ion speed at $T_i \sim 1$ eV. Such a large convective ExB flow would cause significant radial mixing of ions over a timescale of $\tau_{turb} \sim a/V_r \sim 50$ μsec, which is significantly lower than the estimated Bohm diffusion time of $\tau_B \sim 1$ msec for this system. A state-of-the-art plasma simulation code recently showed fluctuation-induced transport much greater than Bohm level [10], so Bohm diffusion is not an upper limit.

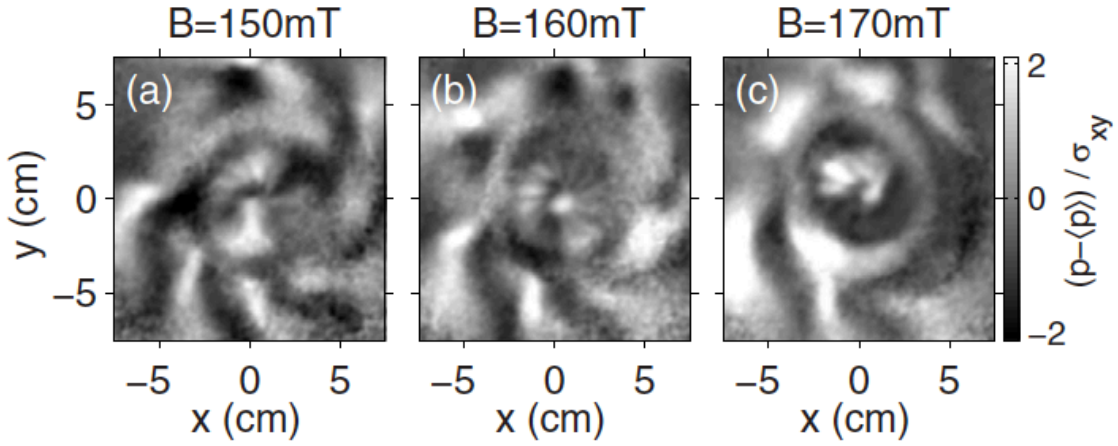

Fig. 3.6 high-speed photograph of instabilities in the CSDX linear device at B=1.5 kG [7]

Plasma instabilities are generically categorized as either electrostatic drift wave [11] or magnetic (MHD) instabilities [12]. The former are commonly seen in linear current-free plasma devices [5-9], while the latter are often seen in high-current arc plasmas [3,4]. Electrostatic instabilities tend to move all ion species together at the ExB drift speed, independent of their charge/mass ratio, so these would not directly affect ion mass separation; however, in MHD instabilities the ions move along the perturbed magnetic fields

at their thermal speed, which does depend on the ion mass. The ion transport rate for these instabilities depends on many factors such as the frequency spectrum, the size scale spectrum, and the fluctuation levels, none of which can easily be predicted. Other types of plasma instabilities might occur at the ion gyro-frequency or bounce frequency in mirror devices, and wave-induced ion transport due to RF electric fields in the plasma might also be significant. The stabilizing/destabilizing role of rotation in magnetized plasma experiments, in particular for separation is discussed in a recent paper [13].

Given the potentially large ion transport rates associated with plasma fluctuations, it is surprising that there seems to be little or no literature on fluctuation effects in plasma processing or plasma chemistry, despite the fact that turbulent transport of ions within these systems may be important. It is not clear whether the effects of fluctuations on ion transport in these systems are negligible, or whether their effects on mixing are so ubiquitous that they are not studied in detail.

[1] D. Bohm, *The characteristics of electrical discharges in magnetic fields*, A. Guthrie and R. K. Wakerling (eds.), New York: McGraw-Hill (1949)
[2] I.E. Ochs et al, Phys. Plasmas 24, 043503 (2017)
[3] R.R. Prasad and M. Krishnan, J. Appl. Phys. 61, 113 (1987)
[4] M.J. Hole et al, Phys. Rev. E 65, 046409 (2002)
[5] R. Gueroult et al, Plasma Sources Sci. Technol. 25, 035024 (2016)
[6] S.C. Thakur et al, Plasma Sources Sci. Technol. 23, 044006 (2014)
[7] S.C. Thakur et al, Phys. Plasmas 23, 082112 (2016)
[8] M. Gilmore et al, J. Plasma Phys. (2015) 81, 345810104
[9] E.E. Scime et al, J. Plasma Phys. (2015) 81, 345810103
[10] E. Shi, Ph.D. Thesis Princeton University (2017)
[11] W. Horton, Rev. Modern Phys. 71, 735 (1999)
[12] E. Faogarone and T. Passot (Ed.), Turbulence and Magnetic Fields in Astrophysics, Springer (2003)
[13] R. Gueroult, J.M. Rax, N.J. Fisch, Phys. Plasmas, 2017, 24, 082102

3.9 Plasma power loss

The loss of plasma energy to the chamber walls will affect the efficiency of nuclear waste separation, as did the radiation loss discussed in Sec. 3.1. This resulting heat loading on the walls can also become an engineering issue if the wall temperature becomes too high locally.

The plasma power loss rate can be written as the total energy in each particle species divided by the confinement time for that species:

$$P_{loss} = W_i/\tau_i + W_n/\tau_n + W_e/\tau_e \qquad \text{Eq. 3.9.1}$$

For plasma systems in which the B field lines intersect the walls (or for B-field-free systems), the plasma power loss will most likely be dominated by the electrons, since their speed is much higher than the ions or neutrals. Neglecting sheath effects (for the moment), the electron confinement time will be: $\tau_e \sim (L_{||}/2)/v_e$ and the power loss per unit area on the wall will be: $P_{loss}/\text{Area} \sim n_e v_e$. Assuming $n_e = 10^{13}$ cm^{-3} and $T_e \sim 5$ eV (as in Table 3.3), the electron heating loss to the wall will be ~150 W/cm^2, which is moderately high but not excessive. This might be reduced by the electrostatic sheath drop associated with an insulated wall, but at the expense of an increase in ion heat flux. Although this heat load may require active cooling external to the vessel wall, this level of heat loss does not seem to be a major issue in engineering a plasma mass

separation device. However, if internal electrodes are incorporated in the design, they would be much more difficult to cool and the danger of leaks may be an engineering show-stopper (see Sec. 4.4).

3.10 Ion throughput and separation efficiency

The goal of a plasma device for nuclear waste remediation is to produce a usefully high throughput of ions which are separated according to their mass. The throughput is generally measured by the total mass flowing through the plasma system (in atoms/sec or grams/sec), assuming that the plasma processes can produce the desired separation of heavy radioactive ions and light non-radioactive ions. As discussed in Sec. 1, the desired throughput is ~100 g/sec, which at ~3×10^6 kg/year could separate a significant fraction of the Hanford waste over ~30 years with 24/7 operation.

The maximum possible (collisionless) ion throughput for a plasma with exhaust area A (cm^2) is:

$$\Gamma \text{ (atoms/sec)} \sim \tfrac{1}{2} n_i v_i A \qquad \text{Eq. 3.10.1}$$

For an assumed T_i=10 eV and an average ion mass M=40, the maximum ion flux at an optimistically high density of $n_i \sim 10^{14}$ cm^{-3} is roughly $\Gamma \sim n_i v_i \sim 2.5 \times 10^{19}$ ions/(cm^2 sec). Assuming an exhaust area of ~10^4 cm^2, this is equivalent to a mass throughput of ~ 10-20 g/sec, which is not far from the desired throughput. Of course, this assumes that the plasma separation physics, the ion source generation, and the waste exhaust process are all operating at this throughput level (Secs. 4.1 and 4.2 for the latter two engineering issues).

More realistic collisional calculations of the ion throughput for a specific MCMF (magnetic centrifugal mass filter) configuration have been made using analytic estimates and a Monte Carlo ion orbit simulation model for an argon/krypton mixture [1]. For almost all cases the plasma is highly collisional (see Sec. 3.6), so the parallel ion transport is diffusive, and the theoretical maximum throughput does *not* increase with density as in Eq. 3.7, since the ion mean free path will also decrease linearly with increasing density. However, the maximum ion throughput does increase as $T_i^{5/2}$ due to the increases in ion velocity and decrease in ion collisionality with T_i. Simulation results for throughput vs. a simplified maximum throughput for a PMFX-U type device in an axial collection model are illustrated in Fig. 3.7. The highest throughputs of $\Gamma \geq 0.1$ gr/sec are associated with high ion temperatures Ti ≥10 eV, given this particular ion species mix, separation efficiency, and plasma geometry. Actual throughputs in existing separation devices are in the range of mg/sec, as previously shown in Table 1.3.

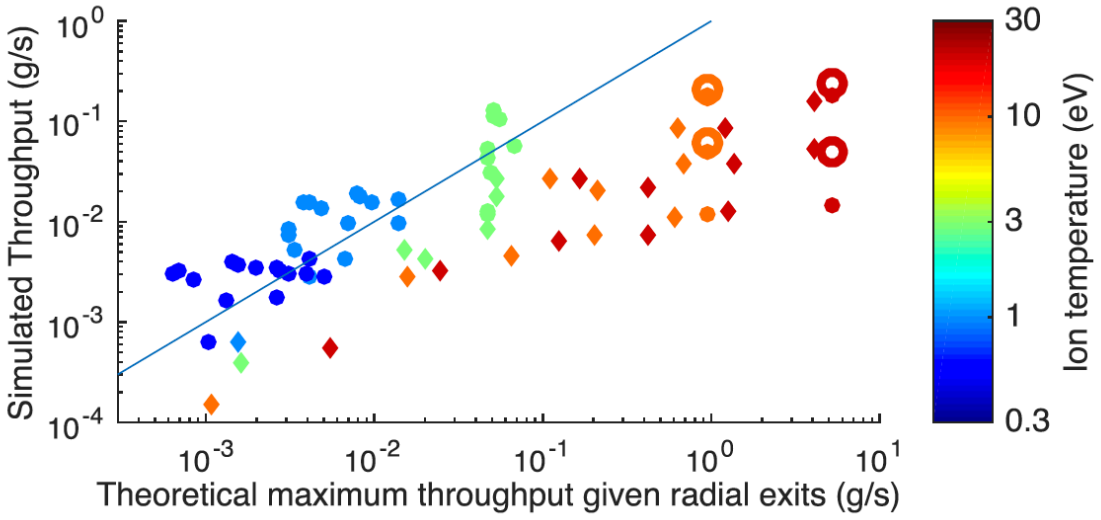

Fig. 3.7 simulated throughput for an MCMF [2]

For this throughput to be useful, the plasma mass filter must of course provide the necessary mass "separation factor", analogous to the "enrichment factor" in isotope separation devices. For nuclear waste remediation, the separation factor is defined as the ratio of the heavy element fraction at the heavy element exhaust to the heavy element fraction in the light element exhaust. For the MCMF simulation results of Fig. 3.7 this factor is in the range ~1-2 for high throughput cases with argon/krypton separation, which is similar to previous MCMF estimates of ~2.3 for separating aluminum from strontium [2]. The required separation factor depends on the ultimate disposition of the wastes; for example, on the desired composition of the glass logs used for vitrification [3].

[1] I.E. Ochs et al, Phys. Plasmas 24, 043503 (2017)
[2] R. Gueroult et al, Phys. Plasmas 19, 122503 (2012)
[3] D. Kramer, "Cleanup of Cold War nuclear waste drags on", Physics Today 70, 28 (2017)

4. Generic technology issues

The main technological issues in plasma mass separation are driven by the large volume of nuclear waste to be processed by this method, estimated as ~10^8 kg (out of a total inventory of ~4×10^8 kg) at Hanford (see Sec. 1.3). Allowing a processing time of 30 years (24/7), this would require a continuous throughput of about ~100 g/sec. A recent estimate of the energy cost for plasma separation gave an upper bound of ~2 GJ/kg [1], so for an optimistic estimate of 1 GJ/kg (400 eV/atom at M=40), this corresponds to ~100 MW CW power. Thus plasma separation of the Hanford nuclear waste would be a huge enterprise, comparable in size-scale and cost to the largest plasma systems, e.g. ITER. This section describes some of the generic technology issues which need to be resolved to achieve a successful plasma nuclear waste separation system. The engineering of specific systems is beyond the scope of this report.

[1] R. Gueroult et al, Plasma Physics Control. Fusion 60, 014018 (2018)

4.1 Plasma sources

Most of the plasma mass separation mechanisms discussed in Sec. 2 require that the nuclear waste be broken down into singly ionized elements or molecules before the separation process begins, since neutral particles will not be separated (see Sec. 3.4). This is already accomplished in laboratory mass spectrometers for a wide range of atoms and molecules, but only at microscopic throughput levels using charged ion clouds (<1 μg/sec) [1,2]. This section describes the technologies which might be used to produce ionized atoms and molecules at a throughput level of up to ~100 g/sec, suitable for the nuclear waste application.

A general issue for nuclear waste handling is the wide variety of physical and chemical waste forms, i.e. liquids, saltcakes (the consistency of beach sand), sludges (the consistency of peanut butter), and solids [1,2]. Some of the liquid waste such water and organic compounds is volatile, and so could fairly easily be transferred to the plasma source chamber in gaseous form. However, most of the waste volume is non-volatile and would have to be fed into the plasma source in solid or powder form.

In general, the plasma ionization source should probably operate at ~10^{-6} bar, since the ionization fraction is increasingly smaller at higher pressures, and since the plasma source needs to be closely coupled with the main separation chamber at a similar pressure. Thus another generic issue for the plasma source is how to load nuclear waste material at atmospheric pressure into the source vacuum system. Presumably this would be done in batch mode, with perhaps 100 kg being loaded (and removed) at each vacuum opening. Possible vaporization and ionization processes are discussed in the following sub-sections, and the mechanical waste handling issues will be discussed further in Sec. 4.2. A schematic illustration of the ion source is shown in Fig. 4.1, and a list of the sources is in Table 4.1.

There is a large literature on the physics and technology of ion beam sources [3]. However, most of this work is oriented toward high energy ions (≥1 keV), which are not useful for nuclear mass separation due to their relatively low throughput and the high energy cost per ion. For example, the negative ion sources for ITER are designed at 33 MW and 500 keV, or ~3x10^{20} atoms/sec [4].

[1] D. Kramer, "Cleanup of Cold War nuclear waste drags on", Physics Today 70, 28 (2017)
[2] http://www.hanford.gov/page.cfm/tankfarms
[3] I.G. Brown, "The physics and technology of ion sources", 2nd edition, Wiley (2004)
[4] M.J. Singh et al, New Journal of Physics 19, 055004 (2017)

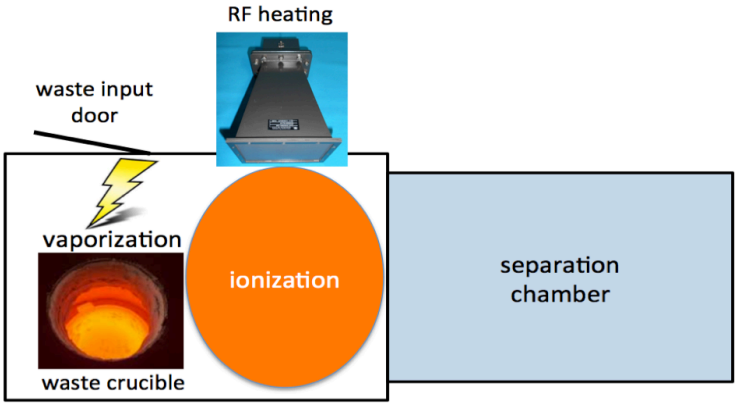

Fig. 4.1 schematic of ion source chamber

4.1.1 Thermal desorption

The simplest method for extracting individual atoms and molecules from solid and liquid waste is through thermal desorption, i.e. heating to vaporization. This technique is used in industry to treat large quantities of hazardous wastes (~2-30 tons/hour) [1], and also in very small samples (μgr) in thermal ion mass spectrometers, including nuclear waste [2]. High temperatures up to ~1000º C can be reached by resistance heating, infrared, or microwave heating. Obviously this method works best for materials with low vaporization temperatures such as organic molecules and some metals, and it is not clear how much of the radioactive material can be evaporated in this way. Thermal desorption can be considered as a chemical pretreatment process to reduce the volume of waste for further separation [3,4], if no significant radioactive material can be vaporized this way. Vaporization of refractory materials such as salts and oxides can be done at higher temperatures using other techniques, as discussed below.

[1] https://en.wikipedia.org/wiki/Thermal_desorption
[2] J.S. Becker, Spectrochimica Acta Part B 58, 1757 (2003)
[3] W.R. Wilmarth et al, Solvent Extraction and Ion Exchange 29, 1 (2011)
[4] L. Nassif et al, Environ. Sci. Technol. 42, 4940 (2008)

4.1.2 Electron impact ionization

One common way to create ions is by the collision of thermal electrons with neutral gas atoms, i.e. electron impact ionization (EII). This is how ions are formed in most laboratory discharges such as helicon or inductively coupled plasmas. The cross-sections for ionization are well known for most atomic gases and common molecules, and depend sensitively on the electron temperature. Roughly, ionization begins when the T_e ~1/3 the ionization energy, since ionization events can be created by the tail of the electron distribution function. The charge state of ions as a function of T_e can be estimated from the Saha equation or more modern data libraries [1,2]. Typically the range of temperatures useful for creating singly charged ions is roughly T_e~2-10 eV. The ionization rate is also linearly proportional to the electron density.

Assuming the nuclear waste is already vaporized into gaseous form, the main difficulty in EII is to maintain the desired electron temperature in the presence of various energy losses, e.g. ionization energy, radiation and charge exchange losses, ion heating (if $T_i < T_e$), and direct electron heat loss to the vessel wall. The last of these is to some extent useful if the electron heat loss goes to vaporizing the solid waste, but could also be damaging to the vessel wall, depending on the chamber geometry. Magnetic fields are of course useful in reducing electron energy loss, but the electron heat loss is usually difficult to calculate from first principles. More discussion of plasma energy loss is in Section 3.9.

The required processing rate of ~100 gr/sec for Hanford nuclear waste separation implies a gas influx rate rate of ~10^{24} atoms/sec (assuming A=60). This is ~10x higher than the DT fuel injection rate in ITER of ~10^{23} atoms/sec at 100 MW of heating power [3], and ~10^5 times higher than the typical argon gas injection rate into a laboratory experiment like PMFX with ~1 kW of heating power [4], which is roughly 10^{14} neutrals/cm^3 x 200 liter/sec (turbopump speed) ~10^{19} atoms/sec. Thus the required ionization rate for nuclear waste separation is extremely high compared to existing plasma devices.

[1] http://open.adas.ac.uk/, or http://open.adas.ac.uk/adf07
[2] K.L. Bell et al, J. Phys. Chem. Ref. Data 12, 891(1983); M.A. Lennon et al, J. Phys. Chem. Ref. Data 17, 1285 (1983)

[3] T. Loarer et al, Nucl. Fusion 47, 1112 (2007)
[4] R. Gueroult et al, Plasma Sources Sci. Technol. 25, 035024 (2016)

4.1.3 Electron beams

Electron beams can be readily created in vacuum using an electrically biased hot filament such as tungsten, or using a plasma cathode [1]. Electron beam ionization at low power is done in mass spectrometers using electrons with energies of ~70 eV near the peak of the electron ionization cross-section for most atoms and molecules [2,3]. However, the electron current emitted from a filament depends on the voltage as $V^{3/2}$, so high power electron beams (such as needed for high throughput) generally operate at much high voltages. For example, commercial high power electron beams for welding can operate continuously at up to ~150 kV and ~60 kW [4]. These high power beams can vaporize almost any (preferably conducting) target, and can be steered using magnetic fields. However, the range of electrons for energies of $\geq$1 keV at a source pressure of ~10^{-6} bar is >10^4 cm [5], so the high energy electron beams are not useful for direct ionization of gases, but rather to heat and vaporize solid source material. It is unlikely that the electron beam vaporization will produce a high fraction of ionized atoms or molecules, so some other process would be needed to ionize the vapor.

[1] D.M. Goebel and R.M. Watkins, Rev. Sci. Instr. 71, 388 (2000)
[2] J.H. Gross, Mass Spectroscopy, A Textbook, Springer 2011, Chapter 2
[3] S.J. Ray et al, Journal of Chromatography A, 1050, 3 (2004)
[4] https://www.ptreb.com/electron-beam-welders-and-systems/ebocam-fixed-gun-systems
[5] http://physics.nist.gov/PhysRefData/Star/Text/ESTAR.html

4.1.4 Laser ablation

Ultraviolet lasers are also used in mass spectrometers for photoionization or multi-photon ionization (for molecules), but with a very low throughput and efficiency [1]. High powered infrared lasers up to ~20 kW are used for cutting and machining [2], but at relatively high cost compared with electron beams. Pulsed high-power lasers are used with LIBS (laser-induced breakdown spectroscopy) to create plasmas on surfaces for chemical analysis [3], but only at microscopic throughputs. Pulsed lasers were also used for triggering the arcing on a metal cathode in plasma centrifuges (see Fig. 2.3). Although lasers are generally less powerful (on average), less energy efficient, and more expensive than electron beams, the wide spectrum of available laser sources, wavelengths, pulse lengths, and optical systems has generated many successful material processing applications, both for pulsed and CW lasers [4]. Their use as a plasma source for nuclear waste processing is worth investigating further, especially for small-scale experiments.

[1] J.H. Gross, Mass Spectroscopy, A Textbook, Springer 2011, Chapter 2
[2] https://www.trumpf.com/en_US/products/machines-systems/laser-cutting-machines/
[3] D.W. Hahn and N. Omenetto, Applied Spectroscopy 64, 335A (2010)
[4] B.N. Chickov et al, Appl. Phys. A63, 109 (1996)

4.1.5 High pressure arcs

Various forms arcs operating near atmospheric pressure are used in industry for welding, melting, spraying and destruction of hazardous wastes, as reviewed for example in [1-3]. For example, electric arc furnaces at power levels of ~100 MW can melt scrap steel at a rate of ~100 tons/hour (30 kg/sec), i.e. at a much higher rate than needed for nuclear waste processing. Commercial plasma waste treatment plants have been operated with various types of plasma torches and jets, transferred and non-transferred arcs, and RF and microwave reactors, performing destruction of toxic organic chemicals, recovery of valuable materials, and vitrification of ash [3], with power levels of up to ~1 MW at throughputs of ~1 ton/hour (~300 g/sec). For example, the RETECH plasma arc centrifugal treatment system is used for metal re-melting and has been certified for treatment of low level nuclear waste by compaction in Switzerland and Japan [3], and a Russian review of radioactive waste treatment with plasma torches is available [4]. A ~50 kW plasma torch was actually proposed and tested as way to assist in vitrification and calcination of Hanford nuclear waste [5,6], and an atmospheric RF plasma torch/centrifuge (PT/C) system for Hanford waste separation was proposed by UCLA/Westinghouse [7].

These atmospheric plasma systems create thermal plasmas with a temperature of T ~1 eV with a very low degree of ionization, and are used mainly for melting and vaporization (incineration). While it might be technically possible to vaporize high-level nuclear waste with such systems, the need for near-perfect waste containment, and the need to rapidly transfer the resulting vapor to the ionization and plasma separation vacuum system, would appear to make the use of this technology rather difficult. In addition, these arc plasmas are generally turbulent on small space/time scales, so may not suitable as a ion source.

[1] U. Kogelschatz, Plasma Phys. Control. Fusion 46, B63 (2004)
[2] A. Schutze et al, IEEE Trans. Plasma Sci. 26, 1685 (1998)
[3] J. Heberlein and A.B. Murphy, J. Phys. D: Appl. Phys. 41, 053001 (2008)
[4] A.N. Bobrakov et al, Russian Journal of General Chemistry 84, 1031 (2014)
[5] C.H. Delegard, Westinghouse Hanford Co. Report WHC-EP-0832 (1995)
[6] G.M. Bunce et al, JOM 51, p. 22 (Oct. 1999)
[7] S.E. Siciliano et al, Westinghouse Report WHC-SA-1821-FP (June 1993)

4.1.6 Vacuum arcs

Vacuum arcs are used for various industrial and scientific purposes such as ion implantation and accelerator ion sources [1-3], and vacuum arcs were used in experiments on the plasma centrifuge (Sec. 2.3). These arcs are usually formed in ≤ 1 msec pulses between two metallic electrodes at a pressure $\leq 10^{-6}$ bar, and ions are created at tiny cathode spots along with metal plasma, neutral gas, and solid "macroparticles". Ion energies can be as low as ~20-50 eV, and mean ion charge states are +1 to +3, depending on the species [1]. The ion erosion rate is typically ≤100 μG/Coul, implying an average arc current of ~1 MA would be needed to erode the ~100 g/sec relevant to nuclear waste separation.

Vacuum arcs might be a simple way to create an ion source for plasma mass separation. However, there are obviously several basic issues: the waste has an uncertain electrically conductivity and may not make a good electrode, most of the ejected material from the arc is in the form of uncharged macroparticles [4], the ions produced have various charge states, magnetic fields can strongly affect the arc, and the vacuum rarc is generally unstable.

Some of these difficulties were overcome using a crucible heated by a diffuse arc [5,6], which produced for example a gadolinium ion flux of ≤3 mg/sec with an average ion charge of near 1. This system was designed as a plasma source for separation of spent nuclear fuels and radioactive wastes, and was operated continuously for many seconds with an arc diameter of ~2 cm, as illustrated in Fig. 4.2. Somewhat similar results were obtained with lead and other cathodes [7]. Light and heavy metal components (e.g. Fe and W) in a vacuum arc system with a curved magnetic field were successfully separated using a centrifugal force mechanism [8], and the authors suggest this could be useful for spent nuclear fuel, especially with macroparticle filtration [9] or with a hot refractory anode vacuum arc [10]. Vacuum arcs would be useful as a plasma source for near-term experiments; for example, a carbon spark plug was used as an impurity source in tokamak experiments [11], or a submerged arc might be useful for liquid waste sources.

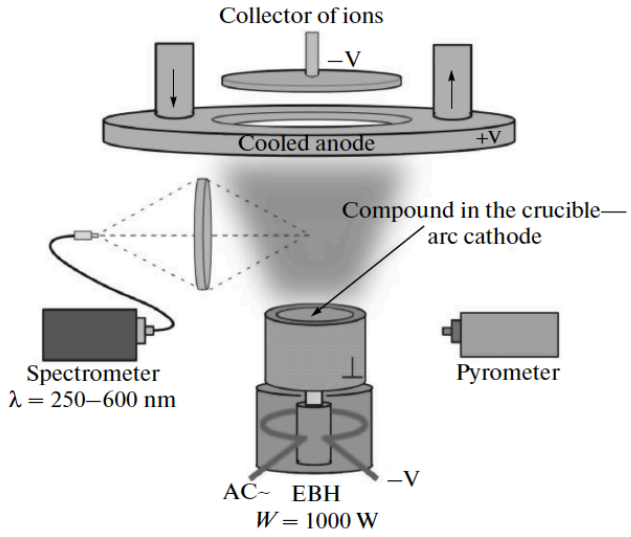

Fig. 4.2 distributed vacuum arc with heated cathode [6]

[1] I.G. Brown, Rev. Sci. Instrum. 65, 3061 (1994)
[2] P. Siemroth et al, Surf. and Coatings Tech. 68/69, 314 (1994)
[3] A. Anders et al, IEEE Trans. Plasma Sci. 33, 1532 (2005)
[4] R.L. Boxman and S. Goldsmith, Surface and Coatings Tech. 52, 39 (1992)
[5] R. Kh. Amirov et al, Plasma Physics Reports 41, 808 (2015);
[6] R. Kh. Amirov et al, Physics of Atomic Nuclei 78, 1631 (2015)
[7] R. Kh. Amirov et al, IEEE Trans. Plasma Sci. 45, 140 (2017)
[8] V.L. Paperny et al, PSST 24, 105009 (2015)
[9] I.I. Beilis et al, J. Ap. Phys. 85, 1358 (1999)
[10] I.I. Beilis et al, Surface and Coatings Technology 122-134, 91 (2000)
[11] F. Levinton and D.D. Meyerhofer, Rev. Sci. Instrum. 58, 1393 (1987)

4.1.7 Sputtering sources

A gentler way to create vaporized atoms and molecules from a solid waste target is by ion sputtering, in which inert gas ions such as argon are electrostatically accelerated to collide with surface target atoms

and eject them individually [1]. Many devices for ion sputtering are used for industrial and scientific applications; for example, RF-driven plasma devices for semiconductor etching [2,3] and magnetron sputtering devices for thin film coatings [4,5]. Normally ionization fractions in sputtering are only ~1%, and the neutral atoms are ejected with a moderate energy, e.g. ~20 eV for an incident argon energy of 400 eV [6]. Thus the mean-free-path of these neutrals would have to carry them to a separate ionization section near the target. In ICRH isotope separation experiments, a metal target plate metal atom sputtering source was used previously to create the ions [7,8]. In mass spectroscopy, an argon glow discharge can sputter small target samples for precise mass analysis, including radioactive samples [9].

Atom sputtering rates can be up to ~1 atom/ion, depending on incident ion energy, mass ratios and self-sputtering, so this source process is limited by the rate of ion current to the target. If the plasma density at the target surface is $n=10^{13}$ cm^{-3} and the incident ion speed is $v_i \sim 3x10^6$ cm/sec (e.g. Ar^+ at 400 eV), the incident ion flux can be $\sim 3x10^{23}$ ions/m^2, corresponding to a sputtering rate of ~30 gr/sec for atoms with M=60. This is not far from the rate needed to process the Hanford nuclear waste. Of course, a large area source of plasma ions would be needed, along with electrical bias to accelerate ions, which would require significant electrical power (~20 MW in this example). An improvement in this source process might be possible using pulsed magnetrons, which can create a high fraction (~70%) of sputtered ions [5]; of course, the sputtered ions will not easily escape the surface when it is negatively biased.

[1] R. Behrish et al, Sputtering by Particle Bombardment: Experiments and Computer Calculations, Springer (2007)
[2] M.A. Lieberman and A.J. Lichtenberg, Principles of Plasma Discharge for Materials Processing (John Wiley & Sons, 1994)
[3] J. Hopwood, Plasma Sources Sci. Technol. 1, 109 (1992)
[4] P.J. Kelly and R.D. Arnell, Vacuum 56, 159 (2000)
[5] K. Sarakinos et al, Surface and Coatings Technology 204, 1661 (2010)
[6] J. Lu et al, Vacuum 86, 1134 (2012)
[7] A. Compant La Fontaine, V.G. Pashkovsky, Phys. Plasmas 2, 4641 (1995)
[8] D.A. Dolgolenko and Yu. A. Muromkin, Physics-Uspekhi 52, 345 (2009)
[9] J.S. Becker, Spectrochimica Acta Part B, 1757 (2003)
[10] W. Eckstein, J. Nucl. Materials 248, 1 (1997)

4.1.8 Dust evaporation

Another possible technique to vaporize and ionize solid nuclear waste is to first grind it into a fine dust, and then introduce the powder into the source plasma chamber or directly into the main separation chamber. The plasma heat flux onto dust particles can be large enough to evaporate all dust, although the process is complicated by charging and possible rocket motion. Figure 4.3 from Ref. [1] shows calculations of dust temperature and lifetime for various metallic dust sizes, done assuming tokamak edge plasma conditions of T~10 eV and $n=2x10^{13}$ cm^{-3}, which are not far from plasma mass separator conditions. To reduce the calculated dust lifetime to ≤10 msec requires a dust size of ≤1 μm, and the energy required for latent heat of evaporation and to overcome the work function is ~5-15 eV/atom for metals, which is comparable to the ionization energy.

There is considerable experience with dust in plasmas. Micron size dust can be levitated without vaporization in low temperature, low density plasmas [2]; lithium and tungsten dust has dropped into and fully evaporated in tokamak edge plasmas [3]; and plasma enhanced chemical vapor deposition uses liquid

droplets to make dielectric coatings [4]. A preliminary test of an aluminum oxide dust dropper in the PMFX experiment was inconclusive [5], perhaps because the dust became charged and deflected. The feasibility of plasma dust evaporation in a plasma at the required ~1 gr/sec remains to be demonstrated. The off-line transformation of nuclear waste into micron-size dust using a plasma torch has been proposed for calcification (see Sec. 4.1.5). There is also an explosion hazard for dust handling which may not be tolerable for nuclear waste treatment (see Sec. 4.4).

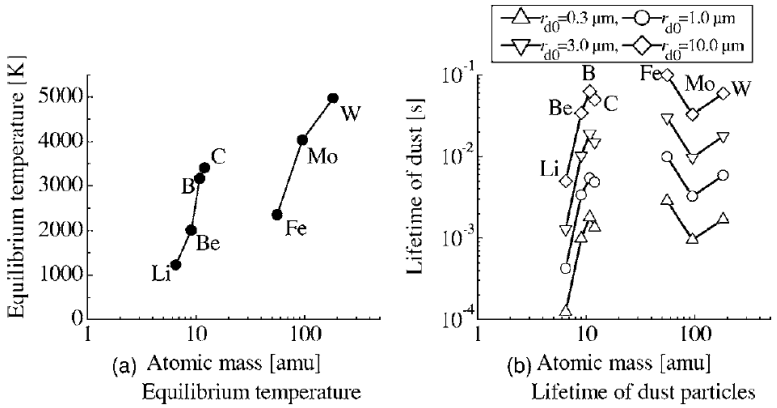

FIG. 4. Equilibrium temperature (a) and lifetime (b) of dust particles for the uniform plasma with parameters: $T_e=T_i=10$ eV, $T_a=3$ eV, $n_e=n_i=n_a=2\times10^{13}$ cm^{-3}. The initial dust radius r_{d0} is changed from 0.3 to 10 μm.

Fig. 4.3 equilibrium temperature and lifetime of dust in a plasma [2]

[1] Y. Tanaka et al. Phys. Plasmas 14, 052504 _2007_
[2] A. Melzer and J. Goree, Fundamentals of Dusty Plasmas, in Low Temperature Plasmas: Fundamentals, Technologies and Techniques (Wiley, 2007)
[3] A.L. Roquemore et al, Fusion Engineering and Design 86, 1355 (2011)
[4] L. M. Poitras, J. Vacuum Sci. Tech. A Vacuum, Surfaces, and Films 18, 2619 (2000)
[5] R. Gueroult et al, Plasma Sources Sci. Technol. 25, 035024 (2016)

4.1.9 RF and other ionization sources

Many of the sources described above provide incompletely ionized atoms, so additional ionization will probably be needed in the plasma source for nuclear waste separation. Conventional ionization techniques mainly involve RF or microwave power coupling to electrons, which then can ionize the neutrals. The simplest of these is electron cyclotron heating, which can be done inexpensively at 2.45 GHz (microwave oven frequency) at B=875 G. Other common plasma sources use inductively or capacitively coupled RF or helicon discharges, typically at 13.56 MHz [1]. The efficient coupling of this RF power to large-volume sources is non-trivial but extensively studied [2-5]. An alternative ionization method uses large-area heated and biased cathodes to emit low energy electron beams (~50-100 V) which can thermalize within the source [5-7].

There are several other methods of ionization used in conventional mass spectrometers at low throughput which might possibly be modified for use for nuclear waste sources. Some of these other methods are [8,9]: electrospray ionization, soft laser desorption, chemical ionization, photoionization,

matrix-assisted laser desorption/ionization, field ionization, thermal ionization, spark sources, and glow discharge sources.

[1] M.A. Lieberman and A.J. Lichtenberg, Principles of Plasma Discharge for Materials Processing (John Wiley & Sons, 1994)
[2] J.H. Bowles et al, Rev. Sci. Instrum. 67, 455 (1996)
[3] B.P. Cluggish et al, Phys. Plasmas 12, 057101 (2005)
[4] S. Shinohara et al, Phys. Plasmas 12, 044502 (2005)
[5] M. Gilmore et al, J. Plasma Phys. (2015) 81, 345810104
[6] S.K. Matoo et al, Rev. Sci. Instrum. 72, 3864 (2001)
[7] W. Gekelman et al, Rev. Sci. Instrum. 87, 015105 (2016)
[8] J.H. Gross, Mass Spectroscopy, A Textbook, Springer 2011
[9] E. de Hoffmann and V. Stroobant, Mass Spectrometry, Principles and Applications (Wiley, 2012)

4.2 Waste handling

The engineering problems of nuclear waste handling and disposal have been studied intensively for many years, both in the US and elsewhere. The handling of "legacy" wastes due to military plutonium and uranium production is generally more difficult than handling of spent nuclear fuel from fission reactors, since the legacy wastes have a much more complex chemical and physical structure. The largest legacy nuclear wastes sites in the US are at Hanford and Savannah River, as discussed in Sec. 1. The remediation of Hanford nuclear waste is far from complete [1,2], and has already experienced many cost and schedule overruns [3].

The potential role of plasma mass separation in nuclear waste remediation has been reviewed recently [4]. Significant savings might be achieved by minimizing the mass of high-level radioactive waste, i.e. physically separating the low volume of high-atomic-mass species from the much higher volume of non-radioactive low-atomic mass species. After this pretreatment, high-level waste would be immobilized by vitrification in glass canisters and placed in long-term underground storage. Plasma separation has a potential advantage with respect to conventional chemical processing in not requiring additional liquid materials during processing. However, many of the difficulties in nuclear waste handling are common to both chemical and plasma separation techniques, such as transportation of the waste from the tanks to the pretreatment plant, remote handling of the waste due to radioactive and chemical hazards, and handling of off-gases and dust released during processing.

One unconventional requirement for plasma nuclear waste separation is the need for all material to pass through a high vacuum system at a pressure of typically $\sim 10^{-6}$ atmosphere. This will require a large amount of vacuum pumping, even though most of the throughput (input and output) will presumably be in solid form and not in gaseous form. Conventional high vacuum pumps (e.g. rotary mechanical or turbo pumps) are not designed to handle dust, which would have to be carefully filtered out to avoid pump damage. The vacuum system interior would need to be cleaned frequently to remove coatings of nuclear waste on almost all exposed surfaces, especially on high voltage electrodes or RF antennae. However, vacuum interfaces have already been used successfully for isotope separation devices such as calutrons (Sec. 1.2), and for analytical instrumentation such as mass spectrometers. One advantage of a vacuum system is that leaks are inward, and not outward.

Mechanical interface chambers will have to be designed to insert the solid waste into the plasma source region, and to remove it from the high and low-mass waste collection regions within the vacuum system. If the total throughput is ~100 g/sec for 24/7 operation at Hanford, and if this was accomplished using ~20 plasma separation devices, the solid nuclear waste handled would be ~400 kg/day in each device. It is possible that source and exhaust chambers could be attached to the main separation device using large vacuum valves, and removed and replaced daily in batch mode. It might also be possible to use conveyer belts to move the waste, but not across a vacuum boundary. If the separated waste can be liquefied at high temperature, they can be removed in flowing films by gravity [5]. Some of these mechanical nuclear waste handling issues may be common to both chemical and plasma separation technology.

In addition to the normal vacuum pumping requirements, there may be substantial additional outgassing due to volatile compounds and chemical reactions in the nuclear waste. Obviously it would be preferable to remove volatile non-radiactive liquids before processing in a plasma system. The off-gas would need to be monitored for radiation and chemical hazards, as it needs to be for chemical separation and some other large-scale industrial processes.

Another unconventional feature of some plasma nuclear wastes separation devices is the use of high voltage electrodes for generation of plasma rotation or electrostatic separation, usually inside the vacuum system. The coating of high voltage components and vacuum feedthroughs would be a serious maintenance issue. There might also be some novel electrochemistry involving nuclear waste. Many plasma mass filters also use strong magnetic fields, which are not normally found in nuclear waste processing. Iron and other magnetic species would be affected by these fields, at least in solids below the Curie temperature.

Most handling of the nuclear waste will probably need to be done with remotely controlled devices and be carefully monitored for radiation and toxic chemical leakage. The average radiation level of Hanford tank waste is on the order of ~1 Ci/kg (see Sec. 1.3), mainly from ^{137}Cs and ^{90}Sr; however, the final vitrified form of the high-level waste canisters can be handled by fork lift operators, as shown in Fig. 4.4, taken from Ref. [2]. On the other hand, dogs which were injected with 3.8 mCi/kg of ^{137}CsCl died within 33 days [6]. Thus the periodic cleaning and maintenance of the entire device will be potentially hazardous. For example, a device with a throughput of 5 g/sec will have to process ~400 Ci per of radioactive material per day, some of which will certainly contaminate the vacuum chamber, interlocks, or pumps with surface coatings or dust. It is interesting to note that the original calutron uranium separation tanks were cleaned by hand using scrapers and wire brushes [7], which would probably not be acceptable today.

[1] https://www.hanfordvitplant.com/
[2] D. Kramer, “Cleanup of Cold War nuclear waste drags on”, Physics Today 70, 28 (2017)
[3] T.C. Perry and C.B. Abraham, “Money for Nothing”, IEEE Spectrum July 2002
[4] R. Gueroult et al, J. Hazardous Materials 297, 153 (2015)
[5] S.N. Suchard, The Plasmas Spearation Process for Generic Isotope Separation, Waste Management Symposium 1983, http://www.wmsym.org/archives/1983/V2/19.pdf
[6] H.C. Redman et al, Radiation Research 50, 629 (1972)
[7] A.L. Yergey and A.K. Yergey, J. Am. Soc. Mass. Spectrom. 8, 943 (1997)

Fig. 4.4 – handling of high-level waste canisters (from [2])

4.3 Plasma heating and magnets

Many plasma mass separation mechanisms will require a dedicated plasma heating system to control the ion and electron temperature downstream from the plasma source. In particular, the need to have singly-ionized species and limit the radiated power forces the desired electron temperature to be T_e ~1-2 eV (see Sec. 3.1), while the need for high ion throughput forces the desired ion temperature to be T_i ~10 eV (see Sec. 3.10). As far as we know, plasmas with this combination of temperatures have never been made in the density range n_e ~10^{13}-10^{14} cm^{-3} needed for plasma mass separation, even with noble gases.

The most common low temperature plasma heating technology is RF heating, as discussed in Sec. 4.1.9. The required RF heating power depends on the ionization energy and radiation (Sec. 3.1), the plasma energy loss mechanisms (Sec. 3.9), and the efficiency of RF coupling (which varies with heating system). Very roughly, this energy will be ~1 keV/atom, so for a throughput of ~100 g/sec or ~10^{24} atoms/sec, this would require ~100 MW of RF heating. This is comparable to the RF heating power planned for ITER, the largest magnetic fusion experiment. Present linear helicon plasma experiments operate with ~1-2 kW of RF power and obtain T_e ~5-10 eV at T_i < 1 eV [1-3]. The largest RF power used for a plasma separation device was the ~4 MW, 6 MHz RF heating system developed for the Archimedes device [4]. Lower power ICRH for heating in isotope separation devices were reviewed in Ref. [5]. Higher power ~10 MW ICRH and ECRH heating systems have been used in tokamaks, and ~1 MW RF source is being developed for fusion materials testing in a linear device [6].

The most likely configuration for RF heating of nuclear waste plasma would have the antenna just outside an insulating vacuum vessel wall made of glass or ceramic. Any conducting coating on the interior wall would interfere with the RF wave propagation, so techniques to avoid or remove such coatings would

have to be developed. High power RF antennas outside the vessel would probably also need to be actively cooled for steady-state operation.

An alternative plasma heating method would be low or zero frequency Ohmic heating due to plasma currents generated inductively or by internal electrodes. This has been used, for example, in pulsed arc centrifuges and with biased electrodes in Archimedes and PMFX (see Sec. 1.2). In general, Ohmic heating is a simpler technology than RF heating, but less powerful and less controllable. Electrodes inside the vacuum vessel would probably suffer from erosion and/or coatings, which may limit their lifetime, and they may also need to be actively cooled, which presents safety issues. Another possible method for ion heating is through bulk plasma ExB rotation, which can produce ion speeds comparable to T_i = 10 eV with modest electric fields of ~3 V/cm at B=1 kG. Of course these ions would have velocity perpendicular to B which would not directly contribute to the ion throughput along B. However, ion orbits effects and collisions could allow this motion to be useful for some separation mechanisms [7].

The magnets needed for plasma separation would most likely be superconducting to minimize power consumption, at least for fields above B~1 kG. Superconducting magnets are conventional technology used for example in MRI scanners, and previously used for isotope separation (see Sec. 5.5). It may be possible to use permanent magnetic for some separation schemes, which would probably be less costly but also less flexible.

[1] E.E. Scime et al, J. Plasma Phys. 81, 345810103 (2016)
[2] M. Gilmore et al, J. Plasma Phys. (2015) 81, 345810104
[3] S.C. Thakur et al, Phys. Plasmas 23, 082112 (2015)
[4] B.P. Cluggish et al, Phys. Plasmas 12, 057101 (2005)
[5] D.A. Dolgolenko and Yu. A. Muromkin, Physics-Uspekhi 52, 345 (2009)
[6] J. Rapp et al, Nuclear Fusion 57, 116001 (2017)
[7] R. Gueroult et al, Plasma Phys. Control. Fusion 60, 014018 (2018)

4.4 ES&H issues

Clearly a major issue in nuclear waste remediation involves the assurance of environmental safety and health (ES&H). The potential development of plasma separation technology must meet the ES&H standards set by DOE and other government agencies, which may be difficult since some of this technology is relatively new and untested. Some specific plasma mass separation ES&H issues are outlined below.

A primary safety issue is leaks of nuclear waste. If the vacuum vessel has insulting parts made of glass or ceramic, as may be needed for RF heating, then cracks or ruptures due to thermal or mechanical stress are possible. Small leaks can be quickly detected with vacuum gauges, perhaps stopping operation but not a major safety issue. Large vacuum vents could potentially distribute some waste to the surroundings, so probably a secondary confinement system would be needed, perhaps a double-walled vacuum system. Electrical sparks and/or arcs are common with high-power RF and high-voltage electrode systems used in plasma technology. Careful protection will be needed against chemical explosions outside the vacuum vessel, e.g. due to hydrogen gas or dust. Electric shock hazards and microwave/RF radiation exposure are also common ES&H issues in plasma devices.

A potentially serious safety issue is the cooling of in-vacuum components, which are not naturally cooled by convection and conduction due to the low pressure. As discussed in briefly in Sec. 3.9, it is not

clear how the plasma heating power will be deposited inside the vacuum vessel due to uncertainties in the plasma transport process, particularly in the presence of a magnetic field. Therefore some in-vessel components may need to be actively cooled for steady-state operation. Water cooling allows the possibility of steam explosion and vessel rupture, such as analyzed in loss-of-cooling accident scenarios for ITER [1]. Helium cooling is a good but costly solution for fusion reactor designs.

Another potentially serious safety issue is the sub-micron nuclear waste dust which may need to be created for the plasma source (Sec. 4.18), or which might be made by the plasma itself. Such dust is a human inhalation hazard and potentially explosive, as shown for example in the ITER safety analysis [1]. Similar dust hazards may present in chemical separation if calcination processes are used [2].

There are serious radiological and toxicological safety issues in handling any nuclear waste, but as far as we know there are no unique issues in plasma mass separation devices, beyond those which are normally handled in chemical separation processing. Possibly these hazards are reduced with respect to chemical separation since the volume of nuclear waste inside a plasma vacuum system will be limited, depending on the plasma waste handling scheme (Sec. 4.2). The alpha and beta emission from all species will certainly be contained by the vacuum vessel. The 662 keV gamma emission from Cs^{137} will largely be shielded by the vacuum vessel, although precautions will be necessary to monitor this emission. No significant neutron emission is expected. There is no known mechanism for plutonium concentration inside plasmas, beyond the coarse-grain atomic mass separation inherent in the plasma mass filter physics. There might be some novel plasma electrochemistry involving electrodes in nuclear waste, but if so the effect on the waste composition should be minimal.

On the positive side, it is not impossible that a plasma mass filter device could be designed to be remotely operated nearby or even inside an existing waste tank such as those at Hanford. In this sense, the plasma mass filter might evolve from the scale of a portable analytical mass spectrometer into a moderate throughput, low resolution plasma mass filter. This proximity could potentially remove some of the hazards of transporting the waste from the storage tanks to the chemical processing facilities.

[1] F. Virot et al, Fusion Engineering and Design 98-99, 2219 (2015)
[2] C.H. Delegard, "Chemistry of Proposed Calcination/Dissolution Processing of Hanford Tank Wastes", Westinghouse Hanford Co. Report WHC-EP-0832 (1995)

5. Research and development (R&D) plan

This section outlines possible components of an R&D plan for the development of a plasma separation device for nuclear waste remediation. A brief summary of the main issues and potential research directions is given in Sec. 5.6. The present report does not attempt to define a specific research proposal. Also note that a separate analysis of physical separation without plasma should be done before embarking on a major plasma separation program, since physical separation will be easier than plasma separation if the waste composition is sufficiently non-uniform (see Sec. 1.5) .

5.1 Staged goals

The steps of an R&D plan for "Plasma Mass Filters for Nuclear Waste Remediation" could be:

1) evaluate plasma mass separation mechanisms with various gases and small samples of solids

2) demonstrate plasma mass separation at low throughput with simulated nuclear waste
3) demonstrate plasma mass separation at low throughput with real nuclear waste
4) demonstrate plasma mass separation at high throughput with simulated nuclear waste
5) demonstrate plasma mass separation at high throughput with real nuclear waste

The goal of stage (1) would be to test the physics and technology of the various plasma separation methods to identify the most promising technique(s). Of course, this step has already been taken in many previous experiments, e.g. vacuum arc centrifuges (see Sec. 1.2), but here different techniques can be directly compared with each other. The design of this device should be flexible and modular to allow quick tests of various options, as illustrated in Fig. 1.4. Initial separation tests can be done with inert (wall recycling) gases or molecular (non-recycling) gases such as sulfur dioxide, or even (toxic) gases such as tungsten hexafluoride. Solid metals or metal oxides can be injected using ion sputtering, laser-blow-off, electric sparks, or powder droppers (see Sec. 4.1). It is important that good diagnostics be available to measure the separation efficiency as well as the plasma physics parameters (see Sec 5.3). No radioactive species would be used in this facility at this stage.

The goal of stage (2) would be to demonstrate one or more promising techniques for plasma mass separation at a low but near-steady-state throughput, perhaps comparable to existing ~1-10 mg/sec of previous plasma (isotope) separation devices. This would most likely require a much larger plasma volume and heating power than used for stage (1), and could evaluate the issues of continuous operation, e.g. buildup of coatings or erosion of internal components. Although this device would be operated with surrogate (non-radioactive) nuclear waste, it might also have near-term applications to other high-value mass separations, such as rare earth metals.

The goal of stage (3) would be to demonstrate plasma mass separation with real nuclear waste, but at a low throughput level of ~1-10 mg/sec. The physics and technology would be based on the most promising device of step (2), but this step would evaluate the ES&H issues of radioactive and toxic materials (see Sec. 4.2 and 4.4), along with remote control of the system. This step could probably be done with a small nuclear waste inventory ~10-100 gr (~1-3 hours of operation), so it might be operated at an off-site lab. For example PPPL had an on-site tritium inventory of ~5 gr (~5×10^4 Ci) for the TFTR tokamak.

The next steps (4) and (5) would attempt to increase the throughput as much up to ~0.1-1 gr/sec, presumably by increasing in the volume and power of the small device tested in (2-3). This would be near to the final scale needed for a Hanford remediation effort, assuming 100 devices of this type operating simultaneously to reach the throughput goal of ~400 gr/sec. The device (4) with surrogate waste would probably require ~1 MW of continuous plasma heating power, and would involve significant engineering efforts to build and operate. The device (5) with real nuclear waste would probably be located near the site to be remediated, since it would need an inventory of ≥10 kg of nuclear waste, which would not be easy to transport.

Obviously each of these depends on the success of the previous step. It is possible but risky to skip stages; for example, the Archimedes program seems to have skipped stage (1), but was not successful in going past stage (2). More steps are desirable since plasma performance is very difficult to predict; for example, intermediate steps between (3) and (4) may be needed, depending on the results.

5.2 Criteria for evaluating separation mechanisms

The first stage of an R&D plan would be to evaluate the various possible plasma separation mechanisms which were outlined in Sec. 2. This evaluation of course needs to be targeted to the specific application; for example, Hanford nuclear waste separation requires a large throughput and only a coarse mass discrimination, whereas separation of spent nuclear fuel requires much lower throughput and targets specific atomic mass ranges [1].

A very preliminary evaluation of these mechanisms with respect to the Hanford application is shown in Table 5.1. The plasma physics mechanisms of Sec. 2 are listed in the left columns, and are evaluated with respect to several qualitative criteria: history, simplicity, robustness, throughput, and efficiency. The numbers in each box reflect a tentative rating: 1=good, 2=average, 3=poor. The total at the right gives a tentative evaluation of each mechanism, where the lower numbers are better rated overall than the higher numbers. Of course Table 1 is just a template for what should be an extensive analysis and test program to evaluate these concepts, corresponding to stage #1 above.

Section	mechanism	history	simplicity	robustness	throughput	efficiency	total
2.1	gyroradius	1	1	2	2	2	**8**
2.2	curved B	1	1	1	1	3	**7**
2.3	centrifuge	1	2	3	3	1	**10**
2.4	rotate in B	2	3	2	2	2	**11**
2.5	rotate vary B	3	3	2	2	3	**13**
2.6	azimuthal B	3	3	2	2	3	**13**
2.7	mobility	3	2	3	1	2	**11**
2.8	advection	3	3	3	2	2	**13**
2.9	ionization	2	2	2	1	3	**10**
2.10	dust	2	2	3	1	3	**11**
2.11	diffusion	2	1	1	2	2	**8**
2.12	transit time	2	2	1	1	3	**9**
2.13	collisionality	3	2	2	2	2	**11**

Table 5.1 – preliminary evaluation of separation mechanisms (1=good, 2=average, 3=poor)

The history column rates the degree to which this separation concept was attempted in previous experiments, presuming that it is good to have some prior history, even if the results were not positive. For example, the gyroradius separation concept was the basis of the calutron and several ion cyclotron resonance separation devices (Sec. 2.1), and the pulsed plasma centrifuge was previously tried several times (Sec. 2.3). At the other extreme, there have been no previous experiments on ion mass separation using plasma rotation in a varying B field (Sec. 2.5), or advection in radial electric fields (Sec. 2.8).

The simplicity column rates each concepts in terms of the simplicity of its physics mechanism, presuming that simpler concepts are good because they are more likely to work as planned. The gyroradius separation mechanisms (Sec. 2.1) are based on the simplest ion property, while the curved B ion drift mechanism is nearly as simple. Also simple is the radial diffusion mechanism (Sec. 2.11), which depends only on the ion collisionality and gyroradius. At the other extreme, the mechanisms which involve plasma

rotation (Sec. 2.4 and 2.5) are intrinsically complex because the physics of plasma rotation is not well understood, even though ExB rotation is observed in nearly all plasma devices.

The robustness column evaluates the reliability of the technology associated with each concept, which will be highly important for nuclear waste applications. The most robust concepts are those with the simplest geometry, the lowest magnetic fields, the fewest high voltage components (which are prone to failure), and the fewest in-vacuum systems (which are difficult to repair). The more robust concepts include the ion drift separation in a curved magnetic field (Sec. 2.2) and transit-time separation (Sec. 2.12), which require low magnetic fields and minimal in-vessel electrodes. The less robust concepts involve pulsed high-voltage, as in the plasma arc centrifuge (Sec. 2.3), or low voltage in-vessel electrodes, such as separation by ion mobility (Sec. 2.7). Use of micron-sized dust as a separation medium (Sec. 2.10) is rated poor since it may involve clogging and a risk of chemical explosion.

The throughput and efficiency columns are meant to evaluate the total mass flow rate and the separation efficiency at the output, which are two different measures of performance. High throughput is always desirable, but separation efficiency should be optimized to the specific application. Quantitative theoretical metrics for comparing plasma mass filters have been discussed previously [2], but there is presently very limited information on the actual performance of relevant systems. The preliminary evaluations of Table 1 are based only on superficial qualitative impressions; for example, that separation in a curved magnetic field (Sec. 2.2) could have a good throughput since its sources can be designed in parallel over a large area, but its efficiency may be poor since the ion drifts are not well separated. Similarly, the throughput of vacuum arc centrifuge system (Sec. 2.3) may be low because of its pulsed nature, but its separation efficiency has been demonstrated on a small scale. Separation based on ionization potential (Sec. 2.9) may have a high throughput, but would be efficient mainly in separating cesium. Dusty plasmas (Sec. 2.10) may have a high throughput due to the relatively large mass of dust particles compared with ions or molecules, but the efficiency would depend on the composition of the dust, which is not likely to match to separation goals.

Obviously, each of these ratings is debatable, and Table 1 should be considered only a framework for starting a serious R&D plan. Ideally all concepts would be tested experimentally at the stage 1 level, and those results plus detailed modeling would be used to select the concept(s) which should move on to stage 2.

[1] R. Gueroult, J.-M. Rax, S.J. Zweben, and N.J. Fisch, Plasma Physics Control. Fusion 60, 104018 (2018)
[2] A.J. Fetterman and N.J. Fisch, Physics of Plasmas 18, 103503 (2011)

5.3 Theory and simulation

Each of the plasma separation mechanisms of Sec. 2 is based on a simple theoretical idea, but few of them have been analyzed using state-of-the-art computation simulations. An R&D program to develop an industrial-scale plasma separation device would certainly benefit from detailed computational simulations of how these ideas would play out in a realistic system.

A list of the generic physics and technology issues from Sec. 3 and 4 is shown in Table 5.2, along with a tentative classification of the type of theory/simulation code needed for each issue. Hopefully each of these codes will able to treat each separation mechanism in order to allow a direct comparison between different approaches. Each type of code should also be able to communicate with the other codes to handle

the coupling between these various generic issues, which is often the most difficult computational task for complex physical systems such as this.

Section	generic issue	theory/simulation code
3.1	ion charge and radiation	atomic physics
3.2	molecules and chemistry	atomic physics
3.3	CX and recombination	atomic physics
3.4	neutral gas transport	particle transport
3.5	large particles	particle transport
3.6	collisional effects	particle transport
3.7	electric fields and rotation	plasma dynamics
3.8	plasma fluctuations	plasma dynamics
3.9	plasma energy loss	plasma dynamics
3.10	throughput and efficiency	atomic+particle+dynamics+engineering
4.1	ion source	engineering systems
4.2	waste handling	engineering systems
4.3	plasma heating	engineering systems
4.4	ES&H	engineering systems

Table 5.2 – theory and simulation needed for plasma mass filtering of nuclear waste

5.3.1 Atomic physics code

As discussed in Sec. 3.1-3.3, there are several crucial issues involving atomic physics which need to be resolved before a plasma can be designed for separating nuclear waste; for example, the ion charge state balance, radiation emission level, molecular ion state, and charge exchange/recombination processes. Many of these atomic processes are governed by cross-sections or reaction rates which can be found in existing codes and databases, and which should be incorporated as much as possible. However, given the unusual atomic composition of a nuclear waste plasma, it is likely that many of these rates will have to be derived or approximated especially for this code.

The basic inputs to this code would be the assumed source species mix derived from the nuclear waste composition (which is highly variable), and the assumed plasma electron density and temperature profiles. The basic outputs would be the ion charge state distribution for each atomic species (including neutrals), the molecular composition (including positive and negative ions), and the radiated power (which is needed for the system energy balance). These code outputs would be used to define the possible operating points, e.g. where the important species are singly charged and the radiated power is manageable. For example, the highly simplified analysis of Sec. 3.1 suggested that the electron temperature needed to be T_e ~1-2 eV to maintain a dominant +1 ion charge state for most species, and that the heavy atom ($\geq$ gold) concentration needed to be <1% to maintain a radiation level of <5 MW/m^3. These estimates should be refined and their uncertainties clarified before finalizing the design of any plasma system for nuclear waste separation.

5.3.2 Particle transport code

The central issue in any plasma device for nuclear waste separation is the transport of all particles from the input stream into the output heavy-atom (highly radioactive) stream and the light-atom (largely non-radioactive) stream. Thus the motion of particle species should be simulated in a realistic geometry, including the ionized atoms and molecules, the neutral atoms and molecules, and any larger particles such as dust in the system. The particle transport code which does this should have the physics of the separation mechanism (e.g. the ion orbits and drifts in a magnetic field), all relevant collision processes (e.g. ion-neutral collisions and charge exchange), and the electric and magnetic fields which influence the particle motion (at least in a time-averaged sense).

The basic inputs to this code would be the assumed particle species, the assumed plasma parameters, and the relevant electric and magnetic fields (excluding fluctuations, which may be too complex to model). The basic output would be a idealized first-approximation to the particle throughput and separation efficiency, including an inventory of where each type of atom will ultimately strike the wall inside the vacuum chamber. Even though the fundamental particle transport processes in plasmas are well known, it will be computationally difficult to track each type of particle and their mutual interactions. To become more realistic, this code will also need to couple to a particle source model (Sec. 5.3.4) and a model for the interactions of particles with the walls (Sec. 5.3.5). The transport of neutral particles will be very important, even though they will not be directly affected by the separation mechanisms.

5.3.3 Plasma dynamics code

Perhaps the greatest difficulty for the theory and/or simulation of a nuclear waste plasma is the possible effect of plasma fluctuations on the separation process. If the plasma is unstable on the timescale of the ion separation process, then the collisional model for particle transport in Sec. 5.3.2 easily can be overwhelmed by unstable flows or turbulent mixing. Although the theory of plasma stability is highly sophisticated and many codes have been developed for applications to basic plasma physics, fusion and astrophysics, little has been done so far to apply these codes to ion mass separation processes. Existing codes use either fluid MHD models, kinetic theory models, or particle-pushing models, and incorporate the fluctuating electric and magnetic fields on the appropriate space and time scales. To calculate transport effects these models must include non-linear physics, and so are computationally expensive and difficult.

The basic inputs to the plasma dynamics code would be the assumed plasma density and temperature profiles, including the externally applied electric and magnetic fields. The basic outputs of the code would be the spectrum of plasma fluctuations and their approximate ion transport effects. However, it is unrealistic to expect that these transport effects can be simulated accurately, since this is still not possible for either simple linear plasma experiments or in magnetic fusion experiments. However, it should be possible to identify the most stable operating regimes in a specific plasma separation scenario, in order to minimize the fluctuation-induced mixing effects.

Two somewhat separate issues might also be handled within a plasma dynamics code: the self-consistent calculation of the plasma rotation and the plasma energy loss. Plasma rotation is crucial for some of the separation concepts, but understanding its physics is difficult since it involves both the parallel and perpendicular transport of ions and electrons, and probably also the friction between ions and neutrals. The plasma energy loss will probably depend on the electron transport, and may be crucial for determining the

plasma heating requirements and wall heat loading. These calculations will be difficult and only approximate solutions and design guidelines are to be expected from such a code.

5.3.4 Engineering systems codes

Each of the generic technology issues discussed in Sec. 4 and listed at the bottom of Table 5.1 will probably need its own simulation code to help design and operate an industrial-scale plasma mass separation device. These would probably be based on existing engineering systems codes, including those used for chemical separation processes at Hanford and other nuclear waste sites.

The various options for a plasma source need to be carefully analyzed and tested before use in a plasma separation system. The conversion of solid or liquid nuclear waste material into neutral atoms or molecules is difficult and largely unexplored. Codes to do this should incorporate the thermal, chemical, and surface properties of each waste form to optimize this conversion. The ionization processes can probably be modeled using existing RF and electron codes. Obviously the source is closely coupled to the main separation volume, so their interactions must be included.

The mechanical handling of the nuclear waste will be crucial for any successful system. An issue specific to plasma systems is the coating of internal vacuum components with deposited vapor and dust, which could be modeled based on the plasma source and particle transport codes. It is very likely that thick coatings will be formed on all surfaces, which might have to be removed *in situ* by mechanical means. Thick coatings are bad because they are likely to flake-off, clog small apertures, and make vacuum pumping and valves problematic.

The plasma separation device will most likely be driven by a high-power RF heating system of some kind in order to control the electron and ion temperatures within the device. These RF systems exist in many applications already, but their application to a nuclear waste system will need careful engineering analysis and design. For example, any in-vessel antennas or microwave horns will most likely be coated with vapor and dust, and ex-vessel access for RF may be blocked by internal conducting coatings. The physics of RF interactions with plasma is a highly complex subject, but with a considerable history of theory and simulation.

Automated control and safety system codes will clearly be needed in a real nuclear waste processing system. The timescale for possible failures such as RF arcing or vacuum leaks is generally in the millisecond range, well below human response time. Thus a control systems code will need to be integrated with a set of sophisticated diagnostics to carefully monitor the device and its environment.

5.4 Process diagnostics

The first research stage will help define the most promising ion mass separation mechanisms, so will use only a small input of non-toxic gases and small samples of solids (e.g. powders). Thus the basic plasma diagnostics can be similar to those on existing plasma devices [1-4]; for example, Langmuir probes for density and temperature measurements, Mach probes for rotation measurements, visible spectroscopy for ion velocity and temperature, and gridded energy analyzers for ion distribution functions, if needed. A fast camera would also be useful to asses plasma fluctuations. These diagnostics are listed in Table 5.3.

However, even at the first stage it will be essential measure particle transport to evaluate the separation mechanisms, preferably on a real-time basis without a vacuum break. Passive broad-wavelength survey spectroscometers can provide qualitative information on the ionization states and approximate location of all the species in the plasma, but quantitative measurements are difficult due to line-integration and the need for electron temperature information to interpret them. Commercial residual gas analyzers would be useful to measure the neutral gas composition in real-time, including points inside the vacuum chamber which could be sampled with movable tubes. But conventional mass spectrometers would not be able to measure the location or concentration of species which are solid at room temperature, which is the main interest in nuclear waste separation.

At the low throughput of a stage #1 device, these solids will form sub-micron thick films on the inner surfaces of the vacuum vessel. Many diagnostics for thin surface films in vacuum systems have been developed for industrial and fusion applications, and these can be adapted for a plasma separation device. Some techniques could be used in real time during plasma operation, such as laser ellipsometry [5] or quartz microbalances [6] for measuring film thickness. Others surface diagnostics could be used *in situ* between plasma pulses (due to background light), such as laser-induced breakdown spectroscopy (LIBS) [7], x-ray fluorescence [8], or Raman spectroscopy [9] for surface chemical composition. Ideally, these diagnostics should be able to scan over a wide area inside the vacuum vessel to look for unexpected depositions.

At the higher throughputs of a stage #2 device the deposition will be nearly macroscopic; for example, a throughput of ~1 mg/sec for 1000 sec would deposit a total of 1 gram on the device walls, or ~1 mg/cm^2 over an area of ~1000 cm^2, i.e. a ~1-10 μm thick layer. These thicker films could be most easily measured using sample coupons removed from the system with vacuum interlocks and analyzed *ex situ* by standard chemical techniques. On the other hand, these thicker films might also coat windows and probes, so could make some of the other diagnostics more difficult; for example, it will be difficult to measure the electron temperature without Langmuir probes. Some diagnostics of the micron-sized dust in the chamber could also be useful, using laser scattering or other techniques developed for dusty plasmas [10].

At the first introduction of actual nuclear waste into a plasma separation device, it will be necessary to install various radiation diagnostics to track radioactive species. For a vacuum vessel inventory of ~1 gr (i.e. 1 mg/sec throughput for 1000 sec) the expected radiation level is ~10^{-3} Ci (3×10^7 disintegrations/sec), mainly due to Cs^{137} and Sr^{90}. The Cs^{137} should be relatively easy to detect due to its 662 keV gamma radiation, which can penetrate ~1 cm of steel. It might be possible to measure the quantity of Cs^{137} and Sr^{90} inside the vacuum vessel by detecting the light emission or ionization due to their betas in a high pressure chamber fill gas (between plasma pulses). Alpha particle and neutron emission from uranium, plutonium and other actinides in the vacuum vessel will probably be too weak to detect.

At the eventual high throughput and power levels (~1 gr/sec and ~1 MW), there will need to be additional diagnostic to control and safely operate the system. The temperature of the outside of the vessel should be monitored by thermocouples and IRTV cameras due to possible hot spots from plasma heat loss. The pressure of all vacuum systems and the room and exhaust gas composition should be monitored for leaks and toxic or flammable gases. The inventory of waste in the system should be tracked as the difference between input and output to the vessel (including exhaust gases). Probably all of these system diagnostics already exist for the chemical separation plants.

diagnostic	measurement
Langmuir probe	electron temperature and density
Mach probe	ion rotation speed
visible spectroscometer	ion flow and temperature
gridded energy analyzer	ion distribution function
survey spectrometers	species location and charge state
bolometer	radiated power
fast camera	plasma fluctuations
residual gas analyzer	gas composition at a few points
laser ellipsometry	thin film thickness
quartz microbalance	deposition thickness
LIBS	surface chemical composition
x-ray flourescence	surface chemical composition
Raman spectroscopy	surface chemical composition
removable coupons	standard chemical analysis
laser scattering	dust in plasma
gamma detector (ex-vessel)	Cs^{137} content and location
beta detector (in vessel)	Cs^{137} and Sr^{90} content
vessel wall temperature	thermocouples, IRTV

Table 5.3 - Process diagnostics for plasma separation

[1] E.E. Scime et al, J. Plasma Phys. 81, 345810103 (2016)
[2] M. Gilmore et al, J. Plasma Phys. (2015) 81, 345810104
[3] S.C. Thakur et al, Phys. Plasmas 23, 082112 (2015)
[4] B.P. Cluggish et al, Phys. Plasmas 12, 057101 (2005)
[5] I.P. Herman, Annual Rev. Phys. Chem. 54, 277 (2003)
[6] C.H. Skinner et al, J. Nucl. Materials 337-339, 129 (2005)
[7] D.W. Hahn and N. Omenetto, Applied Spectroscopy 66, 347 (2012) and 64, 335A (2010)
[8] P.J. Potts and P.C. Webb, J. Geochemical Exploration 44, 251 (1992)
[9] https://en.wikipedia.org/wiki/Raman_spectroscopy
[10] B.A. Annaratone et al, IEEE Trans. Plasma Sci. 37, 270 (2009)

5.5 Example of a second stage scale device

An example of second-stage-scale plasma separation device is reproduced in Fig. 5.1, taken directly from the review of Dolgolenko of the Kurchatov Institute [1]. This review describes a generic ion cyclotron resonance (ICR) isotope separator based on several machines built in the US, Russia, and France. These devices incorporate the gyroradius separation mechanism of Sec. 2.1, but similar designs with lower mass resolution and higher throughput may be possible for Hanford waste separation.

The largest such device was based on a superconducting magnet with $B \leq 1.8$ T, a length of up to 8 meters, an outer diameter of over 2 meters and a bore of about 1 meter [1-4], as illustrated by the model in Fig. 5.2 [4]. This device was developed by TRW in California based on a Dawson patent [5], but classified due to uranium applications, so only indirect design and operation information was published. This device

was operated at TRW until the late 1980's, and then moved to ORNL as part of their isotope enrichment facility (but not used as of 2009). This and similar devices have been successfully used to separate and even sell isotopes of many atomic species, e.g. lithium, calcium, nickel, and potassium.

The source of neutral atoms was either a heated crucible (for volatile materials) or a large sputtering plate biased negatively at 2-4 kV, as shown at the left of Fig. 5.1. The neutrals were ionized inside an electron cyclotron heating region, aided by electron mirroring between the negative sputtering plate and the main magnetic field. The ions flowed into the long solenoid to the right, where cyclotron resonant heating was applied using an inductive four-phase antennas at 0.1-1 MHz to increase the gyroradius of the selected isotopes. The physics of this ion heating is non-trivial, as discussed in some detail in [1,4]. The ions of various gyroradii were collected at the right end by biased plates, also illustrated at the right in Fig. 2.1. The lower gyroradius ions were collected on surfaces directly along B field lines, while the high gyroradius ions were deposited on the sides of these collectors.

This system was capable of processing "several grams to several dozen grams per day", corresponding to a throughput of roughly ~1 mg/sec; for example, the daily production of nickel enriched to 40% with the ^{62}Ni isotope with the TRW device was 13 grams for part of a day [1]. Major modifications of this design would be needed for processing nuclear waste at ~100 mg/sec or 8.6 kg/day (24/7). In principle the nuclear waste processing is simpler since it requires only a coarse mass resolution (above and below A~90), which should simplify the magnet and ICR requirements. However, isotope separation generally uses single metallic species as input, whereas the nuclear waste has a complex mix of species, which will make plasma heating and waste collection much more difficult.

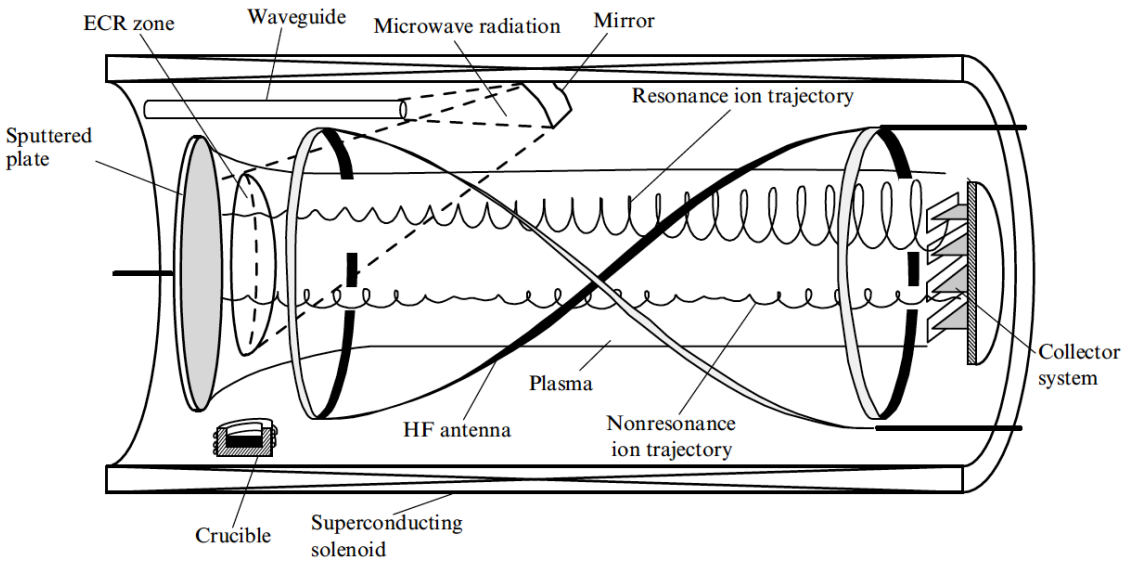

Fig. 5.1 - schematic of the ICR separation device (from [1])

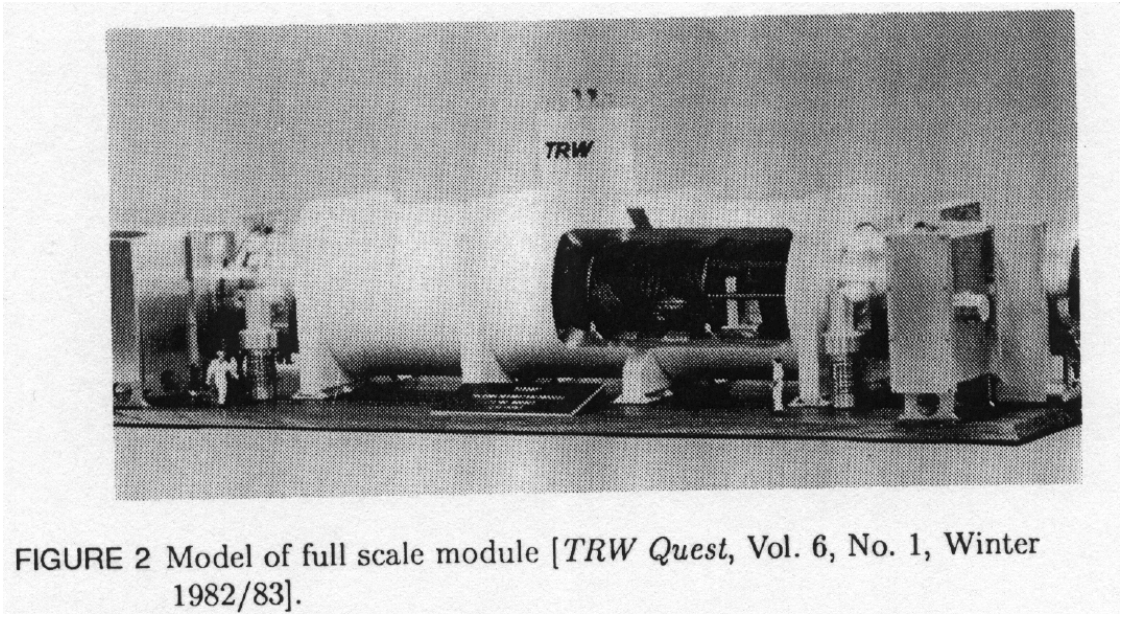

FIGURE 2 Model of full scale module [*TRW Quest*, Vol. 6, No. 1, Winter 1982/83].

Fig. 5.2 - model of full scale isotope separation module at TRW (from [4])

[1] D.A. Dolgolenko and Yu. A. Muromkin, Physics-Uspekhi 52, 345 (2009); D.A. Dolgoenko and Yu. A. Muromkin, Physics-Uspekhti 60, 994 (2017)
[2] A.N. Ezoubtchenko et al, Progress in Nuclear Energy 32, No. 3/4, 729 (1998)
[3] J.G. Tracy and W.S. Aarons, Nucl. Instrum. and Methods in Physics Research A 334, 45 (1993)
[4] F.F. Chen, "Lecture Honoring John M. Dawson", http://www.seas.ucla.edu/~ffchen/Publs/Chen136.pdf
[5] https://www.google.com/patents/US4081677

5.6 Summary of R&D issues and directions

This final section briefly summarizes the generic physics and technology results and issues discussed in Sec. 3 and 4, and points to possible directions for their resolution within a future R&D program. These issues are ordered in terms of section number in the main text.

5.6.1 Charge state and radiated power (Sec. 3.1)

Sample results from atomic physics codes for various species indicate that the average ion charge is mainly in the desired +1 state only when T_e ~1-2 eV, which defines a very narrow operation window for a plasma mass filter. The inevitable deviations in charge state distribution due to spatial variations in temperature would further reduce the ion throughput and/or efficiency of a separation device. These codes also predict a radiated power up to ~5 MW/m^3 at a ~1% concentration level of high mass atoms like gold, which may become too large to support with a practical plasma heating and cooling system. The charge state can be controlled to some extent by varying the external plasma heating, and the radiated power can be controlled by limiting the waste stream fueling rate (at the expense of throughput).

5.6.2 Molecular ions and plasma chemistry (Sec. 3.2)

Based on sample estimates from the literature, a nuclear waste plasma at T_e ~1-2 eV may be dominated by molecular ion species, which could also interact chemically within the plasma during the separation process. Numerical calculations of molecular concentrations and plasma chemical reactions are very complex and may not have much predictive value, given the uncertain and variable composition of nuclear waste. The basic separation mechanisms should not be significantly affected since the charge/mass ratio of most molecules with a heavy atom is not much different than that of the heavy atoms itself, except for negative molecular ions which would not be separated at all. The composition of the output product will be affected by its molecular composition, and may make it more difficult to remove from the system.

5.6.3 Charge exchange and recombination (Sec. 3.3)

Based on estimates from sample cross-sections, charge exchange and recombination processes will be important for some species such as cesium (charge exchange) and nitrogen molecules (recombination). If the timescale for these processes is less than the confinement time of the ion to be separated, then the efficiency will be reduced, since the ion charge changes before the separation is completed. Given the many species expected in a nuclear waste plasma, the detailed calculations of these processes will require a large code and an extensive search for missing cross-sections. One way to minimize these deleterious effects is to reduce the confinement time required for the ion to be separated, e.g. by mechanisms using only a few gyro-orbits. Another way is to reduce the neutral density as much as possible.

5.6.4 Neutral gas transport (Sec. 3.4)

Based on general experience with low temperature plasmas and sample estimates from atomic physics codes, the neutral density in a nuclear waste plasma most likely be comparable to or larger than the ion density. In particular, at the temperatures where easily ionized atoms like cesium are singly charged, the high-ionization-level atoms or molecules like argon (a possible buffer gas) will largely be neutral, and at the temperature where argon-like atoms are singly ionized, atoms like cesium will be doubly ionized. Neutrals will also be formed by charge exchange and recombination. Since neutrals will not be separated by any of the mechanisms discussed here, the separation efficiency can be significantly reduced by their presence, depending on their temperature (transport rate), their wall sticking coefficient (recycling rate), and their exhaust pumping rates. Detailed calculations of neutral flows will be necessary for device design.

5.6.5 Droplets, dust, and nanoparticles (Sec. 3.5)

Particles larger than molecules (i.e. 10 nm - 100 μm) will most likely be created in a nuclear waste plasma and will not be separated by the standard mechanisms since their charge/mass ratio is much too low. These particles may be introduced intentionally by the plasma source (such as a dust dropper), by flaking-off of nuclear waste coatings from the walls, or by coagulation of molecules inside the plasma. Some thermal evaporation of these particles will occur due to plasma heating, but this could take longer than the lifetime of the particles in the plasma. Laser evaporation of particles inside the plasma is possible but most likely inefficient and expensive. The overall separation efficiency will be reduced by the mass fraction of these particles, depending on the particle motion within the system, which will be difficult to predict.

5.6.6 Collisional effects (Sec. 3.6)

Based on simple analytic estimates and simulations, the ion throughput in a nuclear waste plasma will normally be determined by ion-ion and ion-neutral single-particle scattering collisions. Exceptions to this can occur if the ions become collisionless at high enough temperature or at small system size (compared with the gyro-orbit size). Collisions will generally reduce both the ion throughput and the separation efficiency, except for mechanisms which normally operate in the fluid limit (like a plasma centrifuge). More realistic models should eventually include inelastic collisions with molecules, collisions with larger particles in the plasma, and charge exchange and recombination. The collisionality should be assessed before any application of a collisional-radiative model for radiative power loss. Kinetic effects (i.e. non-Maxwellian ions and/or electrons) may also be present due to RF heating or sheaths.

5.6.7 Electric fields and rotation (Sec. 3.7)

Many of the proposed separation mechanisms invoke the application of electric fields to the plasma, either in pulsed form (e.g. arc centrifuge or transit-time separation) or in steady-state operation (e.g. azimuthal rotation or mobility driven separation). However, the prediction of electric fields and their effects on rotation is extremely difficult due to the complex nature of the electrical conductivity of plasmas. For example, the parallel conductivity will depend on the sheath physics and wall geometry, while the cross-field conductivity will depend on the ion-neutral friction and viscosity. Thus the ion separation effects due to electric fields and rotation will most likely need to be measured empirically rather than calculated from the applied fields. External control of these mechanisms will still be possible by varying the applied voltages and their time dependences, but only within limits set by shielding due to electrostatic sheaths and undesired arcing. Electrodes inside the plasma will also be subject to coatings and erosion, and may require active cooling (which can be dangerous in case of a coolant leak).

5.6.8 Plasma fluctuations and mixing (Sec. 3.8)

Self-generated plasma fluctuations can cause rapid cross-field ion mixing, which may significantly reduce the separation efficiency for any of these mechanisms. Plasma instabilities are commonly observed in the density and temperature ranges of interest in both basic plasma research and at the edge of magnetic fusion devices, although the behavior with nuclear waste species is not well documented. Fluctuation-induced transport effects have been very difficult to understand or control despite many years of study, so research on the basic physics should probably not be done in a plasma separation device beyond stage #1. However, the fluctuation levels should be monitored (e.g. using a fast camera), and regimes with large fluctuations should be avoided if possible. In general, the fluctuation-induced transport will also be minimized when the expected confinement time of ions is small, such as for mechanisms with rapid gyro-orbit loss.

5.6.9 Energy loss due to plasma transport (Sec. 3.9)

Plasma energy transport will most likely be dominated by electrons, which will rapidly follow magnetic field lines to the wall. Simple estimates suggest this loss may be up to ~150 W/cm^2 at $T_e \sim 5$ eV, which would require local external cooling of the wall. Plasma heating or erosion of internal electrodes by

electrons or ions will be a more serious issue, since cooling of internal components may be hazardous due to possible leaks. Some of the plasma energy loss might be useful to help evaporate the input waste, but it could just as easily vaporize the output waste, returning it to the plasma. There is a trade-off between reducing plasma energy loss through improved confinement (such as at higher density or magnetic field), and increasing the likelihood of collisional or fluctuation-induced ion mixing at high ion confinement time.

5.6.10 Ion throughput and separation (Sec. 3.10)

A successful plasma separation process for remediation of a Hanford-type site should have a total throughput of ~100 g/sec, with sufficient separation between high mass (A>90) and low mass species (A<90) to satisfy regulatory requirements for high-level and low-level radioactive waste disposal. However, there is presently *no* plasma process which has demonstrated separation of nuclear waste at *any* level of throughput. Thus the R&D program required to reach this goal is extensive, and should start with basic separation tests at very low throughput. Relatively simple calculations for axial collection systems have shown that throughput and separation are dominated by collisions, and that the throughput goal can be only be obtained by raising the ion temperature to $T_i \geq 10$ eV. However, simple charge state and radiation estimates suggest that the electron temperature needs to be in the range $T_e \sim 1\text{-}2$ eV. If this is the case, then maintaining such a non-equilibrium temperature difference will be a major challenge for the plasma separation process.

5.6.11 Plasma sources (Sec. 4.1)

Many possible methods for evaporation and ionization of nuclear waste were discussed, all of which are based on conventional technology, and many of which have been demonstrated at near-relevant levels of throughput. The main issue is to optimize the match between the plasma source and the chosen separation mechanism, since these must be coupled together within the same vacuum system. One criterion for choice is to minimize the macro-particle influx from the source, since particles larger than a single molecule will not be separated in the main chamber. Another criterion is to minimize the plasma instability generated by the source, since these fluctuations can propagate into the main chamber and cause ion mixing. A third criterion is to minimize the energy required to evaporate and ionize the waste. Perhaps the leading candidate based on these criterion is ion sputtering, which has been used successfully for isotope separation devices. The plasma source can probably be developed separately from the separation device at the first stage of R&D, but should be integrated with separation at the second stage.

5.6.12 Waste handling (Sec. 4.2)

Probably the most difficult technological issue in any nuclear waste separation process is simply the handling and transportation of the waste, mainly due to its chemical toxicity and radioactivity. In the case of plasma separation, this includes moving the waste into the plasma source section, removing the separated waste from the output sections, and cleaning and maintaining the vacuum chamber itself. Many of these issues have been studied and/or resolved within the conventional chemical separation program, and obviously these experts should be consulted and included in any plasma separation design process. Specific issues relating to handling corrosive or radioactive waste within vacuum systems may have been resolved to some extent by the isotope separation or industrial plasma processing communities, and these experts should be consulted as well. Clearly major engineering analysis will be required for the development of any large-

scale plasma separation process, even after the physics is completely understood and demonstrated with surrogate waste material.

5.6.13 Plasma heating and magnets (Sec. 4.3)

Probably the most costly technology in plasma separation will be the plasma heating system, which was estimated to need ~100 MW of plasma power for a waste throughput of ~100 g/sec. Given the typical plug-to-plasma RF heating system efficiency of ~50%, operation at this level may require a dedicated power plant. Although the physics of plasma heating systems is understood to a large extent, their application to nuclear waste plasma will require significant new research, engineering design, and testing at each level of R&D. The only analogous plasma heating system is that being designed for ITER, which is a major technological challenge. If the RF antennas are located outside the vacuum system, their coupling to the plasma can be compromised by conducting coatings on the vessel interior, but it the RF antennas are located inside the vacuum vessel they can be compromised by erosion, coatings, or arcing. In either case, high voltages and RF wave radiation will make these systems complicated and hazardous. Even if the RF waves are successfully coupled and heat the plasma, their potential effects on ion transport will need to be understood (although these effects might be useful in ion separation). Magnets would most likely need to be superconducting to minimize power usage, although it might be possible to use permanent magnets for some separation methods.

5.6.14 ES&H issues (Sec. 4.4)

Obviously a necessary condition for plasma separation of actual nuclear waste is a complete ES&H analysis, including monitoring and control system for toxic chemical leaks and radiation. Probably the most serious hazards will be associated with the loading and removal of waste from the vacuum system, and with the routine exhaust of vacuum system pumps. Additional hazards will occur even without nuclear waste, such as dust, high voltage, RF radiation, vacuum systems, and cryogenics for superconducting magnetics.

Acknowledgments:

We thank the following people who have worked with us on this topic: A. Carpe, D. Cylinder, D. DiCicco, E. Evans, M. Galante, M. Mlodik, and J.M. Rax. We also thank P. Efthimion and J. Hosea their support for support this project and K.M. Young for advice. This work was funded by USDOE Contract No. DE-AC02–09CH11466.

.

PPPL PRINCETON PLASMA PHYSICS LABORATORY

Princeton Plasma Physics Laboratory
Office of Reports and Publications

Managed by
Princeton University

under contract with the
U.S. Department of Energy
(DE-AC02-09CH11466)

P.O. Box 451, Princeton, NJ 08543
Phone: 609-243-2245
Fax: 609-243-2751

E-mail: publications@pppl.gov

Website: http://www.pppl.gov